The C-terminus of Troponin T Modulates Calcium Regulation of Actin-Myosin Interactions

by

Dylan James Johnson

May 2019

Director of Dissertation: Joseph Chalovich

Major Department: Biochemistry

Abstract

The highly conserved terminal fourteen C-terminal residues of troponin T play a novel role in the regulation of striated muscle contraction. Elimination of the terminal fourteen residues of the C-terminal region of troponin T stabilizes the functional active state and destabilizes one of two inactive states, the blocked state. We've used a series of functional assays to assess the magnitude of disruption to the actin state distribution by different mutations within that C-terminus. In doing so, we have identified the characteristics of the C-terminus required for its function. To probe the structural mechanism of the C-terminus of troponin T, we used a series of FRET pairs to measure the interactions of the C-terminus of troponin T and how those interactions are disrupted by C-terminal mutation.

Though mutation in the C-terminus of troponin T is associated with a specific cardiovascular disease, hypertrophic cardiomyopathy, the findings from our lab indicate this region's function has broader implications on our fundamental understanding of striated muscle regulation and treatment of cardiovascular disease. Our incomplete

understanding of this cycle's regulation has led to the generation of a variety of hypothesis to explain the gaps in our knowledge. We have taken steps to characterize the functional and structural consequence of mutation within the C-terminus of troponin T and now believe we have closed some of the gaps in our knowledge of this regulated cycle.

The C-terminus of Troponin T Modulates Calcium Regulation of Actin-Myosin Interactions

A Dissertation

Presented to the Faculty of the Department of Biochemistry

East Carolina University

In Partial Fulfillment of the Requirements for the Degree

Doctorate in Biochemistry

by

Dylan James Johnson

May 2019

The C-terminus of Troponin T Modulates Calcium Regulation

of Actin-Myosin Interactions

By

Dylan James Johnson

Approved By:

Director of
Dissertation:_____
Joseph Chalovich, Ph.D.

Committee Member: _____
Colin Burns, Ph.D.

Committee Member: _____
Tonya Zeczycki, Ph.D.

Committee Member: _____
Kyle Mansfield, Ph.D.

Chair of the Department
Of Biochemistry: _____
David Taylor, Ph.D.

Dean of the
Graduate School: _____
Paul J. Gemperline, Ph.D.

Acknowledgements

I would like to thank the members of my thesis committee for their support and guidance and the members of my lab for all of their assistance throughout this research project.

Dr. Joseph Chalovich

Dr. Colin Burns

Dr. Tonya Zeczycki

Dr. Kyle Mansfield

Dr. Yumin Li

Dr. William Angus

Dr. Li Zhu

Dr. Kimberly Kew

Ms. Anita DeSantis

Ms. Amanda Fisher

Micro Summit Processors

A special thanks to Dr. Chalovich for all of his guidance and to Dr. Li Zhu and Dr. William Angus for their support generating the mutant troponin constructs.

Table of Contents

List of Tables

List of Figures

Abbreviations

B State: Blocked Inactive State of Actin

$CaCl_2$: Calcium Chloride

C State: Closed Inactive State of Actin

DABMI: 4-dimethyl-aminophenylazophenyl 4′-maleimide

DTT: Dithiothreitol

EDTA: Ethylenediaminetetraacetic acid

EGTA: Ethylene glycol-bis(2-aminoethylether)-N,N,N′,N′-tetraacetic acid

IAEDANS: 5-(2-iodoacetylaminoethyl) aminonaphthalene 1-sulfonic acid

KCl: Potassium chloride

O state: Open Active State of Actin

$MgCl_2$: Magnesium Chloride

MOPS: (3-(N-morpholino)propanesulfonic acid)

PMSF: phenylmethane sulfonyl fluoride

S1: Myosin Subfragment 1

Tpm: Tropomyosin

Tn: Troponin

TnC: Troponin C

TnI: Troponin I

TnT: Troponin T

Chapter 1: Background

Introduction

This dissertation was developed on the premise that the highly conserved terminal fourteen C-terminal residues of troponin T (C-terminus) play a novel role in the regulation of striated muscle contraction. In this Chapter, I will begin with a brief introduction to cardiovascular disease with a focus on clarifying the broader implications of our work. Although mutation in C-terminus of troponin T is associated with a specific cardiovascular disease, hypertrophic cardiomyopathy, the findings from our lab indicate this region has functions with broader implications to striated muscle regulation and treatment of cardiovascular disease. To realize the significance of this region, it is important to first understand the steps involved in the contractile cycle of myosin-actin interactions required to hydrolyze ATP and produce force. I will detail that cycle including the regulated steps and the proteins involved. Our incomplete understanding of this cycle has led to the generation of a variety of hypothesis to explain the gaps in our knowledge. The data presented in chapters three and four of this dissertation demonstrate steps we have taken to characterize the functional and structural consequence of mutation in the C-terminus of troponin T. I will discuss in Chapter 5 the significance of our findings and how we believe we have closed some of the gaps in our knowledge of this regulated cycle.

The broader implications of the genetic basis of Cardiomyopathy

Cardiovascular disease (CVD) has a prevalence of 48% in the global population with over 121.5 million affected in the United States alone for men and women over twenty years of age [1]. In 2016, over 840,000 deaths were attributed to cardiovascular disease in the United States and over 300,000 of those occurring suddenly or unexpectedly [2]. Coronary artery disease (CAD) accounts for 80% of sudden cardiac deaths while the other 20% is composed of cardiomyopathies and other cardiac disorders[1]. Genes associated with disease have been identified for approximately 50-75% of hypertrophic cardiomyopathy cases and up to 40% of dilated cardiomyopathy cases[1]. Although there are extensive circumstantial risk factors and family history links with CAD [1], there is limited genetic evidence compared to that of heart diseases such as hypertrophic cardiomyopathy. The genetic, epigenetic, shared behavioral and shared environmental risk factors exemplify the complexity of this disease and make evident the difficulty in identifying the root cause[2].

Watkins et al.[3] showed that familial hypertrophic cardiomyopathy was linked to mutations in the actin regulatory component troponin T. Since then, hypertrophic cardiomyopathy has become well established as a disease of the sarcomere[4] as mutations in over ten proteins and over thirty mutations within troponin T alone have been linked to hypertrophic cardiomyopathy [5]. Approximately 1 in 500 individuals have left ventricular hypertrophy, of whom 20% to 30% are likely to have a sarcomere mutation that suggests clinically expressed hypertrophic cardiomyopathy [1]. Additionally, over ten mutations in troponin T have been linked to dilated cardiomyopathies [5]. Hypertrophic cardiomyopathy is characterized by decreased left ventricle volume

resulting from thickening of the ventricle wall. Dilated cardiomyopathies on the other hand is characterized by increased left ventricle volume resulting from dilating of the left ventricle wall. It is interesting that hypertrophic cardiomyopathy and dilated cardiomyopathy can each arise from mutation within a single protein, troponin T, but have seemingly disparate phenotypes[6]. The molecular mechanism of this dual function of troponin T will play a central role throughout this dissertation.

Targeting upstream signaling pathways was a goal of early cardiovascular disease treatments[7]. Those treatments often had wide ranging downstream effects targeting the sarcomere as well as ion channels and smooth muscle. The broad downstream effects of these upstream targets can further increase the chance of arrhythmias and hypotension already commonly present in those with CVD[7]. Targeting proteins of the sarcomere directly would permit safer and more personalized treatment by limiting the pathways affected. In addition to the restoration of compromised sarcomere function in familial myopathies, sarcomere modulation via targeting of sarcomeric proteins may have therapeutic value in a broader range of diseases that affect muscle function[7]. Clinical trials for the treatment of spinal muscular atrophy and amyotrophic lateral sclerosis using sarcomeric modulators for instance have already begun[8].

To modify sarcomeric function, it is essential to understand how the proteins making up the sarcomere interact. These proteins, including actin, myosin, tropomyosin and troponin, interact to convert hydrolysis of ATP into a conformational change that produces force.

The energy of ATP is converted into a force producing conformational change where myosin and actin slide past one another. ATP is hydrolyzed by myosin alone at a

relatively low rate. Interaction of myosin with actin can accelerate this myosin ATPase (ATP hydrolysis) rate by several hundred-fold. The ability of actin to accelerate the ATPase activity is controlled by different mechanisms in different muscle types. Regulation by striated (skeletal and cardiac) muscle occur primarily through the regulatory proteins tropomyosin and troponin although a super relaxed state has recently been observed resulting from a change in myosin head structure[9]. Regulation of this ATPase activity in striated muscle is discussed below.

Actin stimulates myosin ATPase Activity

Myosin hydrolyzes ATP (Myosin ATPase activity) at a relatively low rate through the reaction scheme steps 1', 3' and 5' shown in Figure 1. When crossbridges form between actin and myosin to form actomyosin, hydrolysis of ATP occurs more rapidly[10]. The steps in this acceleration of ATP hydrolysis rate by actin follows the reaction scheme (Figure 1) steps 1, 2, 3',4, 5, 6, 7, and 8.

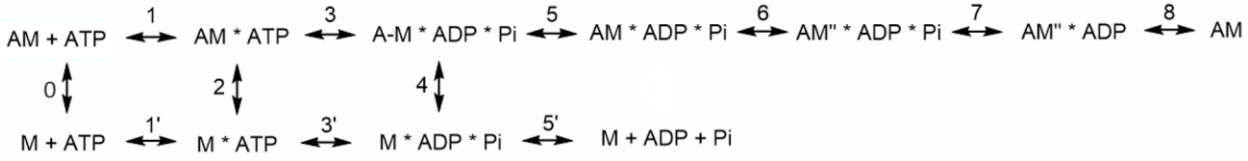

Figure 1: Myosin ATPase Crossbridge Cycle. (-) indicates a weakly bound collision complex. (*) indicates interaction. (") indicates a strongly bound state. Adapted From [11].

Step 1 and step 1' of the reaction scheme refers to the formation of a collision complex of ATP with actin-myosin and myosin respectively. Myosin-ATP rapidly dissociates from actin (step 2 of Figure 1) as ATP decreases the affinity of myosin for

actin. Actomyosin hydrolysis of ATP can be observed at low ionic strengths although it is significantly slower than cleavage by myosin alone and has a K_{eq} of less than one[12].

Myosin retains the ATP hydrolysis products, ADP and Pi. This is thought to be the rate limiting step in the absence of productive interaction with actin (step 5' of Figure 1). Myosin*ADP*Pi forms a collision complex with actin (step 4 of Figure 1) which then isomerizes via step 5 of Figure 1 to form a more stable complex. Eisenberg [13] proposed a model where there is a slow ATPase rate limiting isomerization of myosin before formation of the myosin-ATP collision complex.

Following formation of this more stable complex in step 5, fibers studies [14,15] suggest that myosin undergoes the force producing step (step 6 of Figure 1) responsible for myosin and actin sliding past one another. During or following this step, myosin releases its bound Pi which is thought to be the rate limiting step (step 7 of Figure 1). Steps 6 and 7 are believed to occur in sequence as evidenced by inducing a reversal of the crossbridge cycle via photogeneration of orthophosphate in rabbits psoas fibers and monitoring changes in isometric tension [14–16]. It has also been suggested that steps 6 and 7 or even steps 5-7 occur simultaneously [17–19]. Regardless, it is known that either step 5, 6 or 7 or a combination of them are responsible for the force producing conformational change based on the change in free energy between those states [20,21]. Following these steps, actomyosin undergoes an isomerization followed by a rapid release of ADP (step 8 of Figure 1) [22,23]. This isomerization step could also be the ATPase rate limiting step [24].

Formation of the closely associated complex (step 5 of Figure 1) and the rate limiting step (either step 6 or 7 of Figure 1) are thought to be controlled by calcium and

the troponin complex[11,25,26]. The different models developed to explain how calcium regulates the actin-myosin interaction via troponin are described below.

Calcium regulates actin-myosin interaction via troponin

Productive interaction of myosin with actin in striated muscle is dictated by the conformation of troponin and tropomyosin on actin. The conformation of troponin and tropomyosin on actin is dependent on the calcium concentration. Several models have been hypothesized to explain how calcium binding affects the conformation of troponin and tropomyosin.

The classical steric blocking model describes regulation of the myosin ATPase with only a blocked and an open state of actin (Figure 2A). The blocked state is stabilized by the absence of calcium whereas the open state is stabilized by the presence of calcium. Note that 'low calcium' refers to the virtual absence of calcium, or less than 10^{-7} M (0.1 µM). 'High calcium' or 'saturating calcium' refers to a concentration of greater than 10^{-5} M (10 µM). In this model, the proportion of myosin bound directly correlates with the ATPase rate.

It was observed that myosin S1 can bind actin even at low calcium concentrations and that non-activating species of myosin S1 (such as myosin-ADP) could cooperatively increase subsequent binding[27,28]. Although the apparent binding constant of myosin S1 is unaffected by calcium, the Vmax of the ATPase rate at low calcium concentrations is decreased to about 4% of that at saturating calcium concentrations. These observations suggested that a kinetic step in the hydrolysis or release of ATP was inhibited rather than the binding of myosin S1 to actin. New models were adapted to support this evidence where calcium and myosin function as allosteric

effectors of tropomyosin position rather than tropomyosin sterically blocking myosin binding[28,29].

The Hill model[29] (Figure 2B) consists of three states of actin in which myosin-ATP can bind to any of the states: 1_0, 1_2, or 2_n. In the Hill model, the 1_0 state is at very low calcium concentrations and the 1_2 state is stabilized by saturating calcium but does not have maximal ATPase activity. The 2_n state is stabilized by binding of activating forms of myosin S1 and exhibits maximal ATPase activity regardless of calcium concentration. Equilibrium titrations and kinetics of binding of myosin S1 revealed a discrepancy between the predicted distribution between the 1_0 and 1_2 states.

A model proposed by McKillop and Geeves[30] introduced a blocked state to the Hill model to reconcile that apparent discrepancy. The model proposed by Geeves[30] differs from the Hill model in three ways. That model states: 1) Myosin cannot bind to the blocked state 2) Myosin binds the closed and open states at an equal rate 3) The states are sequential in that actin passes through the closed state when switching between the blocked and open states.

Though the Hill and Geeves models fundamentally differ in explaining the mechanism of troponin-tropomyosin regulating actin-myosin interaction, the results of our experiments presented here are not dependent on these models. The notations can be interchanged where the blocked state is analogous to 1_0, the closed state is 1_2, and the open state is 2_n. This dissertation will use the Geeves notation blocked, closed and open.

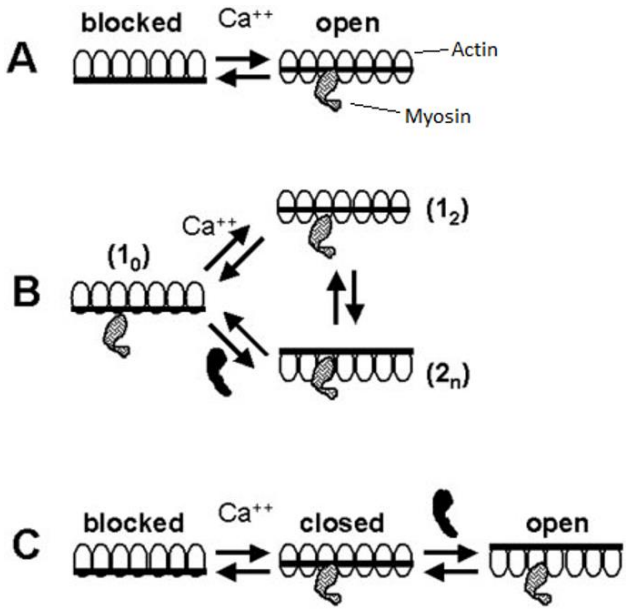

Figure 2: Schematic of regulation as described by each model. Adapted from [31] A) Classical steric blocking Model B) Hill Model C) Geeves Model

Step 4 or step 5 of the reaction scheme in Figure 1 is regulated by calcium via troponin and is the step where troponin is thought to induce tropomyosin movement. Understanding the structure of the regulatory complex and how subunits interact is important to understanding how mutations affect interactions. The structure of the regulatory complex and some of the known interactions of the troponin subunits are described below.

X-ray crystallography, electron microscopy, fluorescence resonance energy transfer (FRET), and atomic modeling have been used to identify three structural states of troponin-tropomyosin on actin [32–38]. Movement of tropomyosin between three distinct positions is well accepted although the specific conformation and interactions of those three positions is not well defined. Tropomyosin's long helical repeating nature allows its position to be measured and mapped onto actin more readily than troponin. Several

groups have used known crystal structures, interatomic distances, and molecular modeling to virtually place troponin on reconstructed thin filaments to predict the conformation of troponin in each of the structural states[35,36,39].

Though there are three structural states of troponin-tropomyosin on actin thought to correspond to the three functional states, the blocked and closed states (using the Geeves notation) were considered functionally redundant in that they do not stimulate myosin ATPase activity. However, disrupting the distribution between the blocked and closed states can lead to cardiovascular disease[40,41]. Though each state is redundant in that they do not stimulate ATPase activity, they are not redundant based on the rate and equilibrium of myosin S1 binding.

The distribution between the blocked and closed states must be considered in addition to the open state distribution. To understand regulation of actin by troponin and tropomyosin, these functionally unique states must be defined as diseases may result from changes in the distribution between each of the three functional states. Our work herein identifies some of the functional and structural differences between these three states.

We know that there are three distinct structural states of actin-tropomyosin-troponin though the position of troponin in each state is less clear. The unique rate of binding, equilibrium of binding, and ATPase stimulation of myosin in each of the three states must be the result of these differences in structure. The known structure and interactions among actin-tropomyosin-troponin have been thoroughly defined elsewhere[42–44]. The known interactions that are most relevant to this project will be summarized below.

Interactions among actin-tropomyosin-troponin

One tropomyosin dimer extends across seven actin monomers (G-actin) in polymeric actin (F-actin) and the overlaps with an adjacent tropomyosin. One troponin complex binds near each tropomyosin overlap region. Actin contains four subdomains (Figure 3). Subdomains 1 and 2 are periphery and are exposed to solvent and myosin binding. Subdomains 3 and 4 are axial and interact with subdomains 3 and 4 of an adjacent actins strand. Alanine residues within tropomyosin force the tropomyosin dimer into a coiled coil that conforms to a long pitch helix on the surface of F-actin. Each tropomyosin monomer contains seven pseudo-repeats with highly negatively charged regions. These pseudo-repeats correspond with the seven actin monomers that each tropomyosin spans. The negatively charged regions of each pseudo-repeat interact with a positively charged region within the long pitch helix of actin. The electrostatic interactions between actin-tropomyosin in the long pitch helix are primarily the result of positively charged amino acids on subdomains 1 and 3 of actin. There is a larger distance between tropomyosin and actin as tropomyosin passes over subdomains 2 and 4[45].

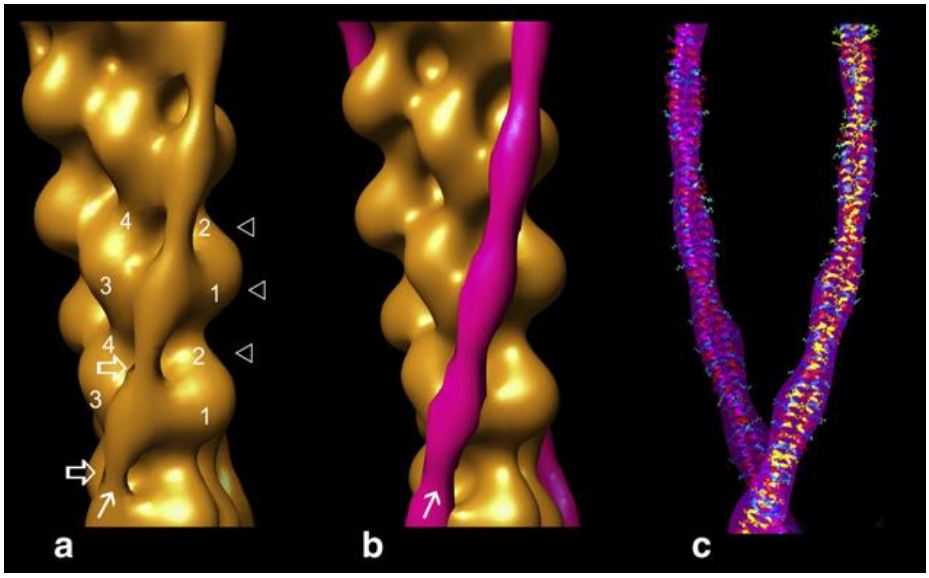

Figure 3: Space filling models from electron micrographs a) actin showing subdomains 1-4. b) actin with tropomyosin position overlayed. c) tropomyosin coiled coil [44,45]

As stated previously, evidence from X-ray crystallography, electron microscopy, FRET, and molecular modeling revealed movement of tropomyosin relative to actin [32–38]. This movement was described as an azimuthal shift of tropomyosin among three locations that differed primarily in their distance from the actin long pitch helix axis. These positions are illustrated in Figure 4. Electron microscopy data showed that addition of calcium resulted in a 25° shift of tropomyosin into the long pitch helix from its low calcium position [46]. Addition of myosin resulted in an additional 10° shift into the long pitch helix.

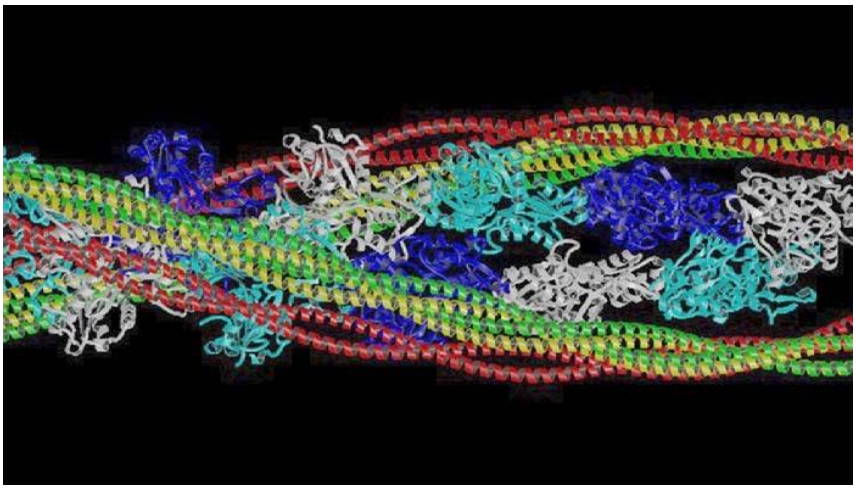

Figure 4: Ribbon Diagram computationally generated from EM data showing actin with tropomyosin in different positions depending on conditions. Red, EGTA; Yellow, Calcium; Green, Rigor (No ATP) [36]

The movement of tropomyosin among those three states is determined by calcium binding to troponin and myosin binding to actin. The troponin complex is composed of troponin C (TnC), troponin I (TnI), and troponin T (TnT) which cooperate to respond to calcium and reposition tropomyosin along actin (Figure 5). This project is primarily concerned with a specific region of troponin, the C-terminus of troponin T, and how it is involved with this process. Functional evidence from our lab suggests this region plays a role in both the normal 25° azimuthal shift of tropomyosin but also in the additional 10° shift usually only achieved with binding of myosin[47]. A high resolution structure of the thin filament[48] showed that tropomyosin is further from troponin at saturating calcium concentrations. The following text details the interactions of each troponin subunit with a focus on the interactions that may be involved with the C-terminus of troponin T and may be influencing this shift of tropomyosin.

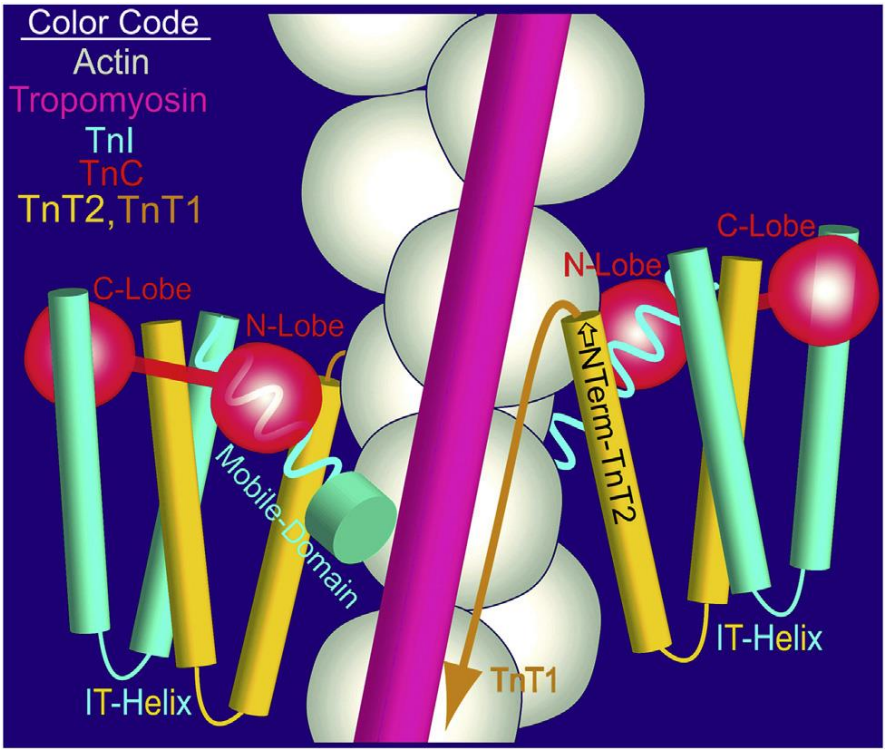

Figure 5: Diagram illustrating the position of tropomyosin and the subunits of troponin along actin [49]

Troponin I: The human cardiac isoform of the troponin subunit troponin I is made up of 210 amino acids and consists of an acidic N-terminal domain (2-32), a structural IT-arm (residues 32-136), inhibitory domain (or inhibitory region) (residues 137-148), regulatory domain (or regulatory region) (149-160) and a C-terminal domain (163-210)(Figure 6)[50].

Residues 44-80 and 91-136 makeup the H1 and H2 alpha helices respectively. Residues 67-80 of the H1 alpha helix interact with the H2 alpha helix of troponin T[51]. The H2 alpha helix of troponin I interacts with the H2 alpha helix of troponin T (residues 227-272) to form the IT-Helix. This point will be emphasized again, but it is important to note here that the IT helix is immediately adjacent to the C-terminal region of troponin T

which this project focuses on. The inhibitory region of troponin I extends from the C-terminal end of the IT-Helix and is composed of residues 138-149 [52] (or 130-149[53]). This is a very well characterized region that plays a critical role in calcium regulation and in this project. At very low calcium concentrations, the inhibitory region of troponin I interacts with a negatively charged region on actin[54] via electrostatic interaction due to its highly positive charge (greater than 50% basic amino acids). This interaction stabilizes tropomyosin in a position that inhibits actin stimulation of myosin ATPase activity.

The affinity of troponin I for troponin C is enhanced as calcium concentration is increased[55]. Little secondary structure was shown for the troponin I inhibitory region residues 138-148 at low calcium concentrations[42,56]. At higher calcium concentrations, residues 136-141 on troponin I form an alpha helix, dissociate from actin and interact with the N-terminal lobe of troponin C [53]. Residues 142-149 of troponin I do not exhibit a secondary structure at either very low or saturating calcium[52].

Adjacent to the inhibitory region, residues 151-160 of troponin I make up the H3 alpha helix (or regulatory domain or switch region) of troponin I [42]. At saturating calcium concentration, the H3 alpha helix interacts with a hydrophobic cleft that opens on the N-lobe of troponin C [57]. Movement of troponin I into the hydrophobic cleft results in dissociation of the inhibitory region of troponin I from actin and release of the mobile domain (residues 163-210) of troponin I from actin and tropomyosin[51,57]. The inhibitory domain of troponin I subsequently binds to troponin C as well.

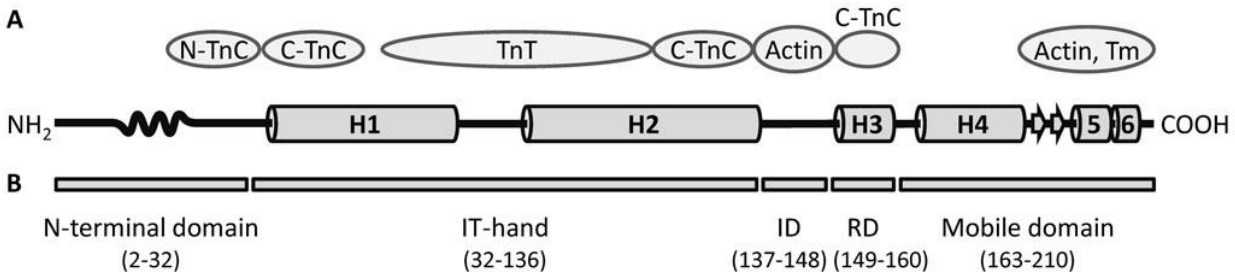

Figure 6: Schematic of Troponin I showing locations of interactions (A) and important regions (B). The inhibitory domain (ID), regulatory domain (RD) and mobile domain are calcium sensitive.

Troponin C: The human cardiac isoform of the troponin subunit troponin C is composed of 161 amino acids [58]. Troponin C is primarily divided into two globular regions, an N-lobe (residues 1-87) and a C-lobe (residues 92-161). A pair of EF hand domains is present in both the N-lobe and C-lobe of troponin C (Figure *7*). In the N-lobe of the cardiac isoform of troponin C, EF-hand 1 is defunct and does not bind metal. EF-Hand 2 in the N-lobe of troponin C is the regulatory, low-affinity, calcium binding region that upon binding calcium leads to a cascade of changes within troponin.

EF-hands 3 and 4 in the C-lobe of troponin C are high affinity and low divalent metal ion specificity. These sites are nearly always filled with either magnesium or calcium at physiological conditions[59]. The C lobe of troponin C interacts with the C-terminal of the IT coiled coil[42]. Though the C-lobe of troponin C does not participate in calcium regulation, the documented interactions of the C-lobe of troponin C with troponin T and troponin I suggests that metal (calcium or magnesium) binding to the EF-Hands in this lobe maintain these interactions. The C lobe of troponin C is therefore closely associated with the IT coiled coil regardless of physiological calcium concentration.

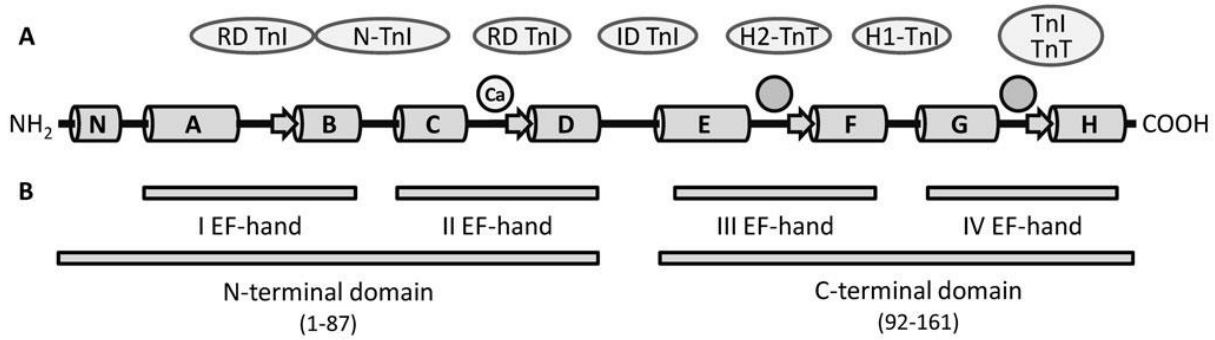

Figure 7: Schematic of Troponin C showing locations of interactions (A) and important regions (B) [43]

Binding of calcium to the regulatory EF-Hand in the N-lobe of troponin C opens a hydrophobic pocket. The H3 helix of troponin I (residues 150-159) known as the regulatory domain (or regulatory region or switch region) binds to that hydrophobic pocket in the N-lobe of troponin C upon opening (Figure 8)[60]. Binding of the regulatory region of troponin I to the troponin C hydrophobic pocket is associated with dissociation of the troponin I inhibitory region and mobile domain from actin and actin-tropomyosin respectively.

Other troponin C binding sites are thought to be made available by the calcium induced conformational changes. These new sites are thought to present alternative binding sites for the inhibitory region (residues 137-148) and mobile domain (residues 169-210) of troponin I for actin-tropomyosin[42]. These sites would reduce the affinity of troponin-actin interactions and result in interactions that position tropomyosin in a more activating position. The entire mechanism linking calcium binding to repositioning of tropomyosin however is not completely clear.

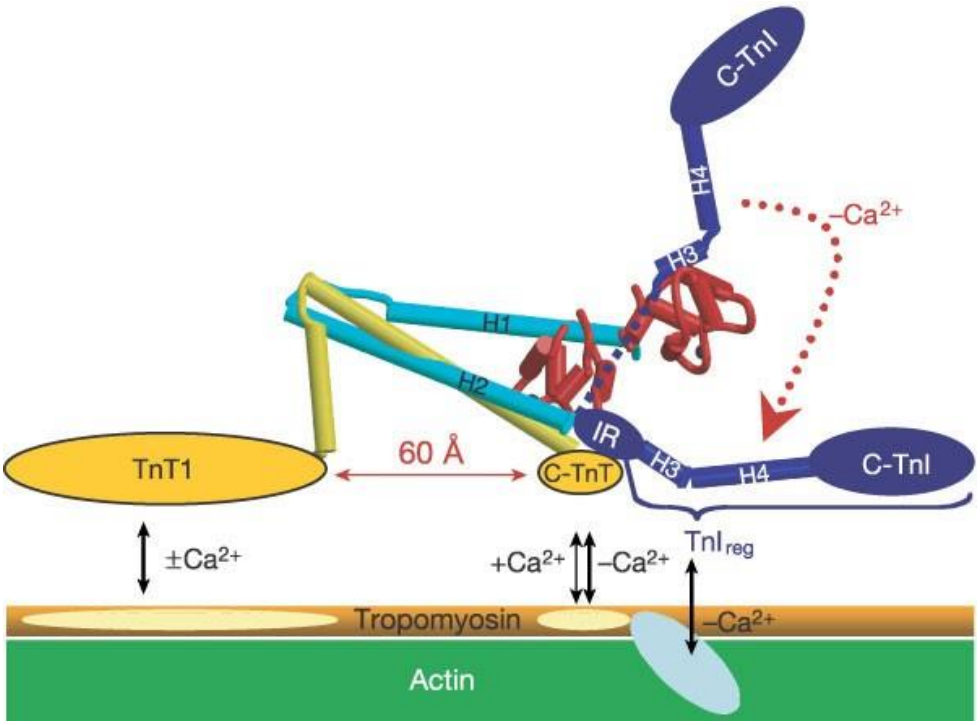

Figure 8: Schematic diagram of the core domain of troponin illustrating subunit domains and possible responses to calcium[42].TnT (yellow), TnI (blue/light blue), TnC (red), tropomyosin (orange), actin (green).

Troponin T: The most common human cardiac isoform of the troponin subunit troponin T is made up of 288 amino acids. The four cardiac isoforms cTnT1-cTnT4 are produced by alternative splicing at exons 4 and 5 [61,62] and are thought to alter thin filament calcium response. Troponin T contains an extended N-terminal region (TnT1,residues 2-68) that extends about half the length of tropomyosin [63] and a globular region (TnT2, residues 69-288) (

Figure 9).

The globular region consists of a conserved region (residues 69-200) and C-terminal region (residues 201-288). The conserved and C-terminal regions are

connected by a flexible linker made up of residues 183-200. Troponin T has two main interaction sites with tropomyosin known as T1 and T2.

The T1 region of troponin T (residues 98-136) is well defined and interacts with the tropomyosin overlap region in a calcium independent manner [43]. Evidence suggests that an alpha-helical region of troponin T interacts with tropomyosin to form a triple stranded coiled-coil with one-third of the length of the tropomyosin C-terminus[64]. Residues 204-220 of the C-terminal domain of troponin T make up the H1 alpha helix and residues 227-272 make up the H2 alpha helix[42]. troponin T residues 257-271 of the H2 alpha helix interact with the calcium binding loops within the troponin C C-terminal domain[42].

The H2 alpha helix of troponin T forms a coiled coil with the H2 alpha helix of troponin I [65] to form the IT-Helix. The last sixteen residues of the C-terminal region of troponin T (residues 273-288) are immediately adjacent to the IT-Helix. The function and structure of these last 16 residues are the central focus of this project. To avoid ambiguity, the last 16 residues of the C-terminal region of troponin T will be referred to as the **C-terminus of troponin T**.

Unfortunately, the structure of the C-terminus of troponin T has not been resolved in crystal structures of troponin. This lack of resolution indicates that the C-terminus is either a flexible, unstructured region or that it binds to actin or tropomysoin[42]. The crystal structures are limited in that they are of troponin alone in the absence of actin or tropomyosin.

The C-terminus of troponin T can be phosphorylated by RhoA associated protein kinase II on residues 275 and 284 or by protein kinase C on residue 284[66,67]. However,

analysis of affinity purified troponin T from human tissue by mass spectroscopy has shown that only serine 2 is phosphorylated physiologically[68]. This brings into question the physiological relevance of phosphorylation to the C-terminus of troponin T.

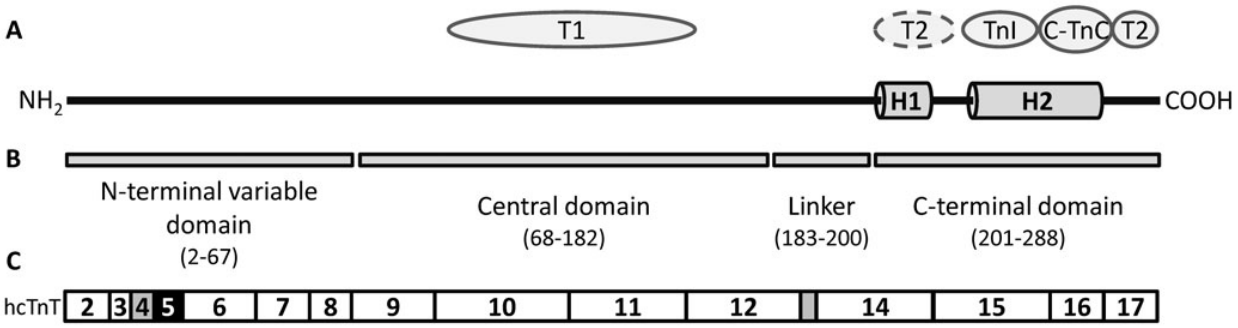

Figure 9: Schematic of Troponin T showing locations of interactions (A) and important regions (B) [43]

A focus of our work investigating the function and interactions of the C-terminus of troponin T is the spatial and sequence similarity of the C-terminus of troponin T with the well characterized inhibitory region of troponin I. Figure 10 shows an alignment of the C-terminus sequence with the inhibitory region of troponin T as they emerge from the IT-Helix. Both regions are highly positively charged. The C-terminal 16 residues of troponin T contains 7 basic residues (arginine or lysine) while the 12 residues of the troponin I inhibitory region contains 6 basic residues.

The hypertrophic cardiomyopathy associated mutation R278C of troponin T has been shown to rescue some effects of the hypertrophic cardiomyopathy associated R145G mutation[69] suggesting the actions of each region are coupled. That same group

suggests these two regions have an evolutionary relationship and came about as a result of gene duplication. This hypothesis will be expounded on later.

Figure 10: Sequence alignment of the C-terminus of TnT (pink) and the inhibitory region of TnI (blue). TnT and TnI have extensive interaction to form the IT-Helix (shown on left). Immediately adjacent to the IT-Helix is the C-terminus of TnT and the inhibitory region of TnI. The inhibitory region is more specifically defined as residues 137-148. Blue letters indicate basic amino acids. Underlined letters indicate known hypertrophic cardiomyopathy associated amino acids.

The possible interaction between the C-terminus of troponin T and tropomyosin is also a focus of our work. A second troponin T-tropomyosin interaction (T2) is present between residues within the C-terminal region of troponin T (residues 201-288) and a region near C190 of tropomyosin [70]. The residues within the C-terminal region of troponin T that are involved in this second tropomyosin interaction consists of either residues 197-239 [71] or the C-terminus (residues 272-288) [43].

Chymotryptic fragments of troponin T, residues analogous to cardiac residues 272-288, were identified as being involved in binding to tropomyosin[72]. That group used affinity chromatography and cosedimentation assays to show that the troponin T T1

fragment had an affinity for actin indistinguishable from whole troponin T. The troponin T T2 fragment (cardiac residues 188-288) had an affinity for actin 20% of that of whole troponin T. A fragment of troponin T T2 (cardiac residues 188-271) missing an additional fourteen residues from the C-terminus had an affinity for actin 10% of that of whole troponin T. Further chymotryptic truncation from the C-terminus of this fragment did not further reduce the affinity.

Another group measured the fluorescence change of an N-(1-anilinonaphth-4-yl)maleimide (ANM) probe on C190 of tropomyosin to measure the binding of troponin T[73]. A fragment consisting of residues analogous to cardiac residues 185-288 caused a fluorescence change indistinguishable from that produced with whole troponin T. A troponin T fragment containing residues analogous to cardiac residues 185-256 did not produce any appreciable fluorescence change of the ANM probe on tropomyosin. This suggested residues 257-288 of TnT were responsible for the ANM fluorescence change.

Using crosslinking of chymotryptic fragments of troponin T, residues analogous to cardiac residues 185-256 were identified as being involved in the C-terminal region interaction with tropomyosin[74]. Interestingly, the crosslinking efficiency was 1.7-fold greater at lower calcium concentrations suggesting this interaction is calcium dependent. Using monoclonal antibody competition experiments, residues analogous to cardiac troponin T residues 197-239 were identified as being involved in the C-terminal region of troponin T interaction with tropomyosin[71].

Each of these studies attempting to identify either the binding partner of the C-terminus of troponin T or the second tropomyosin binding region of troponin T have

important limitations that should be considered. Many of these studies utilize chymotryptic fragments of troponin T to resolve the specific binding region of troponin T to resolve the specific binding region to tropomyosin. The fragments used are often missing half of the total length of troponin T and are sometimes as short as 20 residues. These smaller peptides are necessary in these types of assays to attempt to resolve the binding to a narrow stretch of residues, but the effect on the overall structure should be considered. It is questionable whether those peptides fold as they would in whole troponin T and thus might interact differently outside of its native conformation.

In addition, most of these binding studies were conducted with just a single component of the regulated actin complex. These studies attempting to measure the interaction between troponin T fragments and tropomyosin for instance, only included those proteins in the absence of the other likely potential interacting proteins including, actin, troponin I, and troponin C. Similarly, these isolated systems and corresponding limitations are often necessary for the particular method, but the limitation should be considered, and we should be skeptical of the conclusions.

The second binding site of tropomyosin is believed to include or be near tropomyosin C190. Fluorescence of an ANM probe on C190 of tropomyosin[73] was measured to determine how the fluorescence changed in response to addition of fragments of troponin T. The conclusions from that experiment are limited by only considering C190 of tropomyosin as the binding site. In addition to the previous limitations described for fragments of troponin T, the ANM C190 tropomyosin experiment may be biased toward regions that bind close to that tropomyosin location.

Fragments of troponin T that bind at a location further from C190 of tropomyosin would produce less fluorescence change but may still bind tropomyosin. Additionally, many of these studies are using fragments produced from skeletal troponin. Though the C-terminus region that we are concerned with is highly conserved between skeletal and cardiac troponin T, regions upstream from the C-terminus are less conserved. Most notably, the N-terminal extension is only present in cardiac troponin T.

Fluorescence resonance energy transfer (FRET) is used for identifying regions of proteins that interact by determining the distance between two different residues. Multiple groups have used energy transfer measurements to identify the closeness of different locations between troponin subunits, actin, and tropomyosin. FRET measurements from other groups most relevant to our project are shown in Table 1.

Table 1: Selected distances measured within Actin-tropomyosin-troponin using FRET

Source	Donor	Acceptor	Ca^{2+}	Distance (Â)
[75]	TnI 151	Phalloidin	-	48±1
[75]	TnI 151	Tpm 190	-	52±1
[75]	TnI 151	Actin C374	-	45±2
[34]	TnT 275*	Actin C374	-	29.6±0.4
[76]	TnT 275*	Tpm146	-	44.1
[76]	TnT 275*	Tpm160	-	38.6
[76]	TnT 275*	Tpm174	-	36.1
[76]	TnT 275*	Tpm190	-	35.7
[77]	TnT 276	TnI 145	-	28.2
[77]	TnT 276	TnI 151	-	44.7
[77]	TnT 288	TnI 145	-	39.6
[77]	TnT 288	TnI 151	-	50.1
[34]	TnT 275*	Actin C374	+	36.6±0.2
[76]	TnT 275*	Tpm146	+	46
[76]	TnT 275*	Tpm160	+	41.8
[76]	TnT 275*	Tpm174	+	41.6
[76]	TnT 275*	Tpm190	+	41.6
[77]	TnT 276	TnI 145	+	34.3
[77]	TnT 276	TnI 151	+	53.6
[77]	TnT 288	TnI 145	+	39.5
[77]	TnT 288	TnI 151	+	51.4

*Skeletal troponin used. Skeletal 250 is most analogous to cardiac 275. Skeletal 244 is most analogous to cardiac 269

Using FRET measurements, the C-terminal residues 271-288 were shown to be unfolded in both the low calcium and saturating calcium states[77]. However, the C-terminus was more unfolded when calcium was present[77]. This suggested the region's function is calcium dependent and the region extends a greater distance at saturating calcium. Based on the evidence that the C-terminus of troponin T interacts with tropomyosin, this suggests that the C-terminus would stretch a greater distance to interact with tropomyosin at saturating calcium. This supports the evidence from the

high resolution structure[48] showing that tropomyosin is further from troponin at saturating calcium concentrations. At low calcium concentrations, tropomyosin would be held closer to troponin because the C-terminus of troponin T is in a less extended state.

The FRET between skeletal residue C250 (analogous to cardiac 279) troponin T and actin residue Q41 showed a 93% transfer efficiency at a very low calcium concentration[34]. This was the higher than any other efficiency measured between the C-terminus of troponin T and tropomyosin. The efficiency decreased (increased distance) when calcium was increased suggesting the C-terminus dissociates from that region of actin at higher calcium concentrations [34].

Additionally, the distance between troponin T C250 (cardiac 279) and C190 of tropomyosin was shown to increase at saturating calcium[34]. This suggests as described before, that the C-terminus either dissociates from tropomyosin at saturating calcium concentrations or takes on an extended conformation to span the greater distance observed between the two regions.

Identifying the functional significance of residues within the C-terminus of Troponin T

Cardiomyopathy associated mutations in troponin subunits expose the structure-function relationship of these proteins. Any structural change in troponin, tropomyosin or actin, either from mutation or post-translational modification, can result in functional changes including effects on calcium sensitivity, force generation, crossbridge cycling rate, and calcium cooperativity. One of the primary goals of many labs, ours included, is to investigate these structural “hot spots” where mutations are most detrimental to the structure and function of these proteins.

Over 100 troponin mutations associated with cardiomyopathy have been characterized in terms of their effect on calcium sensitivity, force generation, crossbridge cycling rate, and calcium cooperativity to understand how these mutations lead to disease. A summary of these investigated mutations can be found elsewhere[5,44]. Identifying the functional effects of these different regions allows us to better understand the function of different regions, regions with shared functions, and key locations for targeting with sarcomeric modulators.

The calcium sensitivity, force generation, crossbridge cycling rate, and calcium cooperativity resulting from cardiomyopathy mutations can be described in terms of their distribution between the blocked (B), closed (C) and open (O) states at very low and saturating calcium concentrations. Restoring cardiac function is not as simple as correcting just the calcium sensitivity or force generation; it is necessary to fix every aspect that is disrupted. We believe this can be done by restoring the normal actin state distribution when it is affected. We must understand how regions of troponin influence the action state distribution to identify how we might exploit those regions to restore the distribution.

Evidence from our lab shows a substantial effect of mutation within the C-terminus of troponin T on the actin state distribution. Elimination of the terminal fourteen residues of the C-terminus of troponin T eliminates the blocked state at very low calcium concentrations and stabilizes the open state at saturating calcium concentrations[78]. This apparent function is novel to our understanding of regulation by troponin and may be an ideal target for sarcomeric modulators. One major goal of this project is to identify how mutation in this region disrupts functional outcomes.

Probing the structure-function relationship of mutation in the C-terminus of Troponin T

The functional outcomes of mutations are grounded in disruption of structural relationships. In regions where structure and interactions are known, it is simpler to hypothesize and test mechanisms that describe how mutations disrupt function. The C-terminus of troponin T is absent from the crystal structure of troponin and its binding partner is unknown. This makes identifying these mechanisms difficult. We investigated the distances between the C-terminus and other thin filament locations using fluorescence resonance energy transfer (FRET) to identify possible interactions. The second major goal of this project is to identify interactions of the C-terminus of troponin T and hypothesize a mechanism for its function.

There are many FRET measurements published for distances between different actin-tropomyosin-troponin locations and those most relevant to this project are shown in Table 1. Some of those distances have been used previously to map the crystal structures of actin, tropomyosin, and troponin onto one another to generate a model of their complex. Unfortunately, those modeled complexes are missing the C-terminus of troponin T. We ultimately wish to use our acquired distances, along with those obtained in other labs, to map the location of the C-terminus of troponin T into a model of actin-tropomyosin-troponin

Chapter 2: Experimental Methods

Protein Preparation

Skeletal actin, skeletal myosin, skeletal myosin S1, bovine cardiac ether powder, bovine cardiac troponin, bovine cardiac tropomyosin, human cardiac troponin C, human cardiac troponin I, human cardiac troponin T, and reconstituted human cardiac troponin were prepared by a standard method (Appendix B: Protein Preparation and Protocols). Mutant constructs of troponin T were prepared by Dr. Bill Angus and Dr. Li Zhu. Acrylodan, pyrene, DABMI, and IAEDANS labelling was performed by standard methods with modifications where necessary to improve yield (Appendix B: Protein Preparation and Protocols). Verification of troponin and tropomyosin purity was completed using SDS PAGE gels with a molecular weight marker and by measures of myosin ATPase regulation. Protein concentrations were determined photometrically or using a Lowry assay (Appendix B: Protein Preparation and Protocols).

Actin stimulation of myosin ATPase Activity

Myosin S1 hydrolyzes ATP at a low rate in the absence of actin. Myosin ATPase activity is stimulated by interaction with actin in the O state. The myosin ATPase produces ADP and inorganic phosphate from ATP. An ATPase reaction is initiated by adding S1 to a mixture containing ^{32}P labelled ATP. This mixture might also contain actin, actin-tropomyosin, or actin-tropomyosin-troponin to measure how different combinations of proteins activate or inhibit stimulation of ATPase activity.

For our ATPase assays, the following protocol was followed unless otherwise specified: Rabbit skeletal actin and bovine cardiac tropomyosin were allowed to mix at least twelve hours. Troponin was added approximately thirty minutes before initiating the reaction to provide adequate time to bind. The Actin-tropomyosin-troponin ratio was usually 7:2:2 to ensure saturation unless specified otherwise. The reaction buffer typically contained 31 mM KCl, 10 mM MOPS pH 7, 3 mM $MgCl_2$, 0.5 mM $CaCl_2$, and 1 mM DTT. Solutions were either 1 mL or 0.5 mL final volume and prepared in 4 mL Teflon beakers. The reaction mixture was moved to a water bath set to 25 degrees C over a stir plate. 1 mM ^{32}P ATP was added and the temperature allowed to equilibrate at least two minutes. The reaction was initiated upon addition of 0.1 µM Myosin S1.

At different time points throughout the reaction, an aliquot of the reaction mixture (typically 100 µL) was removed into a disposable glass culture tube and the following steps were completed subsequently without pause: add 0.4 ml of 1.5 N HCl, 1.5 mM $NaPO_4$, 0.2 ml of 1.4 N H_2SO_4, 4.3% Silicotungstic acid, 1 mL of 1:1 isobutanol:benzene and 0.2 ml of 5% ammonium molybdate. The mixture was then vortex mixed for exactly thirty seconds. The generation and movement of free phosphate in the process is summarized in Figure 11.

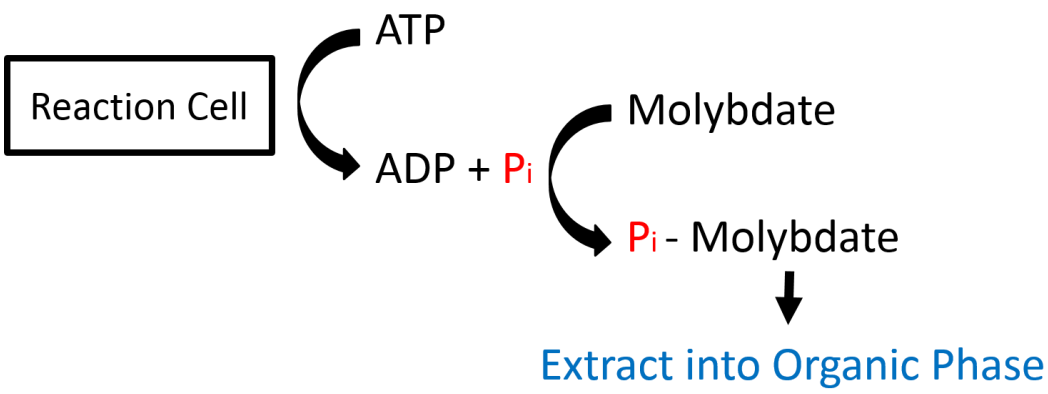

Figure 11: ATPase Experiment Scheme

The purpose of the HCl is to lower the pH and stop the reaction. The P_i in $NaPO_4$ functions to help extract the ^{32}Pi. The silicotungstic and sulfuric acid precipitate the proteins to keep them in the aqueous layer. The molybdate functions to complex with the released Pi. The butanol-benzene is present to provide an organic layer to extract and isolate the phosphomolybdate complex.

0.2 mL was typically removed from the upper organic phase of each resultant aliquot mixture and added to a scintillation vial. 5 mL of Scintiverse scintillation fluid was typically added to the scintillation vial. The extracted $^{32}P_i$ was then counted for each of the aliquots. A slope is measured from a plot of time versus $^{32}P_i$ count for each reaction (Appendix C: Supplementary Data).

A scintillation count of 1 mM $^{32}P_i$ count must be determined to normalize the data and calculate the ATPase rate. That value was typically determined by counting a 20 µL aliquot directly from a mixture following reaction completion without extracting the $^{32}P_i$ into an organic layer. The ATPase rate was calculated using equation 1

Equation 1: $$\text{ATPase Rate (per second)} = \frac{\text{slope} * 1000}{0.1\ \mu\text{M S1} * \text{Count}_{\text{infinity}}}$$

The ATPase rate is also determined each day from an experiment containing myosin S1 alone in the absence of actin. This rate is subtracted from all of the actin stimulated myosin ATPase rates to correct for ATP hydrolysis that was not the result of stimulation by actin. The fraction of actin in the open state was calculated by dividing the observed ATPase rate my the rate when actin is stabilized fully in the active state by N-ethylmaleimide modified myosin S1 or A8VΔ14 troponin[78]. That rate was determined to be approximately 6.5 times the unregulated actin rate.

Stopped Flow Kinetics

Stopped flow kinetics was used to monitor fluorescence and light scattering changes of reactions from less than two milliseconds after rapid mixing. Two solutions are loaded into syringes, then injected into cells. Upon reaction initiation, a volume within each cell is rapidly forced through a mixer then into an optically clear cubical reaction cell. Light of a specified wavelength dependent on the transition being monitored is emitted through one face of the cell. Fluorescence or light scattering are measured at a right angle to the path of the emitted light. A schematic of the stopped flow apparatus is shown in Figure 12.

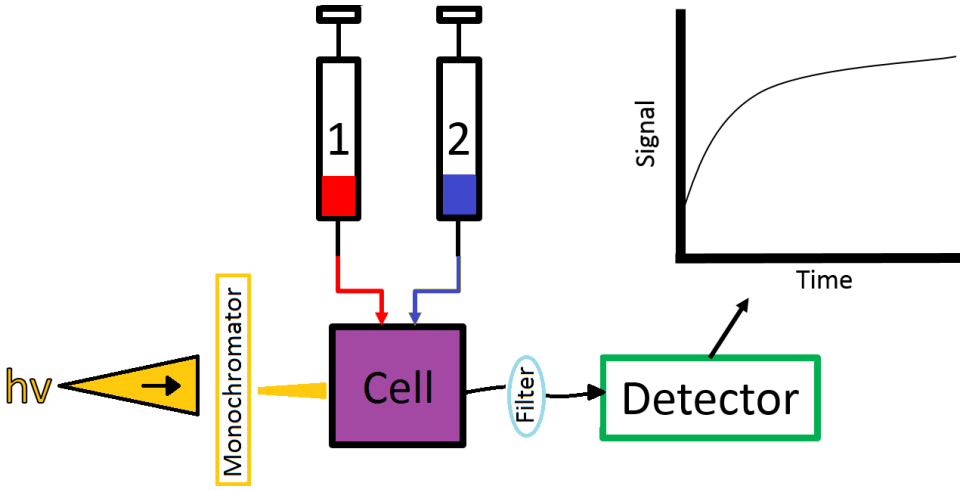

Figure 12: Schematic of stopped flow apparatus

Acrylodan ATPchase Experiment or Dissociation of Myosin S1 from Regulated actin

Rapid dissociation of myosin S1 from regulated actin by addition of ATP (ATPchase) was monitored in a stopped flow spectrometer. Actin is stabilized in the fully open (O) state by formation of myosin crossbridges in the absence of ATP. Reaction solution one contained the proteins actin, tropomyosin, troponin, and myosin S1 typically in a 7:2:2:7 molar ratio. Reaction solution two contained a 1000-fold excess of ATP over actin.

Upon mixing with ATP, myosin S1 rapidly dissociates from actin. Actin the redistributes into a mixture of the closed and blocked states depending on the regulatory proteins present. Tropomyosin was labeled with a fluorescent acrylodan probe on cysteine-190 (Figure *14*). The chemical structure of the acrylodan probe is shown in Appendix C: Supplementary Data. The solution was excited with light of 391 nm wavelength and observed through a 435/451/460 filter.

For actin filaments containing wild type troponin at very low calcium, a rapid fluorescence decrease was observed followed by a slower fluorescence increase (Figure 13). We attribute the rapid initial decrease in fluorescence to a transition from the open (O) to closed (C) state. The slower increase in fluorescence is attributed to the closed (C) to blocked (B) transition[79].

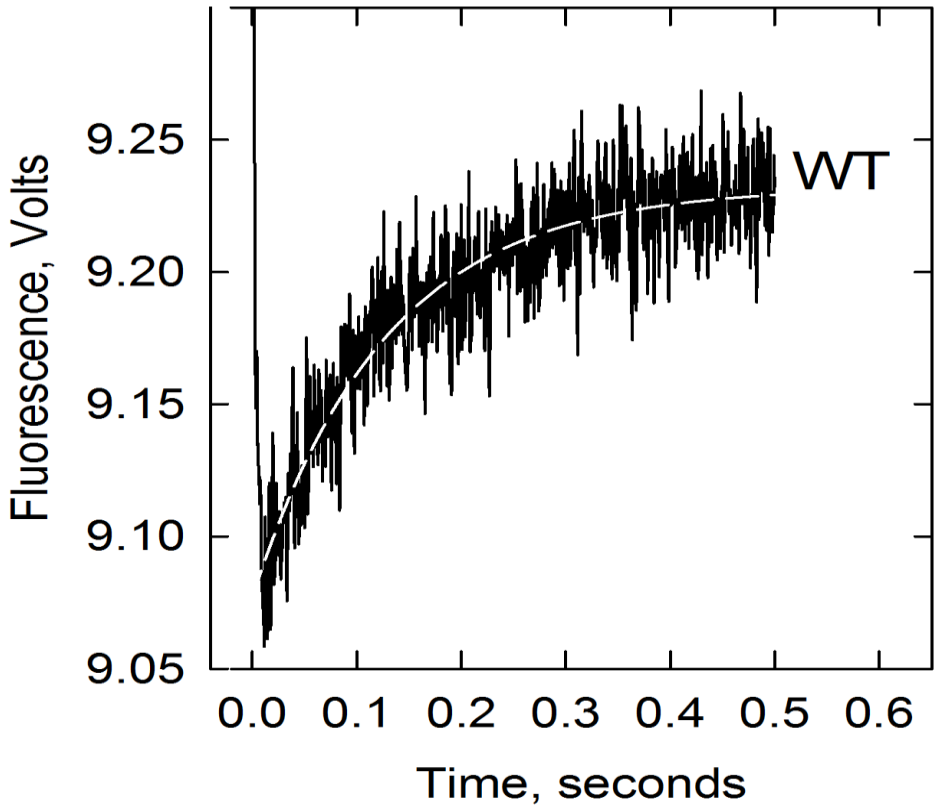

Figure 13: ATPchase experiment of actin regulated by wild type troponin. Initial decrease in fluorescence is attributed to open to closed state transition and the rate is greater than 200/second. The following increase in fluorescence is attributed to the closed to blocked transition and the rate is typically approximately 7/second.

The amplitude of the closed to blocked state transition can be divided by the amplitude of the wild type transition to produce a relative blocked state value using equation 2. The normalized amplitudes for actin regulated by troponin variants tells us how a troponin variant effects the stability of the blocked state as summarized in Table 2.

$$\text{Equation 2: Relative Blocked State} = \frac{\text{amp}_{\text{obs}}}{\text{amp}_{\text{WT}}}$$

Table 2: Mutation Effect on Blocked State

Relative Amplitude	**Blocked State**
Greater than one	Stabilized
Equal to one	Unaffected
Less than one	Destabilized
Zero	Absent

For the ATPchase experiments, rabbit skeletal actin and bovine cardiac tropomyosin were allowed to mix at least twelve hours in a typical ratio of 7:2. Solution 1 typically contained 2 µM Actin, 0.86 µM tropomyosin, 0.86 µM troponin, and 2 µM Rabbit skeletal myosin S1. Solution 2 contained 2 mM ATP. 50 mM ATP stocks were either made fresh or thawed immediately before use. The reaction buffer contained 152 mM KCl, 20 mM MOPS pH 7, 4 mM $MgCl_2$, 2 mM EGTA, and 1 mM DTT. Each solution was typically 1 mL in volume and prepared in 4 mL Teflon beakers.

The actin-tropomyosin solution was mixed with troponin on ice and typically allowed to incubate at least thirty minutes before loading into the stopped flow. After

injecting into cells, solutions were allowed to equilibrate in temperature for two minutes before mixing. Upon mixing solution 1 and 2 in equal parts in the stopped flow, the final concentrations of each protein in the reaction mixture are halved.

Myosin S1 Binding to Pyrene Actin

The rate of binding of myosin S1 to actin is dependent on the regulatory proteins bound to actin and the distribution of actin between the blocked, closed and open states. This experiment takes advantage of the different rates of binding to the different states of actin. In the S1 binding pyrene actin experiment, myosin S1 was rapidly mixed with regulated actin (Actin-tropomyosin-troponin) in a stopped flow apparatus.

Actin was fluorescently labeled with a pyrene probe on cysteine-374 (Figure 14). The chemical structure of the pyrene probe is shown in Appendix C: Supplementary Data This experiment can be performed with either actin or myosin S1 in excess to produce different types of information. The experiment with actin in excess will be described first.

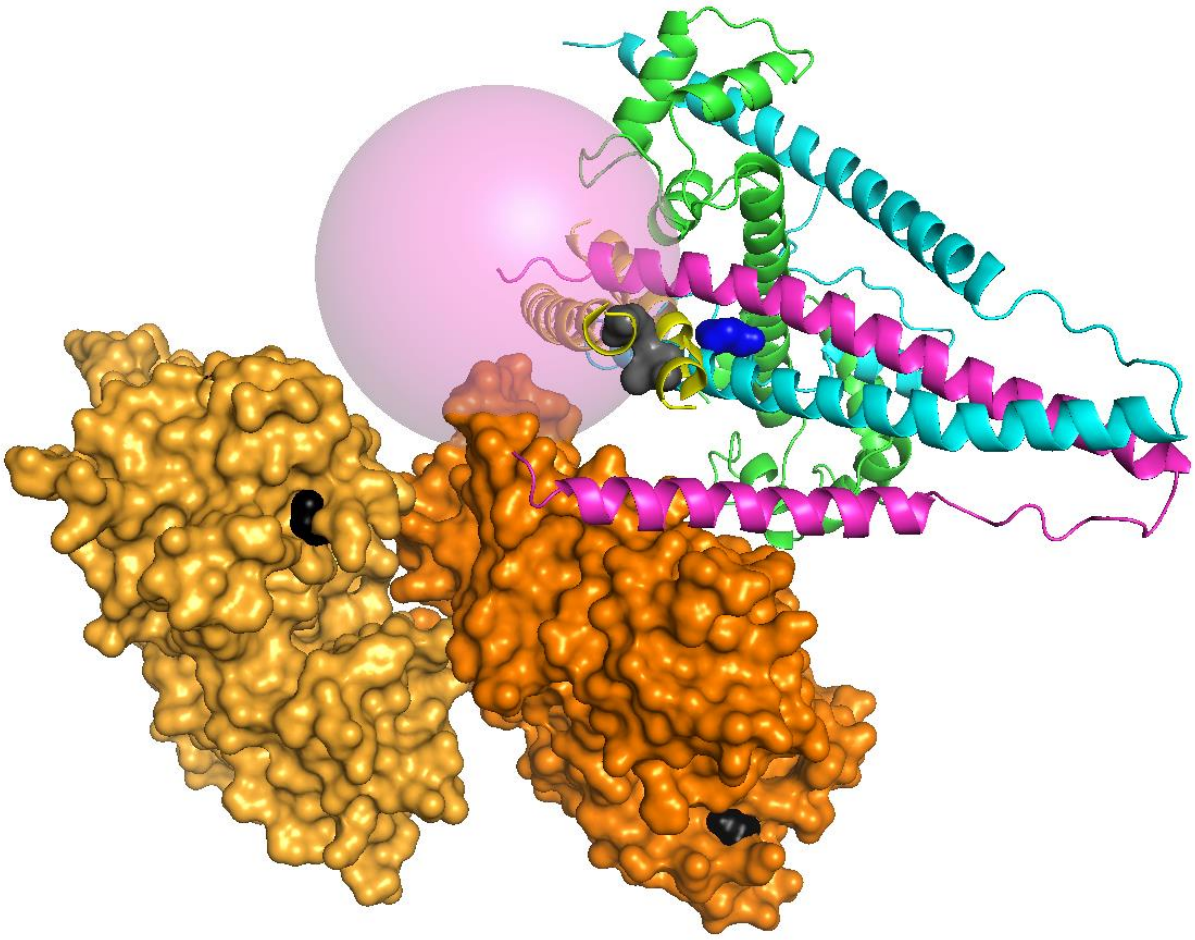

Figure 14: Structure of the Actin-tropomyosin-troponin complex as generated from molecular modelling simulations from crystal structures of actin, tropomyosin and troponin[39]. Only two monomers of actin (orange) are shown). One pseudorepeat of tropomyosin is shown (yellow). Troponin T (pink), Troponin I (Blue), Troponin C (green). The pink sphere indicates the approximate location of the C-terminus of troponin T; the last 16 residues are missing from the troponin T crystal structure. The residue colored black in actin is residue C374. The residue colored grey in tropomyosin is residue C190. The residue colored dark blue in troponin I is residue T143. Thanks to Masao Miki for structure coordinates.

Myosin S1 Binding to Pyrene Actin. Excess Actin.

Reaction solution one contained the proteins actin, tropomyosin, and troponin typically in a 7:2:2 molar ratio. Reaction solution 2 contained myosin S1 in the same buffer as solution 1. The solution was excited with either a monochromator set to 365 nm wavelength or a 360 nm LED and observed through a 370/400/475 filter. After mixing, the final concentration of myosin S1 was 10-fold lower than the actin concentration. The rate of myosin binding to actin is proportional to the distribution of regulated actin states. By combining results at both low and high calcium concentration, qualitative information regarding effects on actin state distribution can be inferred (Table 3).

Table 3: Evidence from S1 Binding Experiment on State Distribution

Relative Rate in EGTA*	**Relative Rate in Calcium***	**State Distribution**
Faster	Faster	Stabilized Open State
Slower	Slower	Stabilized Blocked State
Faster	Slower	Stabilized Closed State
Slower	Faster	Destabilized Closed State

*Relative to Wild Type Regulated Actin

This experiment is a commonly used method of calculating the actin state distribution at low calcium concentrations. From ATPase experiments at very low calcium concentrations, the open state is negligibly occupied, therefore actin is primarily distributed between the closed and blocked states. Equation 3 is used to calculate the closed state population at low calcium concentrations.

Equation 3: $$\text{Fraction C state} = \frac{K_B*(1-M)}{1+K_B}$$

M is the fraction of actin in the open (O) state as determined by ATPase experiments and is typically about 0.01. K_B is calculated from equation 4. K_{EGTA} is the rate of the fluorescence transition when the calcium concentration is very low. $K_{calcium}$ is the rate of the fluorescence transition at saturating calcium concentrations. This value is thought to be equivalent for any troponin species.

Equation 4: $$K_B = \frac{1}{\frac{k_{calcium}}{k_{EGTA}}-1}$$

With the fraction of the open (O) and closed (C) state known, the fraction in the blocked (B) state can be calculated from the conservation of mass as shown in equation 5 where C is the fraction in the C state.

Equation 5: $$\text{Fraction B state} = 1 - C - O$$

For wild type troponin regulated actin at low calcium concentrations, a decrease in fluorescence is observed upon addition of myosin S1 (Figure 15). Before addition of myosin S1 under low calcium conditions, actin is primarily in the blocked and closed states and very little actin is in the open state. It is believed that the fluorescence change corresponds to a myosin S1 binding to each state of actin. There is general

agreement that myosin S1 binds more rapidly to the closed and open states than to the blocked state.

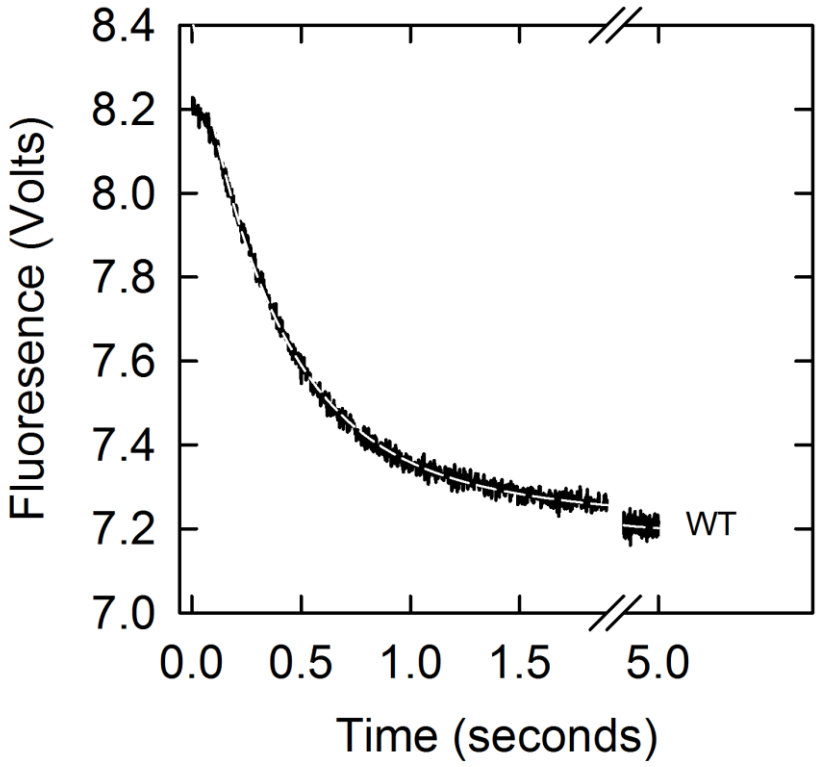

Figure 15: S1 Binding experiment using actin regulated by wild type troponin

For wild type troponin regulated actin in the presence of calcium, a faster decrease in fluorescence is observed compared to the experiment at low calcium concentrations. This is true because calcium removes troponin induced myosin ATPase inhibition and destabilizes the blocked state resulting in higher populations of the closed (C) and open (O) states to which myosin S1 more rapidly binds.

Myosin S1 Binding to Pyrene Actin. Excess Actin. Excess Myosin S1.

Measuring the rate of binding of myosin S1 to pyrene actin with S1 in excess can also be used to measure the relative blocked state distribution of actin as it maintains

pseudo first order kinetics. These traces are more complex due to the cooperative nature of myosin S1 binding when in excess. As S1 binding increases, the O state population and the rate of binding increases as well. An initial lag in the fluorescence time courses where the rate begins slower before increasing represents an initial population of actin that is in the blocked state and unavailable for myosin S1 binding[30,80].

This initial blocked state population of actin inhibiting myosin S1 binding is converted to closed or open actin by the cooperative activation by myosin S1 binding in excess[31,81]. Once in the closed or open state, myosin S1 can bind those sites. Because of the initial unavailability of binding to those blocked sites, the exponential phase following the lag is slowed. The blocked state can be measured using this method by the relative change in both the duration of the lag phase or the rate of the exponential phase that follows.

Fluorescence Resonance Energy Transfer

Fluorescence resonance energy transfer (FRET) is a measure of the transfer of energy between two light sensitive molecules. Transfer of energy can occur when the fluorescence spectra of one molecule (Donor) overlaps with the absorption spectra of another molecule (Acceptor) and when the molecules are close enough to interact. When FRET occurs, the acceptor absorbs the energy from the donor molecule and releases the energy through fluorescence at a higher wavelength or as heat. A decrease in donor fluorescence indicates that the fluorescence has been quenched by the acceptor. By attaching a FRET donor and acceptor to two known locations within a

protein or protein complexes, the closeness of those locations can be measured by quenching of the donor fluorescence. The absolute distance between the donor and the acceptor probe is a function of the efficiency. The absolute distance can also be calculated by also obtaining the quantum yield, overlap integral, dipole orientation factor, and refractive index.

We attached FRET pairs between different locations within the actin-tropomyosin-troponin complex to identify the closeness of different regions. For each FRET pair, the experiment was performed at very low and at saturating calcium concentrations to measure if the regions distances were dependent on the calcium concentration. For each experiment, two solutions are prepared; one solution contains both the donor and acceptor probe, whereas the other contains only the donor probe. This is necessary to determine to what extent the acceptor (DABMI) can quench the donor (IAEDANS) fluorescence.

In the FRET experiments, solutions containing actin-tropomyosin and troponin were mixed in the dark. Actin-tropomyosin were mixed at least 12 hours prior to mixing with troponin for experiment use. Phalloidin was additionally added to stabilize the actin before or along with mixing with tropomyosin.

The FRET experiments contained 2 μM skeletal actin, 0.51 μM bovine cardiac tropomyosin, 0.29 μM troponin. The troponin concentration was chosen for stoichiometric binding to actin. The donor probe is on troponin in each FRET experiment and any excess troponin that is not bound to actin cannot be quenched by the acceptor probe. The tropomyosin concentration was chosen as a titration with DABMI tropomyosin produced maximal quenching at that concentration (Appendix C:

Supplementary Data). The very low calcium concentration solutions were prepared with 2 mM EGTA and no added calcium. The saturating calcium solutions were prepared by adding 0.1 mM $CaCl_2$.

After mixing with troponin, the solutions were given 30 minutes to mix on ice. During this time, the Fluoromax-4 Spectrofluorometer cells were ensured to be clean and the spectrofluorometer was turned on if necessary and temperature of the water bath was ensured to be at 25° C. After this time, the mixed solution to be measured was removed from ice and placed in a water bath at room temperature in the dark for ten minutes. This was done to prevent condensation when added to the spectrofluorometer cells. The solutions were added to the cells and another ten minutes were allowed to pass before taking measurements.

The donor IAEDANS is excited at 336 nm and the fluorescence is measured from 360 to 640 nm. The acceptor DABMI is nonfluorescent and can absorb energy from IAEDANS fluorescence but does not itself fluoresce. Each plot of fluorescence versus wavelength for the IAEDANS-DABMI pair was integrated to obtain the area under each plot. The efficiency was calculated from these integrated values. The exact protocol for taking measurements can be found in Appendix B: Protein Preparation and Protocols.

A representative plot of the raw FRET data is shown in Figure 16. The top panel shows a plot of the fluorescence versus emission wavelength for either donor alone (D) or donor with acceptor (DA). The acceptor used in our experiments is nonfluorescent and quenches the donor fluorescence when nearby. As a result, the plot DA has diminished fluorescence as it has quenched some of the fluorescence from plot D. The area under each of these plots is determined by integrating (after subtracting the

baseline if necessary). This integration process is detailed in Appendix B: Protein Preparation and Protocols.

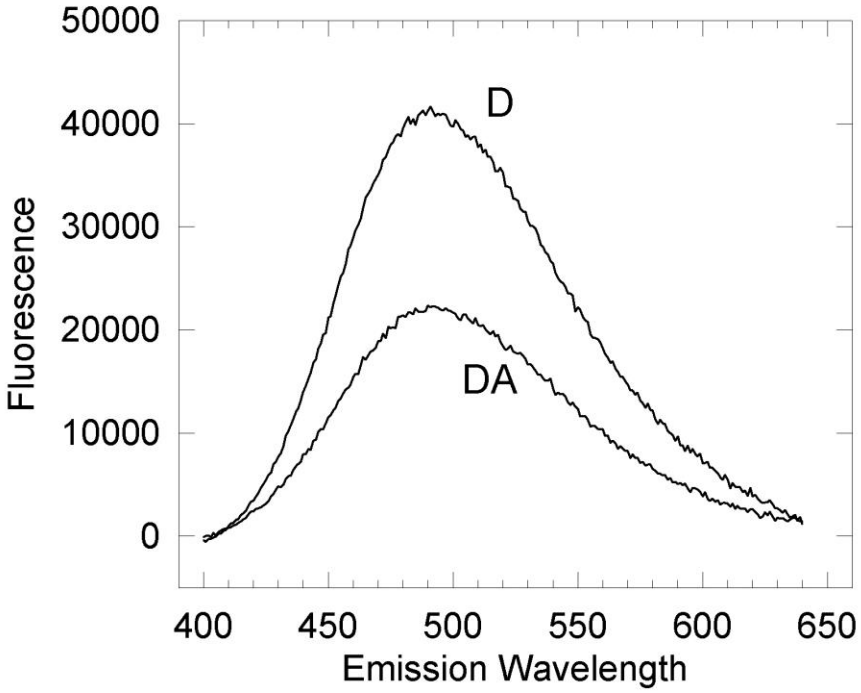

Figure 16: Representative FRET data. D indicates donor in the absence of acceptor probe. DA indicates presence of both donor and acceptor

The efficiency of transfer is a function of these integrated values and the labeling percentage of the acceptor probe. The efficiency is calculated according to Equation 6 where DA is the integrated value when the acceptor probe is present and D is the integrated value in the absence of acceptor. The process of determining the distance from these efficiency measurements is described in Appendix B: Protein Preparation and Protocols.

Equation 6: $\text{Efficiency} = \left(1 - \frac{\text{DA}}{\text{D}}\right) * \left(\frac{1}{\text{acceptor labelling percentage}}\right)$

Chapter 3 Residues within the C-terminus of Troponin T stabilize inactive B state and destabilize active O state

Part 1: Identification of the residues within the C- terminus of troponin T that are responsible for formation of the blocked (B) state at low Ca^{2+}.

Deletion of the fourteen C-terminal residues of Troponin T significantly reduces or eliminates the blocked state of actin at very low calcium concentrations. This has been demonstrated by our lab using three different methods[78,82]. In measures of ATPase activity, actin regulated by Δ14 troponin T at very low calcium concentrations produces an ATPase rate higher than that of wild type regulated actin[83]. Since ATPase activity only occurs when actin is in the active O state, this result suggests that Δ14 troponin T causes a redistribution of actin from the inactive B state to C state. The equilibrium between the C and O states results in an increase in the O state.

In measures of equilibrium binding, wild type troponin regulated actin initially has a low affinity for myosin S1. Cooperative binding of myosin S1 converts binding sites from low affinity to high affinity sites. Those low affinity sites are absent with Δ14 troponin T regulated actin[82]. Myosin S1 binds with a high affinity without requiring cooperative binding. This suggests the blocked state is diminished or eliminated by Δ14 troponin T.

Reduction or elimination of the blocked state by Δ14 troponin T was shown by an independent method developed in our lab. This method measures the relative occupancy of the blocked state through a fluorescence change in an acrylodan probe

on tropomyosin. Acrylodan tropomyosin bound to wild type troponin regulated actin produces a fluorescence change indicative of a closed to blocked state transition upon myosin S1 dissociation by ATP. For actin filaments regulated by Δ14 troponin T, this acrylodan tropomyosin fluorescence change is absent indicating that transition into the blocked state is reduced or absent[79,83].

Reduction or elimination of the blocked state by Δ14 troponin T was also shown by a commonly used method of measuring the fluorescence change of a pyrene probe on actin[78]. This probe is thought to decrease in fluorescence when myosin S1 binds to the closed or open states. Myosin S1 is believed to bind to the closed and open states more rapidly than to the blocked state. Using this method, we showed that Δ14 troponin T produced a higher rate of binding indicating a diminished blocked state population.

The fourteen C-terminal residues of troponin T are highly conserved across isoforms and species. The high conservation along with the results from analysis of Δ14 troponin T made clear the significance of this region. Our next question was, which of those residues are responsible for this effect and why? To help answer this question, we developed a series of truncation mutants missing varying numbers of residues from the C-terminus of troponin T. These included Δ4, Δ6, Δ8 and Δ10 troponin T. The idea behind the generation of this series of mutants was to measure how each affected the state distribution of actin. By comparing the relative change between successive truncation length, we would be able to resolve the specific residues within the C-terminus of troponin T that are important for its function. Some of this work was presented previously[44]. Since then, we have exhaustively confirmed that work by completing additional trials of those experiments with the new protein preparations,

performing those analysis with the remainder of our truncation series, and performing additional assays with the entire truncation series. Our updated progress is presented below, beginning with the truncation series effect on the blocked state of actin.

We performed three independent assays of blocked state accessibility by actin regulated by wild type troponin and each of our five truncation mutants, Δ4, Δ6, Δ8, Δ10 and Δ14 troponin T. It should be noted here, that any time troponin is present in an experiment, it is assumed that tropomyosin is also present. At equilibrium, stoichiometric binding of myosin S1 to actin stabilizes actin nearly 100% in the active O state. Rapid addition of excess ATP causes the myosin S1 to bind ATP and rapidly dissociate from actin. At very low calcium concentrations, the active O state is rapidly depopulated and actin redistributes between a mixture of the closed and blocked state. Two fluorescence changes can be resolved for wild type troponin regulated actin following this dissociation of myosin S1 at the concentrations and conditions of our assay.

The rapid initial decrease in fluorescence is attributed to transition of actin from the active O state to the closed C state[79]. This fluorescence change occurs with a rate >100/sec but slower than the change in light scattering upon S1 dissociation. For wild type troponin regulated actin at very low calcium concentrations, a subsequent increase in fluorescence is observed. We attribute this change in fluorescence to a transition from the closed C state to the blocked B state. The observation that this increase in fluorescence is absent at saturating calcium concentrations further supports this transition is a direct observation of entry into the blocked state. It was previously

observed that ∆14 troponin T similarly eliminated this florescence increase corresponding to reduction or elimination of the blocked B state[47]

Figure 17 shows the results of our analysis of the truncation series effect on the entry of actin into the blocked B state. Figure 17A shows the time course of acrylodan tropomyosin fluorescence for actin regulated by WT (1), Δ10 (2) and Δ14 (3) troponin T. As we've shown previously, WT (1) exhibits a fluorescence increase whereas for Δ14 (3) regulated actin, the transition is absent. Interestingly, for Δ10 (2) regulated actin, the transition can still be observed, but the magnitude of the change is diminished. We attribute this decrease in the magnitude of the fluorescence change to a decrease in redistribution of actin into the blocked B state.

Figure 17B shows a plot of the magnitude of each of the troponin T truncations relative to the magnitude observed with wild type troponin regulated actin. Each successive truncation results in successive decrease in magnitude of that fluorescence change, all of which produce a fluorescence change amplitude that is statistically lower than that produced with wild type troponin regulated actin.

There was insignificant change in the apparent rate constant for the transition from the C state to the B state ($k_7 + k_8$) between WT troponin and each of the truncations Δ4-10 troponin T. As the transition is absent for ∆14 troponin T regulated acting, no rate could be measured. The most significant effect on the amplitude was observed upon elimination of the first four residues from the C-terminus. Elimination of those four residues eliminated approximately half of the B state population accessed by wild type troponin regulated actin. Though those terminal four residues appear particularly important, we conclude from this assay that most or all of the residues within

the terminal fourteen C-terminal residues of troponin T are to some extent important in maintaining the blocked B state.

One limitation of this assay is that it only produces a measure of the blocked state relative to the wild type standard. At the moment, there is not an agreement on the fraction of wild type troponin in the blocked state at low calcium concentrations. By using a standard value of the blocked state population of wild type troponin at low calcium concentrations, the absolute B state population can be calculated. An external assay must be trusted to convert that relative blocked state population into an absolute population value. One method of obtaining a standard value for the blocked state as well as its limitations will be described later.

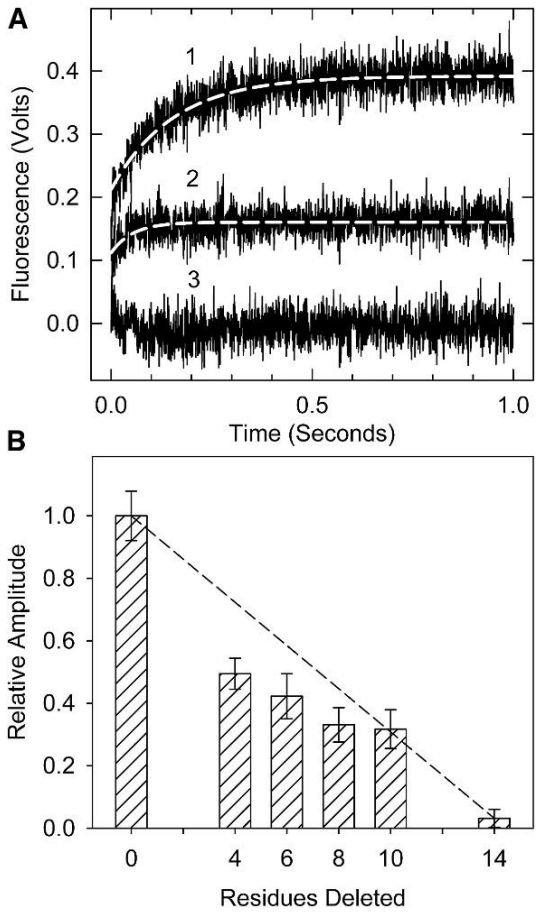

Figure 17: Formation of the inactive B state seen by acrylodan-tropomyosin fluorescence. A. Time courses of acrylodan fluorescence changes for actin regulated by wild type (1), ∆10 (2) and ∆14 troponin T (3) following the rapid detachment of myosin S1 in the absence of Ca^{2+} at 10 °C. Traces shown are averages of at least three different measurements. B. Relative fluorescence amplitude for actin filaments containing wild type and truncated troponin T. The associated apparent rate constants were, 6.8, 6.9, 6.5, 7.4, 6.1 per sec for the wild type through ∆10 mutants, respectively. No rate constant could be determined for Δ14. At 10°C, 2 µM actin, 0.86 µM tropomyosin, 1.4 µM troponin and 2 µM S1 in 20 mM MOPS, 152 mM KCl, 4 mM $MgCl_2$, 1 mM dithiothreitol and 2 mM EGTA was rapidly mixed with 2 mM ATP, 20 mM MOPS, 152 mM KCl, 8 mM $MgCl_2$, 1 mM dithiothreitol and 2 mM EGTA. Acrylodan was excited using a monochromator at 391 nm and 0.5mm slit width. The fluorescence was monitored through a 435/451/460 filter.

Myosin S1 binds to regulated actin at a faster rate at saturating calcium than at very low calcium concentrations. From this we can conclude there is a difference in the rate of binding between the states of actin [30,84]. A pyrene probe on actin is used to measure this difference in binding as it is believed to only exhibit a fluorescence change when myosin S1 binds to the closed or open states[30]. Though we will present new evidence concerning the rates of binding to each actin state later, it is generally accepted that myosin S1 binds the C and O states more rapidly than to the B state. The rate of fluorescence change of pyrene actin in pseudo-first order conditions with either S1 or actin in excess presents two means of measuring the relative blocked state distribution.

Figure 18A shows the time course of myosin S1 binding to excess pyrene actin regulated by tropomyosin and either WT (1), Δ10 (2), or Δ14 troponin T troponin at very low calcium concentrations. Because the fluorescence change only occurs for S1 binding to the C or O states and the O state is population is negligible at low calcium concentrations, the fluorescence change is essentially a measure of S1 binding to the C state. A slower rate corresponds to a greater B state population. Figure *18*B shows the rates of the fluorescence transition for each of the truncation mutants. Stepwise truncation from the C-terminus resulted in a graded elimination of the blocked state where the relative loss of blocked state corresponded with the number of residues removed. As in the results from the acrylodan experiment above, the first four residues from the C-terminus appear disproportionately important to maintaining the blocked state than the other 10 C-terminal residues. Removal of those four residues (GRWK) resulted in a rate halfway between the rates for wild type and Δ14 troponin T regulated

pyrene actin. All of the fourteen C-terminal residues however appear necessary for maintaining the blocked state.

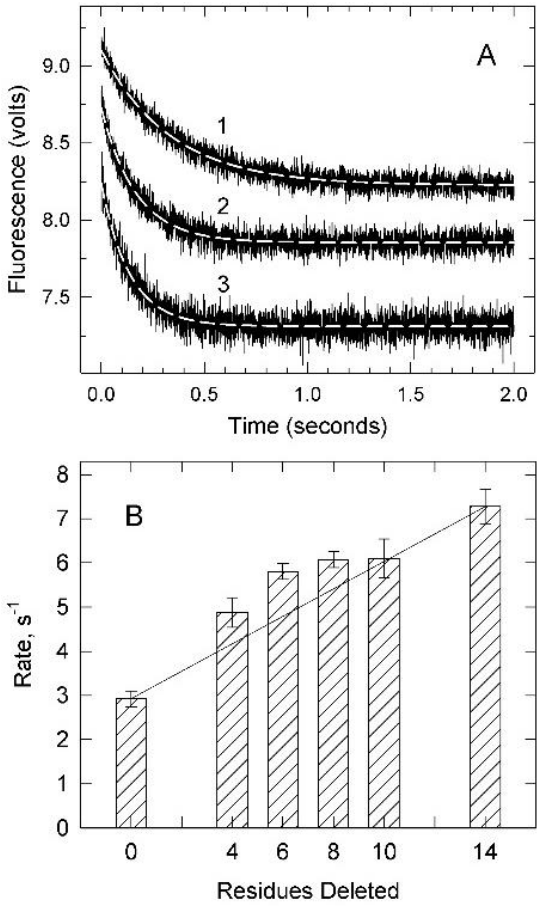

Figure 18: Binding of S1 to an excess of pyrene labeled actin filaments containing tropomyosin and troponin in the absence of ATP at a very low Ca^{2+} concentration. A. Averaged time courses of binding to actin-tropomyosin containing wild type (1); Δ6 (2); and Δ14 (3) troponin T. Dashed lines are single exponential fits. B. Observed rate of binding of S1 to actin-tropomyosin containing troponin with different mutants of troponin T. Error bars shown are standard deviation for at least 5 experiments. At 25°C, 4 μM pyrene-actin (40% labeled), 0.86 μM tropomyosin and 0.86 μM troponin was rapidly mixed with 0.4 μM myosin S1 in 20 mM MOPS, 152 mM KCl, 4 mM $MgCl_2$, 1 mM dithiothreitol and 2 mM EGTA. Pyrene was excited using a monochromator at 365nm with 0.5 mm slit width. The fluorescence was monitored through a 400nm midpoint long pass filter.

Figure 19A shows the time courses for the binding of excess myosin S1 to pyrene actin regulated by wild type (1) or Δ14 troponin T (2). For each truncation, a double exponential was fit to the more rapid phase following the lag. The second phase of that double exponential was the same for each mutant. A higher rate indicates a lower initial population of the blocked state.

Figure 19B plots the duration of the lags for wild type troponin and the truncation mutants Δ4, Δ6 and Δ14. A double exponential was used to resolve the slower initial (lag) phase from the more rapid phase. The time at which the first exponential ends was recorded as the lag time. Successive truncation results in a corresponding reduction in the lag time indicating a decrease in the initial blocked state distribution. A double exponential fit could not resolve multiple phases for actin regulated by Δ14 troponin T Tn indicating that no lag phase or blocked state could be resolved. Each truncation had a statistically lower lag time than wild type troponin.

Figure 19C plots the rate of the first exponential in that double exponential fit corresponding to the rate of transition following the lag phase. A stepwise effect is observed where successive truncation results in a corresponding increase in the rate of the exponential fit indicating a greater initial accessibility of closed and open actin sites for myosin S1 to bind. Each truncation had a statistically higher rate than wild type troponin.

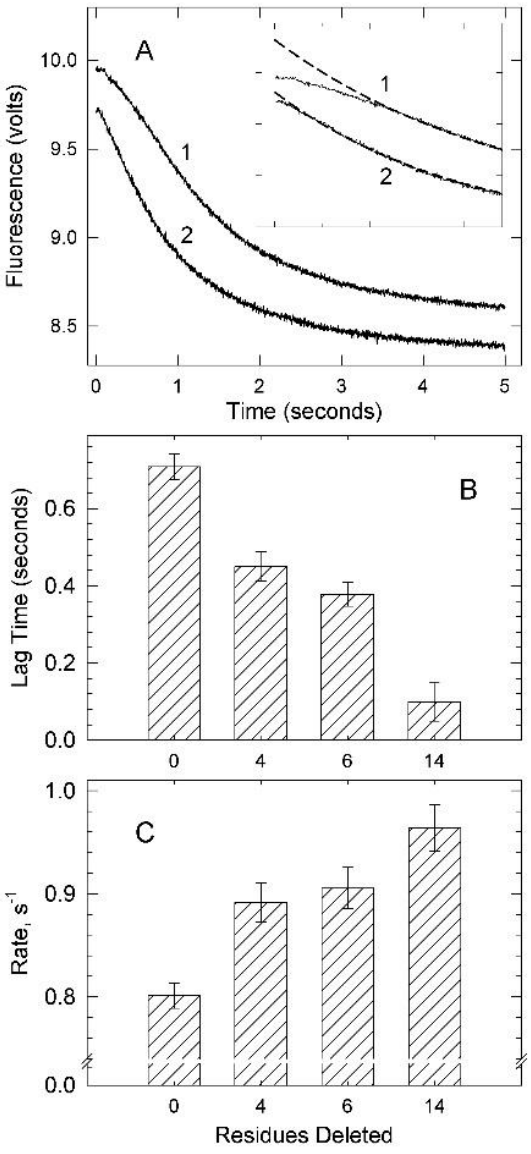

Figure 19: Binding of excess S1 to pyrene labeled actin filaments containing tropomyosin and troponin in the absence of ATP at very low Ca^{2+}. A. Averages of ≥ 5 time courses of S1 binding to actin filaments containing troponin with wild type troponin T, curve 1 or Δ14 troponin T, curve 2. Dashed lines are double exponential fits. B) Lag time preceding the exponential phase against troponin type. C) Apparent rate constants for the major rapid exponential phase of binding against troponin variant. Error bars shown are standard deviation. Conditions: At 25°C, 0.2 μM pyrene-actin (40% labeled), 0.086 μM tropomyosin and 0.086 μM troponin was rapidly mixed with 2 μM myosin S1 in a buffer containing 152 mM KCl, 20 mM MOPS buffer pH 7, 4 mM $MgCl_2$, 1 mM dithiothreitol and 2 mM EGTA. Pyrene was excited using a monochromator at 365 nm with 0.5mm slit width. The fluorescence was monitored through a 400 nm midpoint long pass filter.

As described and shown previously (Figure 18), binding of myosin S1 to excess pyrene actin allows us to identify the relative effect of troponin mutants on the blocked state distribution at very low calcium concentrations. What was not described previously is that these measurements are commonly used to calculate the absolute distribution of actin across all three states (Equations 5-7). This technique relies on the assumption that myosin S1 binds at an equal rate to either the closed or open O state. Since the blocked state is absent at saturating calcium concentrations, measuring the rate of binding at saturating calcium is thought to be a direct measure of the rate of binding to the closed and open states. As such, regardless of the troponin species regulating actin, this rate should be equal since in the absence of blocked state, the total combined population of closed and open states is maintained. With this standard value of the rate of binding to the closed and open state $k_{calcium}$, equation 5-7 is used to calculate the state distribution at very low calcium concentrations. Our experiments attempting to use this method produced an unexpected result.

We repeated the experiment shown in Figure 19 under the same conditions except the calcium was saturating. Figure 20A shows the time course of the fluorescence change for WT (1), Δ8 (2), and Δ14 (3) regulated pyrene actin. As stated, this commonly used method of calculating the actin state distribution relies on the rate at saturating calcium concentrations being unaffected by different troponin mutants. Upon fitting these time courses with a single exponential, we found that the rates of binding increased as the number of residues in the C-terminus of troponin T was reduced and as the population of the open state increased relative to the closed state. Figure 20B shows the measured rates of the fluorescence transition for pyrene actin

regulated by each truncation mutant at saturating calcium. Because Equation 6 assumed that the rate of binding to the closed and open states are equal, this equation is invalid. The implications of this finding will be discussed in Chapter 5.

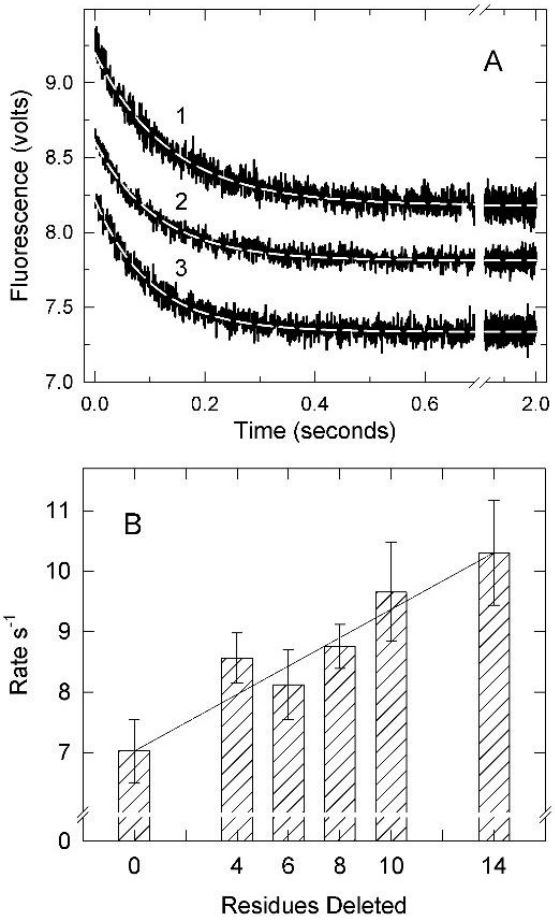

Figure 20: Rate of binding of S1 to an excess of pyrene labeled actin filaments containing tropomyosin and troponin in the absence of ATP at a very saturating Ca^{2+} concentration. Plots are averages of at least five time courses of binding to actin-tropomyosin containing wild type (1), Δ8 (2), and Δ14 troponin T (3). Dashed lines are single exponential fits of the data. At 25°C, 4 μM pyrene-actin (40% labeled), 0.86 μM tropomyosin and 0.86 μM troponin was rapidly mixed with 0.4 μM myosin S1 in 20 mM MOPS, 152 mM KCl, 4 mM $MgCl_2$, 1 mM dithiothreitol and 0.1 mM $CaCl_2$. Pyrene was excited using a monochromator at 365nm with 0.5mm slit width. The fluorescence was monitored through a 400 nm midpoint long pass filter.

Part 2: Identification of the residues within the C- terminus of troponin T that are responsible for inhibiting formation of the open (O) state at saturating Ca2+

A key observation in our studies is the dual effect of mutation in the C-terminus of troponin T on the actin state distribution. The Δ14 troponin T mutant was shown previously to affect the blocked-closed state distribution at low calcium concentrations and also the closed-open state distribution at saturating calcium. To identify the residues within this C-terminus that are most important for stabilizing the open state at saturating calcium, ATPase measurements of actin-myosin were made with a series of troponin T truncation mutants. Because actin only stimulates ATPase activity in the open O state, the rate of ATPase activity is a direct measure of the O state. The ability to measure this state directly is of crucial importance to our studies and this technique will be reviewed here.

The ATPase rate was measured for actin regulated by wild type troponin and each of the truncation mutants Δ4, Δ6, Δ8, Δ10, or Δ14 troponin T. These data were collected across multiple actin, tropomyosin, troponin and myosin S1 preparations as well as with different batches of 32P ATP and reagents.

Figure 20 is a plot of corrected rates for wild type troponin and each truncation mutant. The average from all wild type troponin experiments was found to be 2.4/sec. Each truncation produced a statistically higher ATPase rate than wild type troponin. As well, Δ14 produced a rate that was significantly higher than WT, Δ4, Δ6 and Δ8 troponin T troponin. Though there is no statistical difference between Δ4, Δ6, and Δ10, the general trend is that as residues are removed from the C-terminus, the ATPase rate is increased. The solid straight line connecting the rate for wild type and Δ14 troponin indicates the rate that would be obtained if each residue within the C-terminus

contributed equally to maintaining the active O state. As can be seen, each residue does not contribute in this way and instead some residues appear disproportionately more important. The greatest differences occur between WT and Δ4 and between Δ10 and Δ14.

To calculate the O state from these rates, we must know the rate of myosin ATPase activity in the presence of actin fully stabilized in the active O state under the same condition. This value is typically measured by stabilizing actin fully in the O state with binding of a small amount of NEM S1. Our lab has shown that this rate can also be obtained in the absence of activating myosin species using the troponin construct A8VΔ14 Troponin[78]. This was a very important observation and the significance of this finding will be discussed later in the context of the data presented in this dissertation. That rate was found previously to be 6.5* the rate of unregulated actin (Baxley 2017). If we know the ATPase rate produced under the same conditions by actin stabilized fully in the active O state (V_{max}), the O state population for any actin-tropomyosin-troponin mixture can be calculated by normalizing to that rate (equation 10). These calculated O state populations are plotted in Table 3.

Equation 10:

Fraction O state =

Corrected ATPase Rate / (6.5 * unregulated actin ATPase rate)

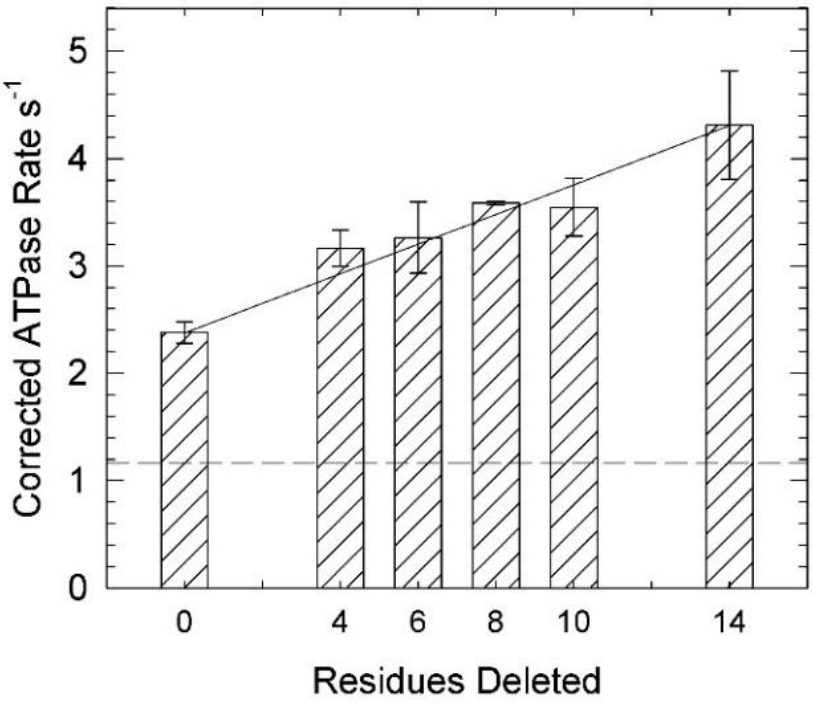

Figure 21: ATPase rates of myosin S1 in the presence of actin and actin-tropomyosin containing troponin with different mutants of troponin T at saturating Ca^{2+}. Measurements were made at 25° C and pH 7.0 in solutions containing 1 mM ATP, 3 mM $MgCl_2$, 34 mM KCl, 10 mM MOPS, 1 mM dithiothreitol and 0.1 mM $CaCl_2$. The concentrations of S1, actin, tropomyosin, and troponin were 0.1, 10, 2.2, and 2.2 µM, respectively. The average rate for wild type regulated actin over all experiments was 2.4 /sec (+/- 0.1). Corrected rate = average of all wild type experiments*(measured mutant rate / measured wild type rate). Error bars are standard deviation.

Table 4: Fraction of actin in the O state for actin filaments at saturating Ca^{2+} and containing various mutants of TnT.

TnT mutant	F_O[a]
wild type	0.34
Δ4	0.45
Δ6	0.46
Δ8	0.5
Δ10	0.5
Δ14	0.62

[a]O state = (ATPase rate) / (6.5* Unregulated actin ATPase rate)

Part 3: HAHA troponin T and ∆14 troponin T exhibit similar functional properties as at very low Ca^{2+} concentration

Our truncation study revealed that: 1) the entire C-terminus was required to maintain the Blocked state and 2) removal of the entire C-terminus is required for the full activating effect. We had previously entertained the idea that the basic residues within this region (6 of last fourteen and 7 of last 16 residues) are responsible for this regions function. The truncation study affected the state distribution of the blocked and open states in a graded manner. Truncation from the C-terminus loosely corresponded with removal of those basic residues. Importantly, ∆4 troponin T troponin, which removed two basic residues, produced a marked effect in each of our assays.

We generated a new troponin construct where the seven basic residues within the terminal sixteen residues of the C-terminus of troponin T were substituted with the neutral amino acid alanine. As the goal of this mutant was to develop a high activity construct and since the mutant contained an abundance of alanine substitutions, we named this mutant high alanine high activity troponin T (HAHA troponin T) (Figure 22). Mass spectrometry was used to verify the amino acid sequence of the purified protein (Appendix C: Supplementary Data).

Additionally, we constructed and analyzed a 289C and S275C troponin T mutant that retains the basic amino acids but has an additional Cysteine attached to the C-terminus and a serine substituted to cysteine at residue 275 respectively. 289C troponin T was designed as a control for HAHA 289C to demonstrate that terminal cysteine did not appreciably affect function. Both 289C and 275C troponin T were designed with the idea of targeting with fluorescent probes.

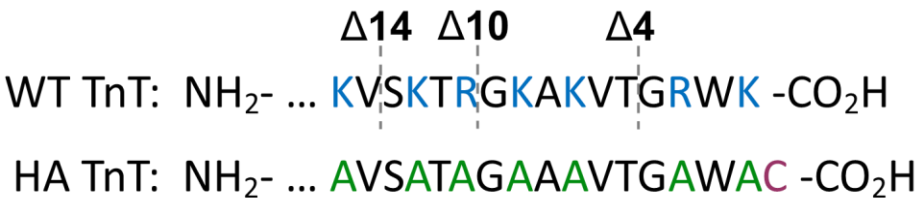

Figure 22: Amino acid sequence of the C-terminus of wild type and HAHA troponin T. The Δ4, Δ10, and Δ14 notations and corresponding dotted lines indicated the position at which the C-terminus was truncated for the different mutants. The residues indicate in blue are the seven basic residues within the terminal sixteen residues. The residues indicated in green are the alanine residues that were substituted in place of the basic residues. Note the additional C-terminal cysteine on HAHA TnT which was used for the attachment of fluorescent probes.

This construct was developed for three major reasons. Firstly, in order to identify how removal of those basic residues affected the state distribution of actin. Secondly, to develop a full-length mutant for potential use in fiber studies. Thirdly, to utilize the full-length open-state stabilizing mutant in fluorescence assays.

The HAHA troponin T construct was analyzed by the methods used previously to characterize the truncation series. The acrylodan tropomyosin assay was used to measure the relative blocked state distribution. Figure 23 shows the time course of the fluorescence change of acrylodan tropomyosin upon rapid dissociation of myosin S1 by ATP. Actin rapidly transitions out of the open O state and redistributes into the closed and blocked states. The closed state produces a low fluorescence whereas the blocked state produces a high fluorescence.

In Figure 23, Curves A and B are for wild type troponin and 289C troponin respectively. The 289C mutant produces an amplitude of the closed to blocked

transition that is equivalent to that produced by wild type troponin regulated actin. We also completed this experiment with 275C troponin T (Appendix C: Supplementary Data). Both experiments with 275C and 289C demonstrated that an addition or modification to cysteine within the C-terminus of troponin T could be made without disrupting the blocked state distribution.

The HAHA troponin T construct however, appears to eliminate that fluorescence change from the closed state to the blocked state. This corresponds to an elimination of the blocked state by the HAHA troponin T construct. Since we showed the terminal cysteine present in this construct did not produce any change to the blocked state relative to wild type troponin, we can attribute this loss of blocked state to the elimination of the basic residues within this region. As was described previously and will be expanded on in chapter 5, this assay only gives a relative blocked state value and does not give an absolute value.

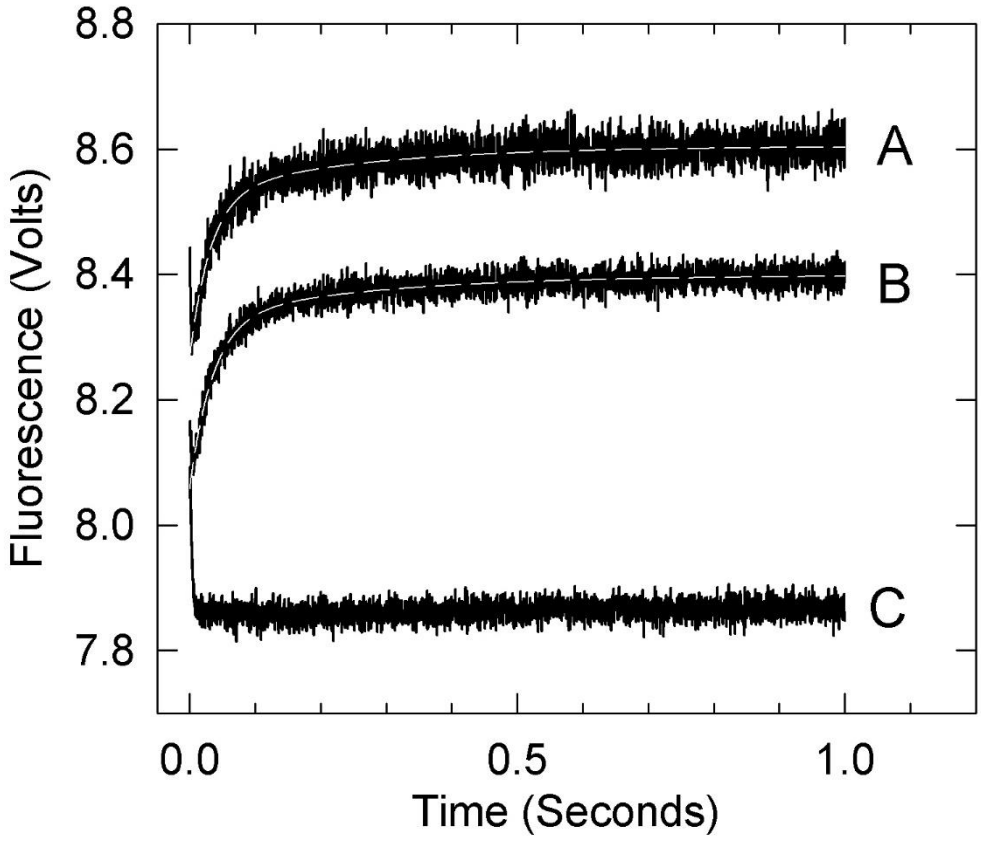

Figure 23: Formation of the inactive B state seen by acrylodan-tropomyosin fluorescence. Time courses of acrylodan fluorescence changes for actin regulated by wild type (A), 289C (B) and HAHA troponin T (C) following the rapid detachment of myosin S1 in the absence of Ca^{2+} at 10 °C. Traces shown are averages of at least five different measurements. The associated amplitudes of the closed to blocked transition were 0.28 for both wild type and 289C TnT troponin. The associated apparent rate constants were, 32 and 29 per sec for wild type and 289C TnT troponin, respectively. No amplitude or rate constant could be determined for HAHA TnT. 2 µM actin, 0.43 µM tropomyosin, 0.43 µM troponin and 2 µM S1 in 20 mM MOPS, 152 mM KCl, 4 mM $MgCl_2$, 1 mM dithiothreitol and 2 mM EGTA was rapidly mixed with 2 mM ATP, 20 mM MOPS, 152 mM KCl, 8 mM $MgCl_2$, 1 mM dithiothreitol and 2 mM EGTA. Acrylodan was excited via a 390 nm LED and observed through a 435/451/460 filter.

The acrylodan tropomyosin assay was additionally completed on another mutant, S275C troponin T, where serine 275 corresponding with the fourteenth residue from the C-terminus was substituted with a cysteine. This mutant was designed for FRET studies and we wanted to ensure that mutation did not appreciably affect the blocked state population. The S275C mutant behaved identically to wild type troponin T. Figure 24 shows a summary of the results from the acrylodan experiment incorporating HAHA, 289C and 275C troponin T troponin as well as wild type and ∆14 troponin T troponin.

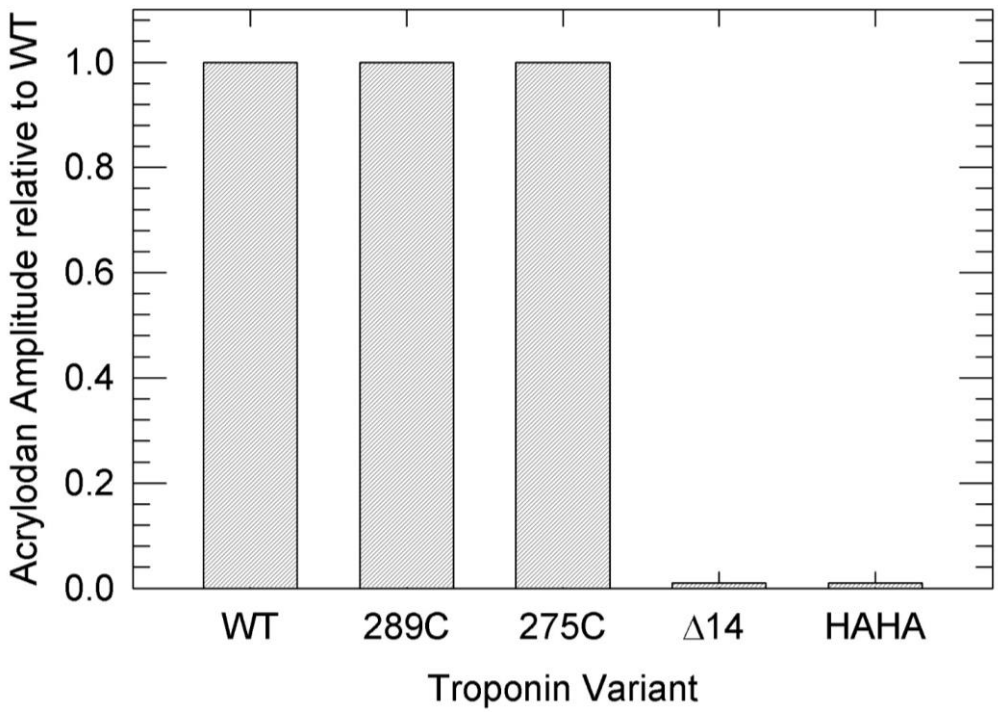

Figure 24: Ampltidues of acrylodan tropomyosin relative to wild type troponin regulated actin. ∆14 and HAHA TnT did not produce any measurable fluorescence amplitude.

As an additional means of measuring the effect of the HAHA troponin T construct on the relative blocked state distribution, we measured the rate of fluorescence change of pyrene actin upon binding of myosin S1 with actin in excess at different calcium concentrations. This assay takes advantage of the differential rates of binding to each state of actin. Because myosin S1 binds the closed and open states more rapidly than the blocked state, a lower rate of binding at low calcium indicates a greater population of the blocked state. Figure 24 shows the time course of pyrene fluorescence upon myosin S1 binding. Curves A and B are for wild type and 289C troponin T troponin respectively. The 289C mutant produced a rate of fluorescence change equivalent to that of the wild type troponin regulated actin indicating that the additional C-terminal cysteine did not affect rate of myosin S1 binding and presumably does not affect the blocked state population.

Curve C is the time course of fluorescence change for actin regulated with HAHA troponin T. Actin regulated by this mutant produces a more rapid fluorescence change corresponding with a lower initial blocked state population. Because the 289C mutant did not produce a rate of this transition that differed from that produced by actin regulated with wild type troponin, this observed increase in the rate of the pyrene fluorescence change can be attributed to the elimination of the basic residues from the C-terminal region of TnT. From this assay, it appears the elimination of those basic residues greatly diminished or eliminated the blocked state.

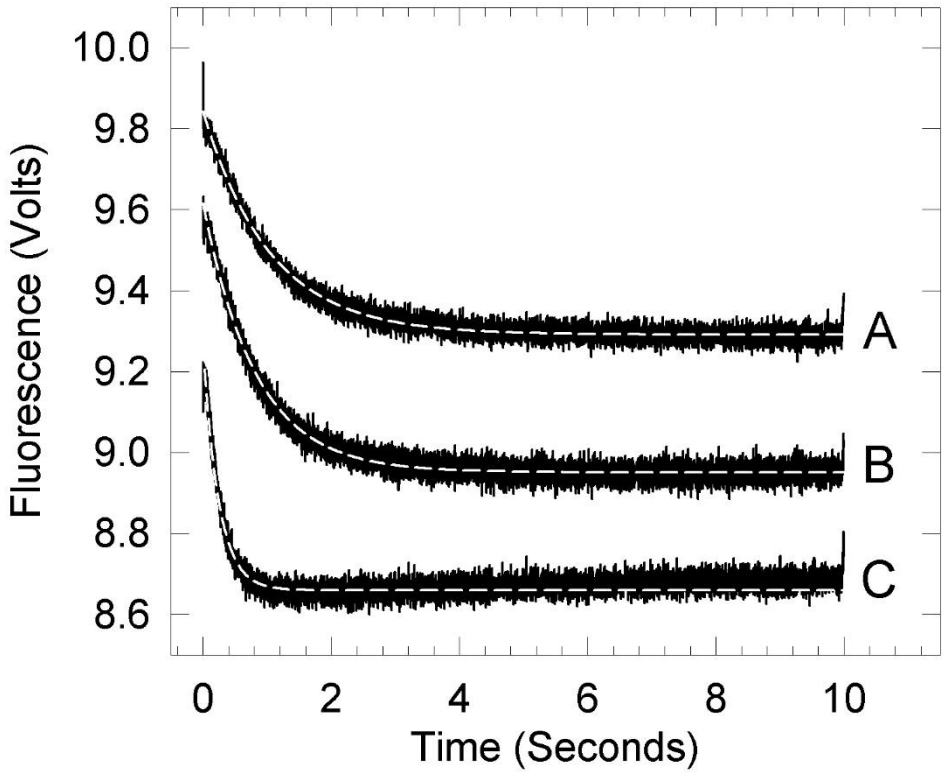

Figure 25: Rate of binding of S1 to an excess of pyrene labeled actin filaments containing tropomyosin and troponin in the absence of ATP at a very low Ca^{2+} concentration. Plots are averages of at least five time courses of binding to actin-tropomyosin containing wild type (A); 289C (B); and HAHA troponin T (C). Dashed lines are single exponential fits. The apparent rate constants were 1.0, 1.2, and 4.1 per second for wild type, 289C, and HAHA TnT respectively. At 25 °C, 4 μM pyrene-actin (40% labeled), 0.86 μM tropomyosin and 0.86 μM troponin were rapidly mixed with 0.4 μM myosin S1 in 20 mM MOPS, 152 mM KCl, 4 mM $MgCl_2$, 1 mM dithiothreitol and 2 mM EGTA. Pyrene was excited using a 360nm LED. The fluorescence was monitored through a 400 nm midpoint long pass filter.

We also monitored the fluorescence change of pyrene upon binding of myosin S1 to an excess of pyrene actin regulated by wild type, 289C troponin T, and HAHA troponin T troponin (Figure 24) at saturating calcium concentrations. By the assumptions made in the equations described previously (Equations 6-8), the saturating calcium rate should be a constant and is necessary for calculating the low calcium actin state distribution by this method. There was minimal difference in the rate of fluorescence change for wild type (1/sec) and 289C (1.2/sec) troponin T troponin regulated actin showing again that the introduction of the terminal Cys residue did not affect function. However, HAHA troponin T produced a more rapid rate of binding similar to that observed earlier for Δ14 troponin T in Figure 25. Under these conditions, HAHA troponin T stabilized the active O state. Contrary to the assumptions made in Equation 8, the rate of binding appears to follow the pattern open > closed > blocked.

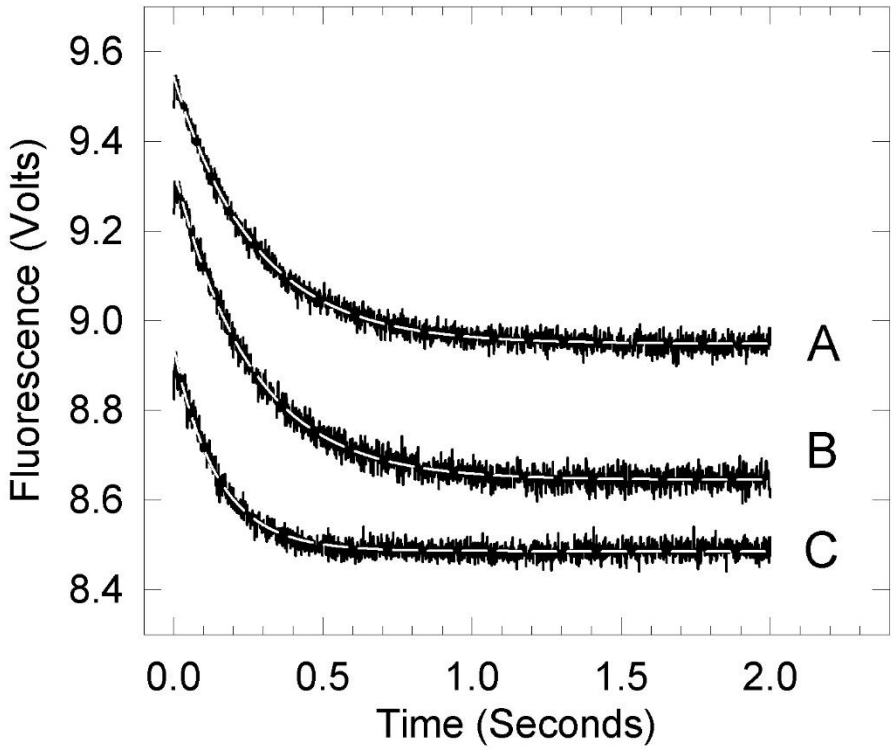

Figure 26: Rate of binding of S1 to an excess of pyrene labeled actin filaments containing tropomyosin and troponin in the absence of ATP at a saturating Ca^{2+} concentration. Plots are averages of at least five time courses of binding to actin-tropomyosin containing wild type (A); 289C (B); and HAHA troponin T (C). Dashed lines are single exponential fits. The apparent rate constants were 3.7, 3.9, and 6.8 per second for wild type, 289C, and HAHA TnT respectively. At 25 °C, 4 μM pyrene-actin (40% labeled), 0.86 μM tropomyosin and 0.86 μM troponin was rapidly mixed with 0.4 μM myosin S1 in 20 mM MOPS, 152 mM KCl, 4 mM $MgCl_2$, 1 mM dithiothreitol and 0.2 mM $CaCl_2$. Pyrene was excited using a 360nm LED. The fluorescence was monitored through a 400 nm midpoint long pass filter.

Part 4: At saturating Ca^{2+} concentration HAHA troponin T behaves similarly to ∆14 troponin T

The high alanine high activity (HAHA) troponin T construct appears to significantly diminish or eliminate the blocked state to an equivalent extent as ∆14 troponin T at very low calcium concentrations. We also wanted to identify if this HAHA troponin T construct stabilized the open O state at saturating calcium concentrations. We measured the ATPase rates of unregulated, wild type, 275C, 289C, and HAHA troponin T to determine the extent to which each stabilizes the active O state (Figure 24). Wild type, 275C, and 289C troponin T troponin each produced an ATPase rate of about 2 per second. The additional cysteine at the C-terminus or the cysteine substitution at residue 275 did not appreciably disrupt the open O state distribution relative to wild type troponin regulated actin.

The HAHA troponin T construct, on the other hand, increased the ATPase rate to 3.9 per second. This doubling of the ATPase rate relative to wild type troponin regulated actin is what was previously observed with Δ14 troponin T regulated actin. It appears from this assay that the HAHA troponin T construct stabilizes the O state to a similar extent as the Δ14 troponin T mutant. Because the 289C mutant did not appreciably affect the O state, this increase in O state population by HAHA troponin T can be attributed to substitution of the seven basic residues within the 16 C-terminal residues. By each of our measures of quantifying the actin state distribution, the HAHA troponin T construct appears to mimic the effects of the Δ14 troponin T construct.

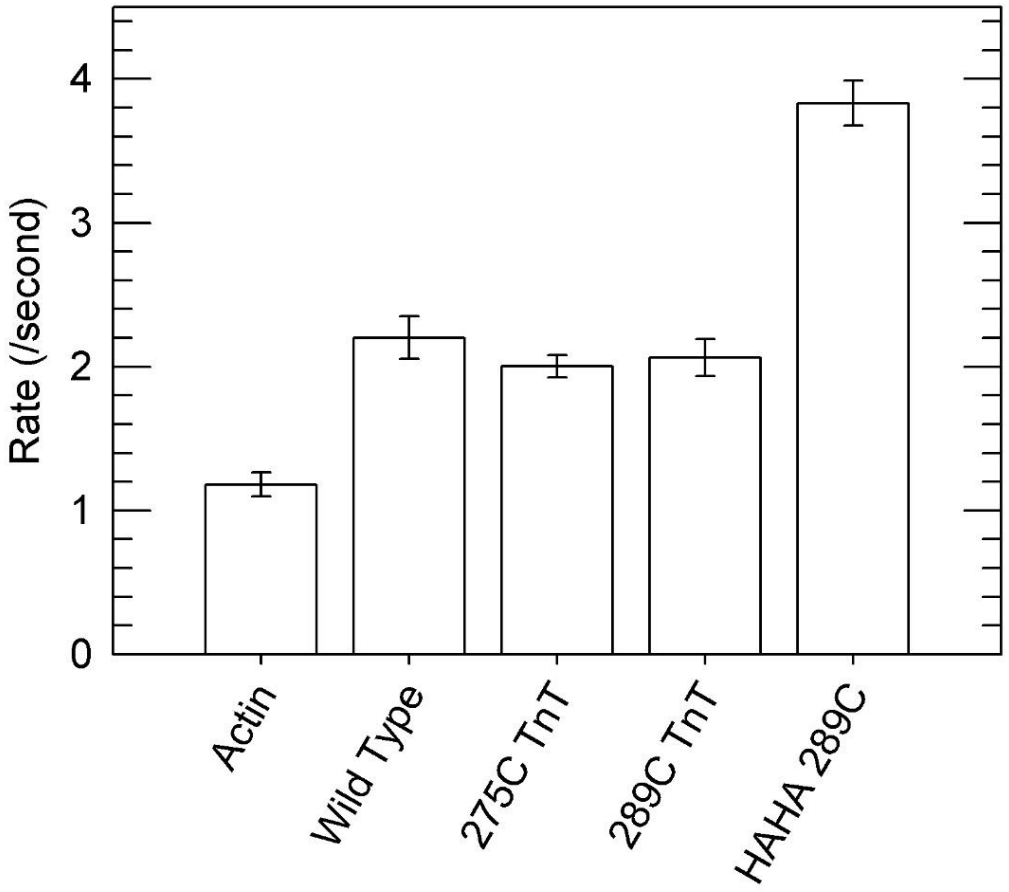

Figure 27: ATPase rates of myosin S1 in the presence of actin and actin-tropomyosin containing troponin with different mutants of troponin T at saturating Ca^{2+}. Measurements were made at 25^{o} C and pH 7.0 in solutions containing 1 mM ATP, 4 mM $MgCl_2$, 31 mM KCl, 10 mM MOPS, 1 mM dithiothreitol and 0.1 mM $CaCl_2$. The concentrations of S1, actin, tropomyosin, and troponin were 0.1, 10, 2.2, and 2.2 µM, respectively.

Part 5: A8VΔ14 troponin T affects Km but not Vmax

Our lab observed that troponin containing Δ14 troponin T or A8VΔ14 troponin[47,78] substantially increased the open state population. This observation was made at an actin concentration well below the K_M and the rates were proportional to V_{max}/K_M. We studied the rates at increasing actin concentrations to determine if the increase in rate was due to an increase in V_{max} or a decrease in K_M. The importance of this distinction will be discussed in Chapter 5

We repeated the ATPase assay of unregulated actin and actin regulated by A8VΔ14 at a variety of actin concentrations. We chose to use A8VΔ14 in these experiments because this mutant produces the highest ATPase rate by a troponin mutant thus far observed. We used actin concentrations ranging from 10 to 400 μM for unregulated actin and 5 to 150 μM for actin regulated by A8VΔ14 Tn.

Figure 28 shows a plot of the ATPase rate versus the actin concentration for unregulated actin (circles) and actin regulated by A8VΔ14 (squares). At 10 μM actin, the rate was about three times that of unregulated actin. The rate at this concentration corresponds to the conditions used in our previously described ATPase assays (Figure 21). As the actin concentration increased, stimulation of the myosin ATPase rate increased. At very high actin concentrations, the rates converged.

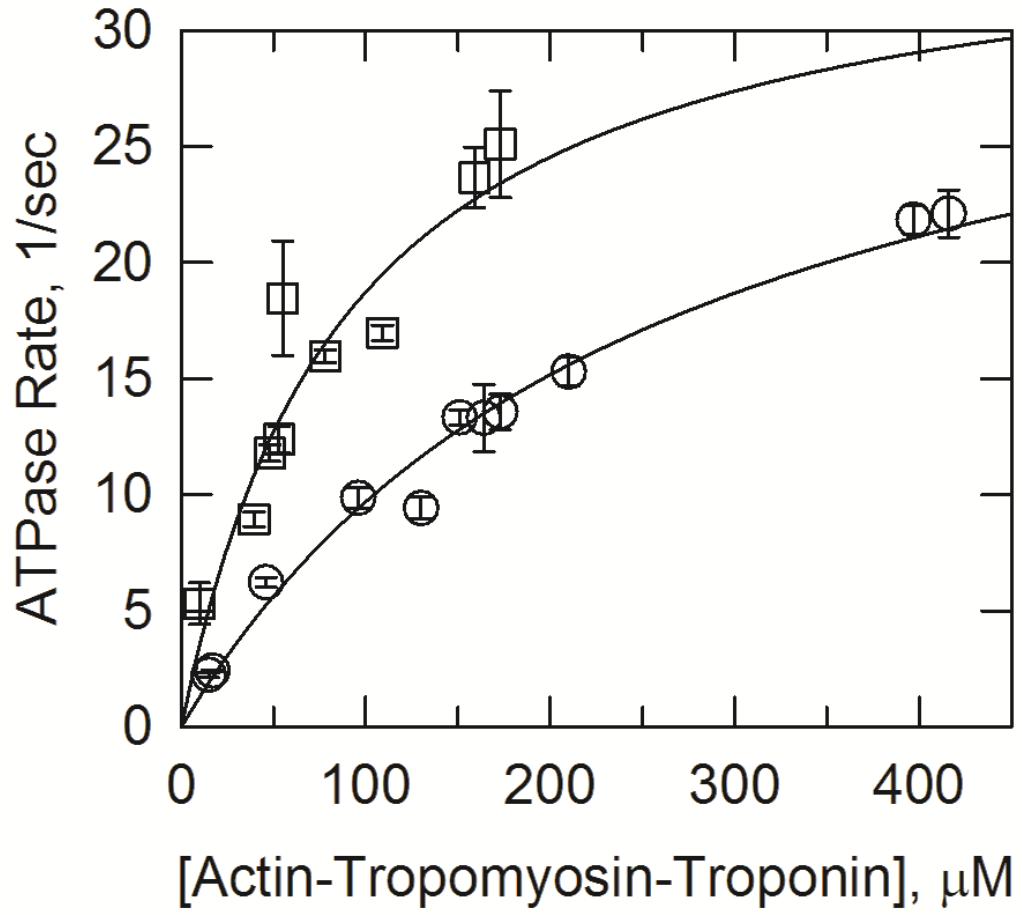

Figure 28: ATPase rates of myosin S1 in the presence of unregulated actin (circles) and actin regulated with tropomyosin and A8VΔ14 troponin at saturating Ca^{2+}. Measurements were made at 25° C and pH 7.0 in solutions containing 1 mM ATP, 4 mM $MgCl_2$, 31 mM KCl, 10 mM MOPS, 1 mM dithiothreitol and 0.1 mM $CaCl_2$. The concentrations of S1 was 0.1 μM. The actin concentration was varied. Tropmyosin and troponin were maintained in a 7:1.1 ratio relative to actin. The Vmax was 35 (±4) and 35 (±8) /second for unregulated actin and A8VΔ14 regulated actin respectively. The K_M was 258 (±49) and 90 (±36) for unregulated actin and A8VΔ14 regulated actin respectively.

The Vmax was 35 (±4) and 35 (±8) /second for unregulated actin and A8VΔ14 regulated actin respectively. There was no appreciable change in the Vmax. The K_M was 258 (±49) and 90 (±36) for unregulated actin and A8VΔ14 regulated actin respectively. From these results, it appears that the activating quality of A8VΔ14 is primarily the result of a decrease in the K_M. The implications of these results and the significance of a troponin construct that can stabilize the open state will be described in Chapter 5.

Chapter 4: Dynamics of the C-Terminus of Troponin T and structural consequence of mutation

Part 1: Using FRET to map the location of the C-terminus of troponin T.

The previous chapter (Chapter 3) focused on the functional consequence of mutation within the C-terminal 16 residues of troponin T. In that chapter, we established that truncation from the C-terminus results in a graded elimination of the blocked state at low calcium concentrations and stabilization of the open O state at saturating calcium concentrations. We generated a construct, HAHA (high alanine, high activity) troponin T to assess the importance of the positive charges on the function of the C-terminus of troponin T. Analysis of that construct revealed elimination of those basic residues corresponded with loss of the blocked state at low calcium concentrations and stabilization of the open O state at saturating calcium concentrations. This HAHA troponin T construct exhibited functional properties that were by our measures, equivalent to the properties of the Δ14 troponin T mutant observed previously.

This chapter focuses on the structural properties of the C-terminus of troponin T in an attempt to elucidate the structural basis for the functions of the C-terminus of troponin T. The interactions required for the C-terminus function are fundamental to our basic understanding of regulation by troponin. These interactions present novel targets for sarcomeric modulators to affect the distribution between actin states. Modulators that specifically inhibit or enhance these interactions may allow fine tuning of actin states to restore normal contractile activity in those with cardiovascular diseases.

To investigate the interactions of the C-terminus, we designed a series of fluorescence resonance energy transfer (FRET) experiments to measure the efficiency of transfer between probes on the C-terminus of troponin T and other locations within the thin filament. These measures of transfer efficiency indicate the closeness between the probed locations. Each measurement was conducted at both a very low calcium concentration and at saturating calcium to identify the structural response of each probed pair to changes in activation status. Additionally, we can convert these efficiencies to absolute distances using additional parameters. Along with the distances obtained from other labs, our acquired distances will ultimately be used as constraints in molecular modelling simulations. The goal of which is to map the location of the C-terminus into a model of the actin-tropomyosin-troponin complex.

We designed each FRET measurement to strategically answer a targeted question (Table 5). We ultimately plan to incorporate these measurements as constraints in molecular modelling simulations.

Table 5: Summary of justifications for each FRET measurement.

Donor	Acceptor	Justification
TnT 275C	C374 of actin	Identify possible interaction of highly basic TnT C-terminus to the highly negatively charged surface of actin
TnT 289C	C374 of actin	Identify possible interaction of highly basic TnT C-terminus to the highly negatively charged surface of actin
HAHA TnT 289C	C374 of actin	Identify possible disruption of interaction of TnT C-terminus and highly negatively charged surface of actin resulting from elimination of basic residues in C-terminus
TnI T143C	C374 of actin	Develop a FRET sensor to measure the known interaction between the TnI inhibitory peptide and actin
TnI T143C Δ14 TnT	C374 of actin	Identify disruption to the inhibitory peptide binding actin resulting from the activating mutant, Δ14 TnT
TnT 275C	C190 of Tpm	Test external evidence that these two regions interact or bind
TnT 289C	C190 of Tpm	Test external evidence that these two regions interact or bind
HAHA TnT 289C	C190 of Tpm	Identify possible disruption of interaction of TnT-C terminus and Tpm resulting from elimination of basic residues in C-terminus
TnI T143C	C190 of Tpm	Approximate distance between inhibitory peptide binding site on actin and Tpm as very low calcium concentration. Approximate distance between TnI binding site on TnC and Tpm at saturating calcium concentration
TnI T143C Δ14 TnT	C190 of Tpm	Identify disruption to this distance resulting from activating construct, Δ14 TnT
TnT 275C	143C of TnI	Identify how the inhibitory region of TnI and C-terminus of TnT emerge from the IT helix. Approximate closeness of 275C TnT to inhibitory region binding site of actin at very low calcium concentrations. Approximate closeness of 275C TnT to TnI inhibitory region binding site of TnC at saturating calcium.
TnT 289C	143C of TnI	Approximate distance between 275C and 289C TnT. Approximate closeness of 289C TnT to inhibitory region binding site of actin at very low calcium concentrations. Approximate closeness of 289C TnT to TnI inhibitory region binding site of TnC at saturating calcium.

We developed the troponin T constructs 289C and S275C to attach fluorescent probes in our FRET experiments. For each of these constructs, the added cysteine is the only cysteine available for labelling. The 289C construct is the wild type troponin T sequence with an additional cysteine appended to the C-terminus. The S275C construct is the wild type troponin T sequence with residue S275 substituted with a cysteine. The effect of those modifications on our measures of the blocked and open O state were measured and described in the previous chapter (Chapter 3). We found that both 289C and S275C are statistically equivalent to wild type troponin by each of our measures of the actin state distribution at very low and saturating calcium.

Those two locations on the C-terminus of troponin T, 275 and 289, compose the boundaries of the C-terminus that we are interested in mapping into a model of actin-tropomyosin-troponin. Residue 289 is at the far C-terminus and residue 275 is fourteen residues from the C-terminus, corresponding with the Δ14 mutation. Ideally, efficiency measurements at both locations will allow us to better triangulate the exact position and orientation of the C-terminus relative to other locations within actin-tropomyosin-troponin.

We also targeted the HAHA troponin T construct with a fluorescent probe. Recall that mutant has the seven basic residues of the C-terminus substituted with alanine and an additional cysteine appended to the C-terminus at 289C. Measurements with HAHA troponin T will be most directly comparable to those made with 289C troponin T as the probe for each is at the 289 position. These efficiency measurements are important for identifying the position of the C-terminus when actin is stabilized almost entirely in the O state at saturating calcium and when the blocked state is virtually absent at very low

calcium concentrations. This will assist us in better understanding the conformation of actin-tropomyosin-troponin when fully activated.

A T143C troponin I construct was developed for a variety of reasons. Residue 143 of troponin I is within the well characterized inhibitory region of troponin I that is in known to interact with actin at very low calcium concentrations and troponin C at saturating calcium concentrations. The relative location of T143C can be seen in (Figure *14*). Because the inhibitory region of troponin I is known to interact with actin at low calcium concentrations, we propose that measuring the efficiency of transfer between the C-terminus of troponin T and the inhibitory region of troponin I at low calcium concentrations is a method of approximating the efficiency of transfer between the C-terminus of troponin T and that corresponding inhibitory region of actin. This will provide some insight into our hypothesis that the C-terminus of troponin T might interact with actin similarly to the inhibitory region of troponin I.

Because the inhibitory region of troponin I is known to interact with troponin C at saturating calcium, we propose that measuring the efficiency of transfer between the C-terminus of troponin T and the inhibitory region of troponin I at saturating calcium is a method of approximating the efficiency of transfer between the C-terminus of troponin T and the inhibitory peptide binding location on troponin C. This will provide some insight into our hypothesis that the C-terminus of troponin T might interact with the hydrophobic pocket of troponin C similarly to the inhibitory peptide.

The inhibitory peptide of troponin I and the C-terminus of troponin T are both immediately adjacent to the IT helix and are known to be in relatively close proximity, at least at the N-terminus of each domain. Based on the sequence alignment of troponin I

and troponin T composing the IT helix, residues T143 of troponin I and S275 of troponin T must be in relatively close proximity. Measuring the transfer efficiency between those two locations will resolve how those two domains emerge from the IT helix.

Because it is known that S275 of troponin T is relatively close to T143, we propose that the transfer efficiency between T143C and 289C is an approximation of the transfer efficiency that would be measured between 275C and 289C. This measurement allows us to determine whether the C-terminus of troponin T adopts a relatively compact or expanded structure based on the approximate distance from each end of the C-terminal domain. This strategy was designed to circumvent the inability to attach a donor and acceptor probe within the same protein to measure an inter-troponin T distance.

In addition to the T143C construct, we also developed a T143C troponin I – Δ14 troponin T construct where T143C troponin I was reconstituted with wild type troponin C and Δ14 troponin T. The idea here was to identify how the activating Δ14 troponin T construct affected the efficiency of transfer between the inhibitory region of troponin I and other locations within actin-tropomyosin-troponin. This was designed in hopes of identifying a structure-function relationship resulting from mutation in the C-terminus of troponin T.

Actin contains two native cysteine residues. One of the cysteines can be selectively targeted with fluorescent probes while leaving the other unaffected. This actin cysteine, C374, was labelled with a FRET acceptor probe. The efficiency of transfer was measured between actin C374 and each of the probed troponin T and troponin I constructs.

One limitation of the use of actin as an acceptor is that it is possible that multiple actin monomers are within range of accepting energy transfer from the donor on troponin. Our analysis of this data assumes that only one actin is available for accepting the energy transfer. In future molecular modelling simulations, we will be able to account for the possibility of multiple acceptors.

Tropomyosin contains one native cysteine at position 190. The efficiency of transfer was measured between tropomyosin C190 and each of the probed troponin T and troponin I constructs as well. There is also a limitation to having an acceptor probe on tropomyosin. Because tropomyosin is a dimer and each subunit has a cysteine at position 190, both subunits can be labelled with a probe. This introduces a variety of combinations of labelling on each tropomyosin. Tropomyosin can be unlabeled, labelled on one of two subunits or labelled on both subunits. Our analysis of the data assumes the location of the acceptor probe on tropomyosin as being one location.

Each of the troponin constructs were labeled with an IAEDANS probe to function as a donor in the FRET experiments. Actin and tropomyosin were labeled with a nonfluorescent DABMI probe to function as an acceptor in FRET experiments. The troponin I construct was additionally targeted with the acceptor probe DABMI for inter-troponin distances between troponin T and troponin I.

It is expected that labelling these proteins with bulky fluorescent groups would disrupt their ability to maintain the normal actin state distribution to some extent. To make valid conclusions from our FRET data, we must determine the extent to which the probes affect the proteins function. Ideally, the actin state distribution will not be appreciably disrupted by mutation.

We performed ATPase measurements on each of the constructs used in our FRET experiments to determine any disruption to their regulatory properties resulting from attachment of a bulky fluorescent group. These data are shown in Figure 24. The DABMI probe on actin slightly inhibited the unregulated actin stimulation of myosin ATPase activity. We proceeded in our FRET experiments with each of these constructs as we determined that they either regulate sufficiently or exhibit disruption to activity that was consistent with previous observation.

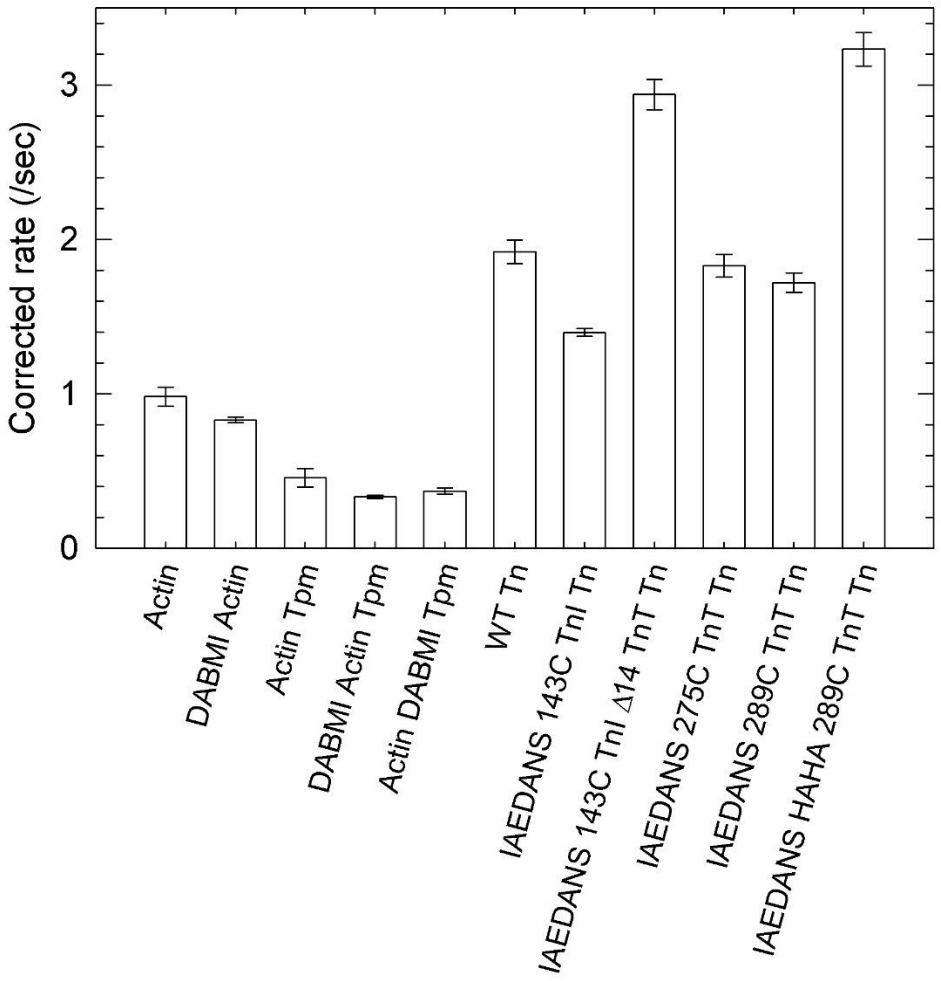

Figure 29: ATPase rates of myosin S1 in the presence of actin and actin-tropomyosin containing troponin with different mutants of troponin T at saturating Ca^{2+}. Measurements were made at 25° C and pH 7.0 in solutions containing 1 mM ATP, 4 mM $MgCl_2$, 31 mM KCl, 10 mM MOPS, 1 mM dithiothreitol and 0.1 mM $CaCl_2$. The concentrations of S1, actin, tropomyosin, and troponin were 0.1, 10, 2.6, and 2.2 µM, respectively.

The FRET measurements were completed as described previously in chapter 2. The data from our FRET experiments are divided into three tables based on the acceptor probe location. These data will be described in more detail in chapter 5. Table 6 shows the data for our FRET experiments where DABMI C374 of actin is the acceptor.

A particularly interesting result was that the transfer of the troponin I T143C – DABMI actin FRET pair was dependent on the absence and presence of Δ14 troponin T. This pair appears to be a direct measure of the binding of the inhibitory region of troponin I to actin which is a characteristic mechanism of calcium regulation and presents a new method for measuring mutation effects on regulation. In the presence of Δ14 troponin T, the efficiency between that pair decreased at both low and saturating calcium. This suggested Δ14 troponin T disrupted that interaction between the inhibitory region of troponin I and actin. We looked further into this pair and describe the results in part 3 of this chapter.

Table 6 shows the data for our FRET experiments where DABMI C190 of tropomyosin is the acceptor. We observed a particularly high transfer efficiency between IAEDANS 275C troponin T and DABMI C190 tropomyosin. Though the efficiency at saturating calcium was not high enough to explicitly suggest those locations interact, it is possible a nearby location of both regions may interact. This is supported by evidence of other labs that suggest the C-terminus of troponin T interacts with tropomyosin near C190 of tropomyosin. That pair also exhibited an appreciable decrease in efficiency at saturating calcium suggesting the regions move further apart or possibly dissociate. The high resolution crystal structure of troponin modeled onto the actin crystal structure[48] at

low and saturating calcium concentrations showed a similar calcium response of these two regions relative to one another. The next section of this chapter will focus on the FRET pairs monitoring distances between troponin and DABMI C190 tropomyosin.

Table 6 shows the data for our FRET experiments where DABMI T143C of troponin I is the acceptor. Although the efficiency of transfer is high, the distance between T143C and S275C was greater than that expected based on the sequence alignment emerging from the IT-Helix[69]. The implications of this result will be discussed in Chapter 5.

Table 6: Distances to DABMI on C374 of actin

Donor	Efficiency EGTA	Efficiency Calcium	Distance EGTA	Distance Calcium
IAEDANS TnT 275C	0.24	.13	48	55
IAEDANS TnT 289C	0.11	.09	56	58
IAEDANS HAHA TnT 289C	0.05	.06	65	63
IAEDANS TnI T143C	0.25	.09	48	58
IAEDANS TnI T143C Δ14 TnT	0.20	.04	50	68

Table 7: Distances to DABMI on C190 of tropomyosin

Donor	Efficiency EGTA	Efficiency Calcium	Distance EGTA	Distance Calcium
IAEDANS TnT 275C	0.86 (.04)	.55 (.10)	30	39
IAEDANS TnT 289C	0.70 (.07)	.51 (.02)	35	40
IAEDANS HAHA TnT 289C	0.53 (.01)	.35 (.01)	39	44
IAEDANS TnI T143C	0.73 (.02)	.48 (.02)	34	40
IAEDANS TnI T143C Δ14 TnT	0.38 (.01)	.25 (.01)	43	48

Table 8: Distances to DABMI on T143C of TnI

Donor	Efficiency EGTA	Efficiency Calcium	Distance EGTA	Distance Calcium
IAEDANS TnT 275C	0.60 (0.02)	.65 (0.02)	37	36
IAEDANS TnT 289C	0.43 (0.02)	.55 (0.02)	42	39

Part 2: Time course of FRET upon deactivation of regulated actin

With the FRET measurements described above, we developed a general idea of the location of the C-terminus of troponin T relative to other locations within the actin-tropomyosin-troponin complex. The most likely interaction of the C-terminus of troponin T at saturating calcium is with tropomyosin near C190. As well, we showed a calcium response for some of the distances suggesting the mechanism of regulation. The distance between the C-terminus of troponin T and tropomyosin C190 increased with calcium indicating the C-terminus takes on an extended conformation or dissociates.

A series of rearrangements occur upon calcium binding to troponin C causing a repositioning of tropomyosin. Though we do not yet know all of these rearrangements, at minimum, they include opening of a hydrophobic pocket of troponin C and a resultant enhanced association of troponin I with troponin C. Another step toward understanding the mechanism of the C-terminus function is to determine which rearrangements in the troponin calcium response is affected by the C-terminus of troponin T. The C-terminus of troponin T must be involved in one or more of the steps in that series or directly influence one or more of those steps. The previous FRET studies help to define interacting partners. Time courses of FRET help to define where in time the changes in troponin T occur in the sequence. This work presents some of the first steps taken to achieve that goal.

We wanted to identify a FRET pair involving the C-terminus of troponin T that had a high transfer efficiency and a dependence on calcium concentration. This was in the interest of finding a reliable FRET pair whose efficiency change could be monitored in the time course of our kinetic assays. This would allow us to identify if the C-terminus

is required for a transition, if the C-terminus is dependent on that transition, or if the C-terminus is coupled to that transition.

The acrylodan ATPchase assay measured the redistribution of actin from the fully active open state to a distribution of the closed and blocked states (Figure *13*). Based on past results from the acrylodan fluorescence time course of that assay at 10° C, actin is primarily in the closed state at 0.1 seconds. At 0.5 seconds, actin is equilibrated between the closed and blocked states when wild type troponin is regulating actin. The troponin mutants 289C and 275C troponin T did not appreciably affect the state distribution. The HAHA troponin T mutant eliminated the fluorescence transition attributed to the blocked state.

We measured the efficiency of the IAEDANS troponin – DABMI C190 tropomyosin FRET pairs over the time course of that same reaction. The FRET pairs between troponin and DABMI tropomyosin exhibited a high transfer efficiency and a notable change in efficiency with change in calcium concentration. This allowed us to measure how different regions of troponin move relative to tropomyosin as actin redistributes from the open state into the closed and blocked states.

Figure 24 shows the results of the S1 dissociation experiment following the fluorescence of IAEDANS 289C troponin T with and without the acceptor probe DABMI on C190 tropomyosin. Plot A shows the fluorescence time course of donor IAEDANS in the absence of acceptor DABMI at 10° C. That trace remains relatively constant over the normal time course of the reaction. Plot B shows the fluorescence time course of donor IAEDANS in the presence of acceptor DABMI at 10° C. This plot is shifted downwards indicating quenching of IAEDANS fluorescence by the DABMI acceptor

probe. A decrease in fluorescence is observed over the course of the reaction. This decrease in the IAEDANS is the result of an increase in fluorescence quenching by the DABMI acceptor.

These traces were replotted as efficiency versus time by converting the fluorescence plots to efficiency using the equation 1-(DA/D) where DA is the fluorescence time course when the acceptor is present, and D is the fluorescence time course when the acceptor is absent. Plot G shows the resulting plot of efficiency versus time for IAEDANS 289C troponin T transfer to DABMI C190 tropomyosin as S1 is dissociated from actin at 10° C. These plots show the efficiency before it has been corrected for the extent of labelling on the acceptor probe. The increase in efficiency means that the IAEDANS and DABMI probes moved closer to each other throughout the time course of the reaction. This experiment was repeated at both 18° C and 25° C. An Arrhenius plot of the temperature dependence is shown in Appendix C: Supplementary Data. The linearity of the plot shows that the rate limiting step is not affected by the temperature.

The initial and final efficiency of the IAEDANS 289C troponin T - DABMI C190 tropomyosin FRET pair at 10° C was 0.29 and 0.46, respectively. The efficiencies and distances from this experiment are summarized in Table 9. We attribute the initial efficiency value of 0.29 to the transfer between IAEDANS 289C troponin T and DABMI C190 tropomyosin when actin is stabilized fully in the closed state.

The final efficiency is a measure of the efficiency of transfer when actin has equilibrated between the closed and blocked states. That distribution is dependent on the troponin construct that is regulating actin. As described previously, we question the

validity of the methods available to estimate the blocked state population at low calcium concentrations, however, we previously published a value of 87% blocked state for wild type troponin regulated actin at low calcium concentrations as determined by the pyrene method[78]. Therefore, the final efficiency value 0.46 corresponds to the efficiency of transfer between IAEDANS 275C troponin T and DABMI C190 of tropomyosin when actin is approximately 87% in the blocked state.

From these efficiencies, we calculated the distances to be 46 and 41 Å for the initial and final distance, respectively. These values follow the same trend that was observed in the steady state FRET measurements between IAEDANS 289C troponin T and DABMI C190 of tropomyosin. In both cases, 289C of troponin T is closer to C190 of tropomyosin when actin is in a more active state.

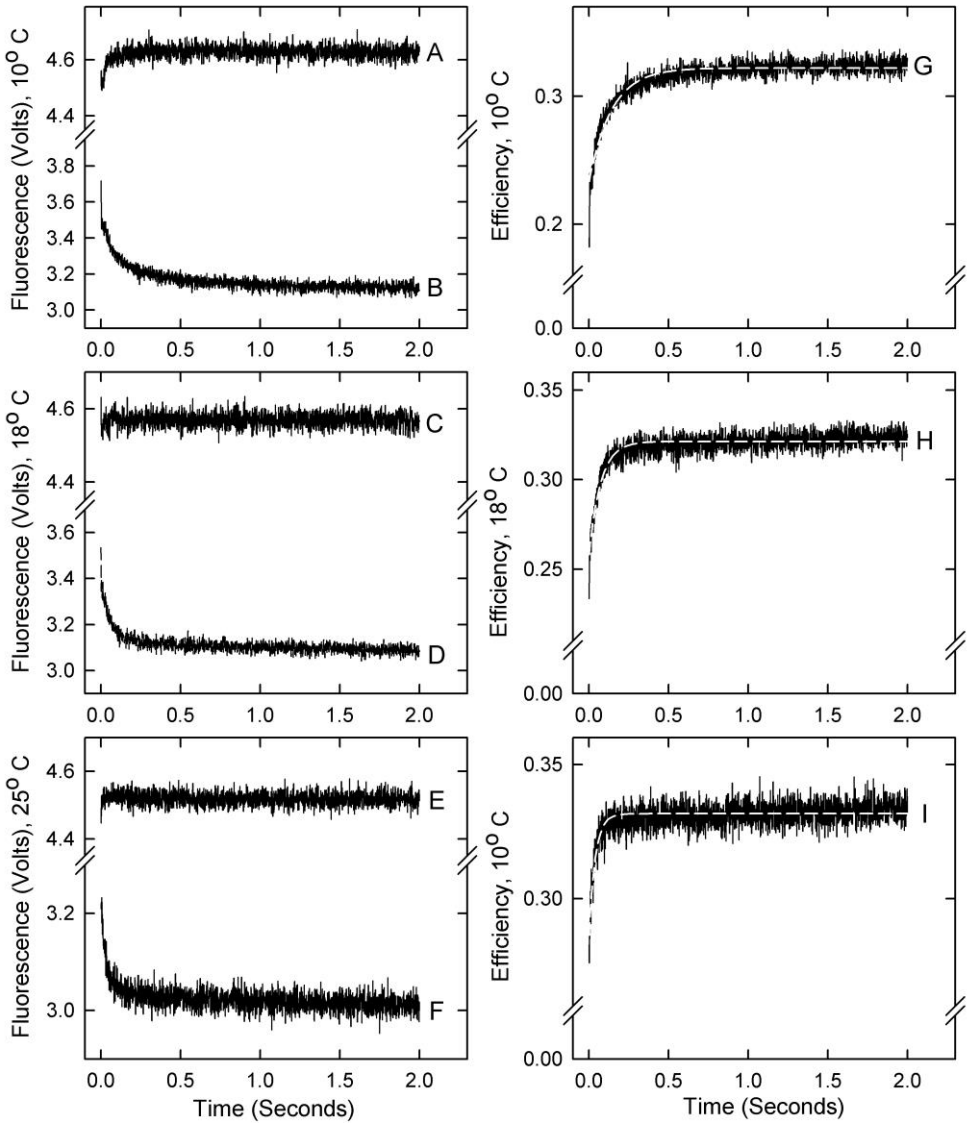

Figure 30: Time courses of IAEDANS 289C TnT fluorescence change in the absence and presence of a DABMI fluorescence acceptor probe on C190 of tropomyosin following the rapid detachment of myosin S1 from actin at very low Ca^{2+} concentrations. Traces shown are averages of at least three different measurements. Traces A, C and E are in the absence of acceptor DABMI. Traces B, D and F are in the presence of acceptor DABMI. Traces G, H, and I are the efficiency of transfer between IAEDANS and DABMI. 2 µM actin, 0.51 µM tropomyosin, 0.43 µM troponin and 2 µM S1 in 20 mM MOPS, 152 mM KCl, 4 mM $MgCl_2$, 1 mM dithiothreitol and 2 mM EGTA was rapidly mixed with 2 mM ATP, 20 mM MOPS, 152 mM KCl, 8 mM $MgCl_2$, 1 mM dithiothreitol and 2 mM EGTA at 25° C. IAEDANS was excited using a 340nm LED and the fluorescence monitored through a 435/451/460 filter. Apparent rates: G, 7.0(±0.1); H, 13.7(±0.3); I, 25(±1).

One of the primary goals of these structural measurements was to determine how mutation in the C-terminus of troponin T affects the structural response of the region. We monitored the fluorescence time course of IAEDANS HAHA 289C troponin T as myosin S1 dissociated from actin in the absence (Figure 24A) and presence (Figure 24B) of DABMI C190 tropomyosin. The resultant efficiency change from that pair is plotted in Figure 24C. This pair is analogous to that shown in Figure 24 above with the exception that this pair contains the HAHA troponin T sequence which enhances activity by stabilizing the O state at saturating calcium and eliminating the B state at very low calcium.

We did not observe an appreciable change in efficiency over the course of this reaction. The efficiency of the IAEDANS HAHA 289C troponin T - DABMI C190 tropomyosin FRET pair at 18° C over the course of the reaction was 0.34. This corresponds to a distance of 45 Å. Because HAHA troponin T is present in this pair, actin is stabilized nearly 100% in the closed state following dissociation of myosin S1 at a low calcium concentration. As we expected, no change in efficiency is observed as there is no transition from the closed to blocked state.

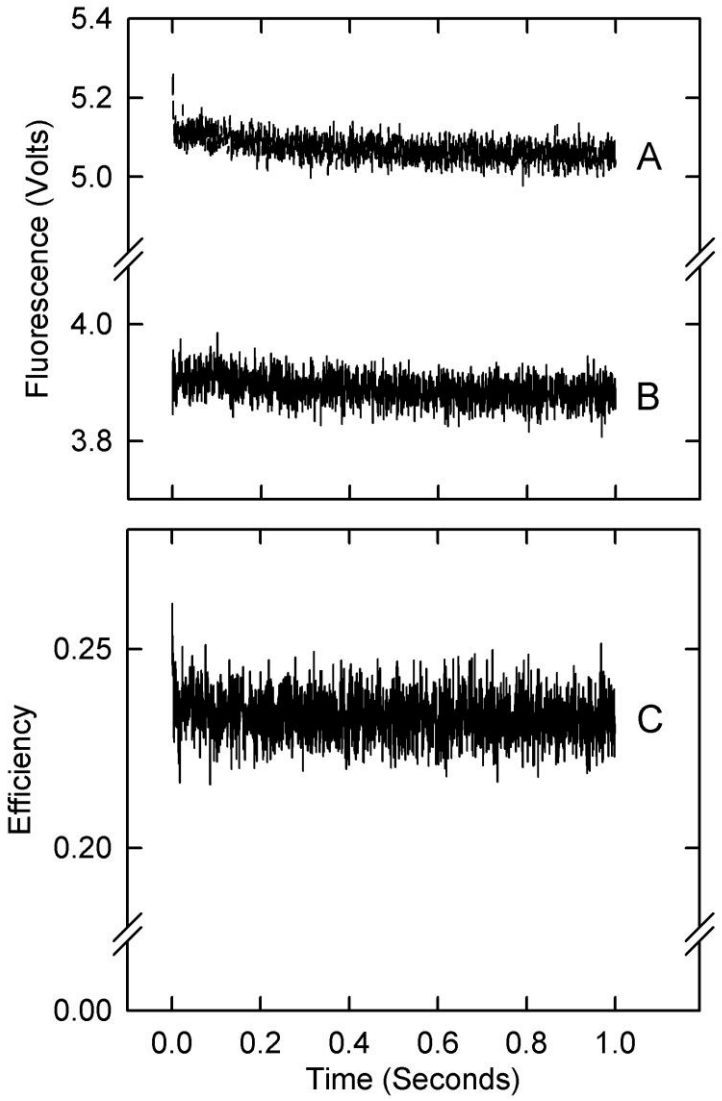

Figure 31: Time courses of IAEDANS HAHA 289C TnT fluorescence change in the absence and presence of a DABMI fluorescence acceptor probe on C190 of tropomyosin following the rapid detachment of myosin S1 from actin at very low Ca^{2+} concentrations. Traces shown are averages of at least three different measurements. Trace A, donor alone; B, donor and acceptor; C, efficiency. 2 µM actin, 0.51 µM tropomyosin, 0.43 µM troponin and 2 µM S1 in 20 mM MOPS, 152 mM KCl, 4 mM $MgCl_2$, 1 mM dithiothreitol and 2 mM EGTA was rapidly mixed with 2 mM ATP, 20 mM MOPS, 152 mM KCl, 8 mM $MgCl_2$, 1 mM dithiothreitol and 2 mM EGTA at 25° C. IAEDANS was excited using a 340 nm LED and the fluorescence monitored through a 435/451/460 filter.

The fluorescence of IAEDANS 275C troponin T was followed as myosin S1 dissociated from actin in the absence and presence of the DABMI acceptor probe on tropomyosin (Figure 24). In the absence of acceptor, the fluorescence of this probe remains relatively constant throughout the time course of this reaction (Figure 24A). In the presence of acceptor, the IAEDANS fluorescence decreased throughout the time course of the reaction (Figure 24B). The efficiencies were replotted using the equation described above (Figure 24C).

The initial and final efficiency of the IAEDANS 275C troponin T - DABMI C190 tropomyosin FRET pair was 0.66 and 0.74 respectively. The efficiencies and distances from this experiment are summarized in Table 9. We attribute the initial efficiency value of 0.66 to the transfer between IAEDANS 275C troponin T and DABMI C190 tropomyosin when actin is stabilized fully in the closed state. We attribute the final efficiency value 0.74 to the efficiency of transfer between IAEDANS 275C troponin T and DABMI C190 of tropomyosin when actin is approximately 87% in the blocked state.

From these efficiencies, we calculated the distances to be 36 and 34 Å for the initial and final distance respectively. These values follow the same trend that was observed in the steady state FRET measurements between IAEDANS 275C troponin T and DABMI C190 of tropomyosin. In both cases 275C of troponin T is closer to C190 of tropomyosin when actin is in a more active state.

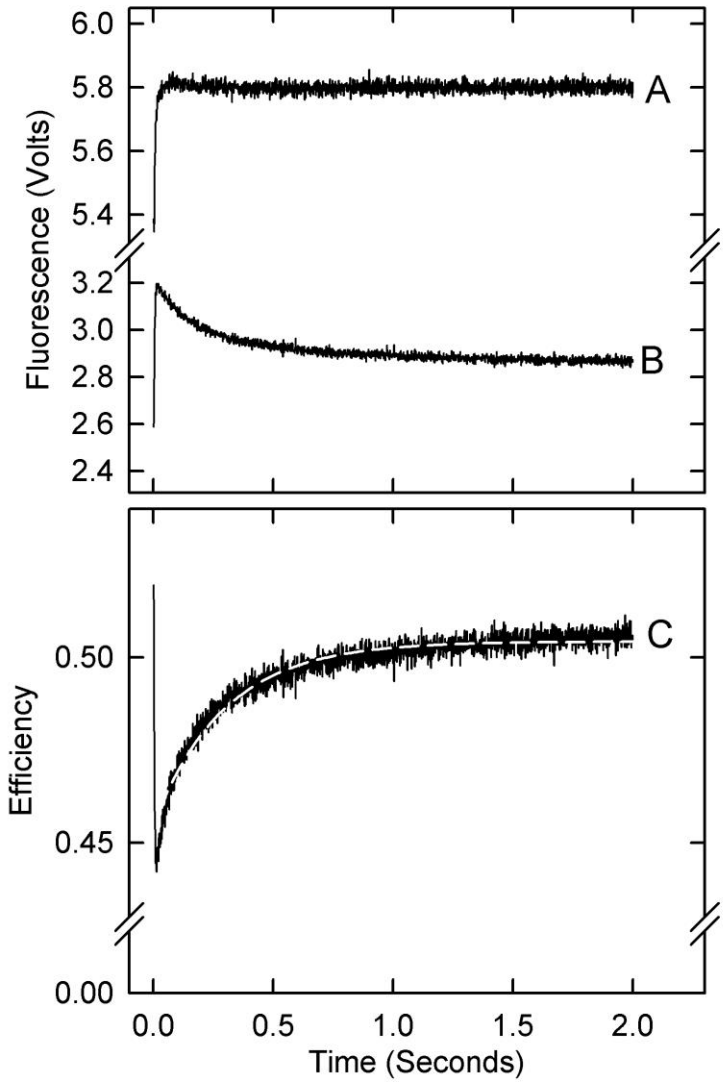

Figure 32: Time courses of IAEDANS 275C TnT fluorescence change in the absence and presence of a DABMI fluorescence acceptor probe on C190 of tropomyosin following the rapid detachment of myosin S1 from actin at very low Ca^{2+} concentrations. Traces shown are averages of at least three different measurements. Apparent rate: 3.4/second. Trace A, donor alone; B, donor and acceptor; C, efficiency. 2 µM actin, 0.51 µM tropomyosin, 0.43 µM troponin and 2 µM S1 in 20 mM MOPS, 152 mM KCl, 4 mM $MgCl_2$, 1 mM dithiothreitol and 2 mM EGTA was rapidly mixed with 2 mM ATP, 20 mM MOPS, 152 mM KCl, 8 mM $MgCl_2$, 1 mM dithiothreitol and 2 mM EGTA at 25° C. IAEDANS was excited using a 340 nm LED and the fluorescence monitored through a 435/451/460 filter.

We additionally monitored the fluorescence change of IAEDANS T143C troponin I as myosin S1 dissociated from actin in the absence (Figure 24A) and presence (Figure 24B) of an acceptor DABMI probe on tropomyosin. Since the locations of this inhbitory region of troponin I are well characterized, this experiment additionally measures the distance between tropomyosin and those known locations as actin is deactivated. As shown previously, these traces were replotted as efficiency versus time (Figure 24C). The efficiency of this pair also increased over the time course of the reaction. This indicates that IAEDANS T143C troponin I moves closer to DABMI C190 of tropomyosin as actin redistributes from the open O state into the closed and blocked states.

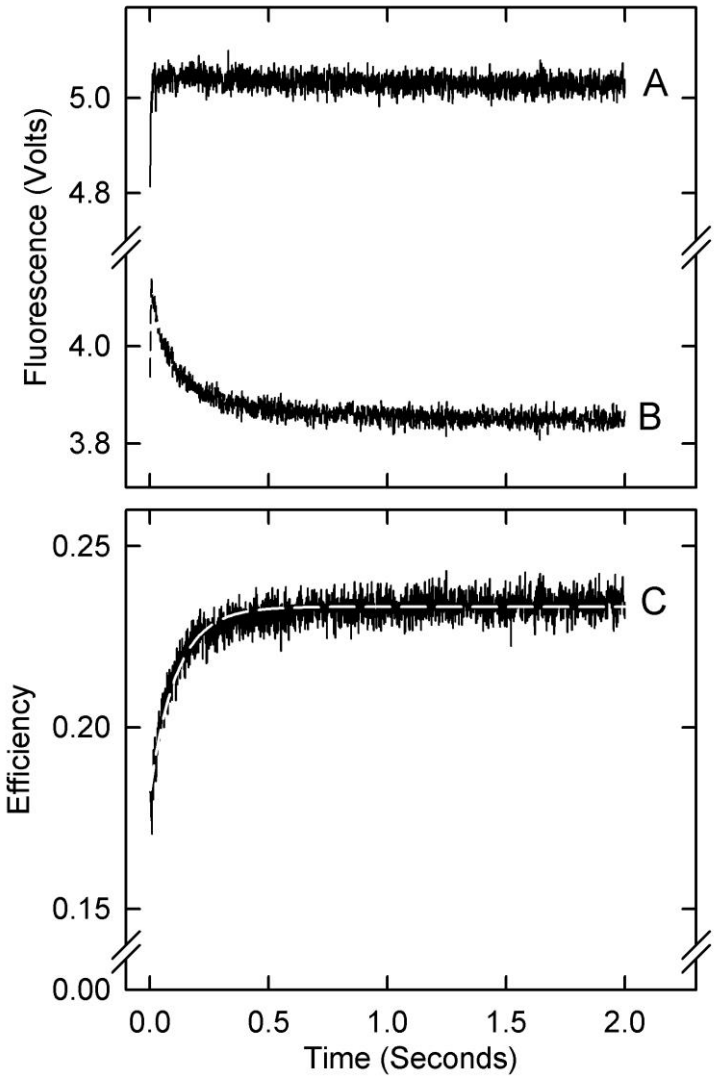

Figure 33: Time courses of IAEDANS T143C TnI fluorescence change in the absence and presence of a DABMI fluorescence acceptor probe on C190 of tropomyosin following the rapid detachment of myosin S1 from actin at very low Ca^{2+} concentrations. Traces shown are averages of at least three different measurements. Apparent rate: 8.9/second. Trace A, donor alone; B, donor and acceptor; C, efficiency. 2 µM actin, 0.51 µM tropomyosin, 0.43 µM troponin and 2 µM S1 in 20 mM MOPS, 152 mM KCl, 4 mM $MgCl_2$, 1 mM dithiothreitol and 2 mM EGTA was rapidly mixed with 2 mM ATP, 20 mM MOPS, 152 mM KCl, 8 mM $MgCl_2$, 1 mM dithiothreitol and 2 mM EGTA at 25° C. IAEDANS was excited using a 340nm LED and the fluorescence monitored through a 435/451/460 filter.

Table 9: Efficiency of transfer, distances and rates of FRET from IAEDANS to DABMI C190 tropomyosin from timecourses

	Efficiency initial	Efficiency final	Distance initial	Distance final	Rate*
IAEDANS TnT 275C 10° C	0.66	0.74	36	34	3.4(±0.1)
IAEDANS TnT 289C 10° C	0.29	0.46	46	41	7.0(±0.1)
IAEDANS TnT 289C 18° C	0.35	0.47	44	41	13.7(±0.3)
IAEDANS TnT 289C 25° C	0.41	0.49	42	40	25(±1)
IAEDANS HAHA TnT 289C 18° C	0.34	0.34	45	45	NA
IAEDANS TnI T143C 10° C	0.26	0.34	47	45	8.9(±0.2)

*Typical rate of acrylodan fluorescence transition is 7/second for wild type troponin regulated actin at 10° C. Error is standard deviation of fit to single exponential.

Part 3: Mutation in C-terminus of troponin T is coupled to Troponin I – Actin interaction. A structure-function relationship.

We found from our FRET measurement between IAEDANS T143C troponin I and DABMI C374 of actin, that the efficiency of transfer decreased with increasing calcium concentration. This indicated that the inhibitory region of troponin I was further from C374 of actin when the calcium concentration was higher. The location of that donor probe, T143C, is in the well characterized inhibitory region of troponin I that is known to interact with actin at low calcium concentrations and troponin C at saturating calcium concentrations. This is the result that we expected from this experiment as we observed the inhibitory region of troponin I apparently dissociating from actin. We had now developed a FRET sensor that could apparently directly monitor the binding of the inhibitory region of troponin I to actin.

We utilized this FRET sensor to monitor how mutation within the C-terminus of troponin T effects the interaction between the inhibitory region of troponin I and actin. We reconstituted IAEDANS T143C troponin I with ∆14 troponin T and wild type troponin C. We measured the FRET sensor at very low and saturating calcium in the absence and presence of the activating ∆14 troponin T mutant. At a very low calcium concentration, the FRET transfer efficiency was markedly lower for ∆14 troponin T regulated actin than that obtained when actin was regulated with wild type troponin T. This suggests that the inhibitory region of troponin I had weaker binding to actin or was bound differently so that the probes were further away when the C-terminal region of troponin T was missing.

At saturating calcium concentrations, the efficiency of transfer was also lower for ∆14 troponin T than for wild type troponin T regulated actin. In the wild type case, the

troponin I inhibitory region distance to actin increased as expected since the inhibitory region is known to dissociate from actin at saturating calcium. In the case of the Δ14 troponin T mutant, the distance from actin is even greater. One explanation is that at saturating calcium, the binding target for the C-terminus of troponin T is either different or in an altered position. That change is the key to understanding how removing the last fourteen residues of troponin T leads to activation.

We performed a calcium titration of this FRET sensor monitoring the inhibitory region of troponin I binding to actin. One purpose of this experiment was to determine if this FRET sensor functioned over the physiological calcium concentrations associated with calcium regulation. Additionally, by performing this titration we could determine if the Δ14 troponin T mutant affects the pCa_{50} or the hill coefficient of this FRET sensors calcium response.

We used a Ca-EGTA buffer to prepare the FRET sensor solutions at a variety of calcium concentrations with either wild type troponin T or Δ14 troponin T (Appendix C: Supplementary Data). After initial FRET measurements, the results were plotted to identify the necessary calcium concentrations for the solutions needed to obtain an accurate fit of the data. The resultant plot from this experiment is shown in Figure 34.

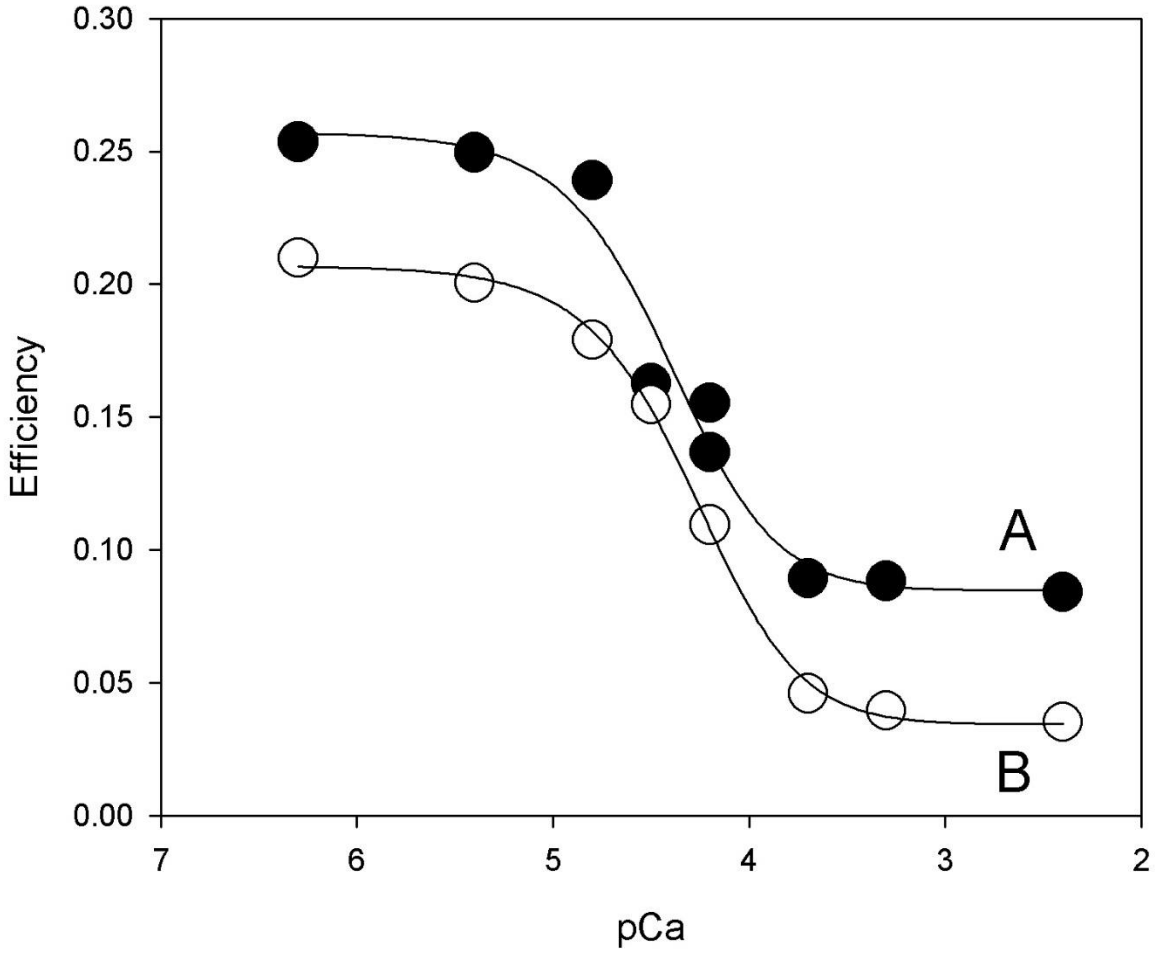

Figure 34: Calcium dependence of IAEDANS T143C TnI– DABMI C374 FRET pair in the absence (closed circles) and presence (open circles) of ∆14 TnT. Conditions of FRET measurements: 2 µM actin, 0.51 µM tropomyosin, 0.43 µM troponin in 20 mM MOPS, 152 mM KCl, 4 mM $MgCl_2$, 1 mM dithiothreitol and mixture of Ca^{2+}-EGTA buffer, Ca^{2+} and EGTA to reach desired pCa at 25° C. Excitation at 336 nm. Fluorescence integrated from 460-600nm. Slit widths were 3nm.

This plot shows the IAEDANS T143C troponin I – DABMI C374 actin efficiency versus the calcium concentration with wild type (closed circles, A) or ∆14 troponin T (open circles, B) troponin. The curve overlayed on each set of data is a fit to the Hill

equation. This fit gave a hill coefficient of 16.1 and 15.7 for wild type and Δ14 troponin T respectively. This indicated that the slope of the change in efficiency was lower in the Δ14 troponin T case. The movement of T143C troponin I relative to actin was less cooperative in the Δ14 troponin T case.

The pCa_{50} was 4.4 and 4.3 for wild type and Δ14 troponin T respectively. This indicated that the FRET sensor was less sensitive to calcium in the Δ14 troponin T case. A higher calcium concentration was required for movement of T143C troponin I relative to actin when Δ14 troponin T was present.

Part 4: Δ16 troponin T peptide in Myosin ATPase Assay

We purified a Troponin T peptide consisting of the last sixteen residues of the C-terminus of troponin T. The idea was to determine if this peptide could act as a small molecule modulator of the actin state distribution. We predicted this region would bind in a similar manner to the C-terminus of troponin T and either enhance the functional outcome of the C-terminus or compete for binding with the C-terminus and inhibition function.

We incorporated the peptide at varying concentrations into the myosin ATPase assay under the same conditions performed previously in Figure 21 in the presence of unregulated actin. Those results are shown in Figure 35. We found that as the peptide concentration was increased, the myosin ATPase rate decreased. This suggested that the peptide was binding to actin in such a way that inhibited actin stimulation of myosin ATPase activity.

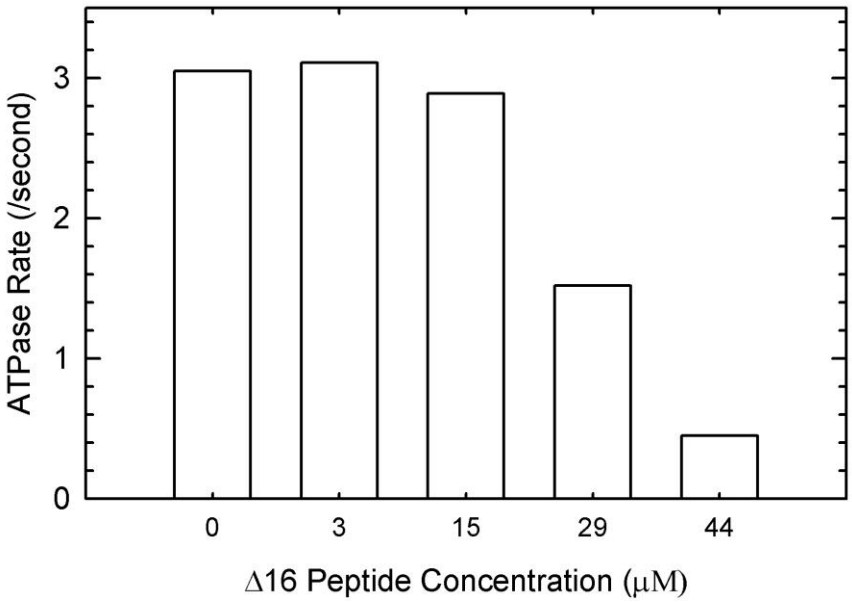

Figure 35: ATPase rates of myosin S1 in the presence of actin and different concentrations of the Δ16 troponin T peptide. Measurements were made at 25° C and pH 7.0 in solutions containing 1 mM ATP, 3 mM $MgCl_2$, 34 mM NaCl, 10 mM MOPS, 1 mM dithiothreitol and 0.1 mM $CaCl_2$. The concentrations of S1 and actin were 0.1 and 10 µM, respectively.

However, we noticed what appeared to be some precipitation in our reaction mixtures. A spin down assay was used to determine if this was in fact precipitation and if the precipitation correlated with the concentration of peptide added. The reaction mixtures were made as they were in the myosin ATPase assay experiment but excluding ^{32}P ATP and myosin S1. After thirty minutes, the mixtures were spun at 20,000 RPM in a rotor for 30 minutes in a Sorvall Legend Micro 21R centrifuge. The supernatant was carefully removed and 20 µL water was added to each tube. An SDS-PAGE gel was run for each of those samples. This gel revealed that as the peptide concentration was increased, a greater amount of actin was precipitated. The gel is shown in Appendix C: Supplementary Data.

Chapter 5 Discussion

Previous data from our lab demonstrated that the cardiomyopathy mutation Δ14 troponin T, missing fourteen residues from the C-terminus, produces marked changes in ATPase activity, binding of myosin S1 to actin, conformational changes associated with regulatory status, and contraction of muscle fibers. Those observations showed that Δ14 troponin T eliminated or substantially diminished the blocked state at very low calcium concentrations and stabilized the open O state at saturating calcium concentrations. These effects are presumably a result of changes to the interactions among the components of the regulatory complex of actin, tropomyosin and troponin. One goal of this project was to identify the specific residues within the C-terminus of troponin T that modify these interactions. The second primary goal of this project was to identify the interactions normally maintained by the C-terminus of troponin T and how those interactions are changed by mutation.

Stepwise elimination of C-terminus eliminates the blocked state in a graded manner

To identify the relative importance of each residue within the C-terminus, we developed and characterized a series of truncation mutants of troponin T. That truncation series included Δ4, Δ6, Δ8, and Δ10 troponin T, missing 4, 6, 8, and 10 residues from the C-terminus, respectively. In our characterization of that truncation series at very low calcium concentrations, we showed that all fourteen of those C-terminal residues are required for maintaining the blocked state. The number of residues removed from the C-terminus corresponded with progressive elimination of the

blocked state at very low calcium concentrations. Removal of all fourteen residues from the C-terminus appeared to be required to reach the maximal effect of reducing or eliminating the blocked state.

The different methods used to calculate the distribution of actin in the blocked state were in agreeance that the blocked state was diminished as successive residues were removed from the C-terminus. There was some discrepancy between the different methods as to the magnitude of elimination of the blocked state by each truncation mutant. Figure 36 shows a plot of the relative blocked state population for each truncation mutant by the three different methods used. The acrylodan (circles) and excess myosin S1 (squares) method are in general agreement for every truncation. The excess pyrene actin method (triangles) is in agreeance with the other two methods for truncations Δ4, Δ6, and Δ8. For truncations Δ10 and Δ14, the excess pyrene method produces a greater relative blocked state population than the other two methods.

The dashed line in Figure 36 is a representation of the blocked state population as a function of the number of residues deleted from the C-terminal of troponin T. By the acrylodan method of measuring the blocked state distribution, the first four residues from the C-terminus (residues 285-288) were disproportionately important in maintaining the blocked state at very low calcium relative to the other C-terminus residues. Those four residues (29% of the C-terminus composition) appear responsible for 50% of the blocked state stabilizing function of the C-terminus. Notably, those residues are particularly conserved in the already highly conserved C-terminus.

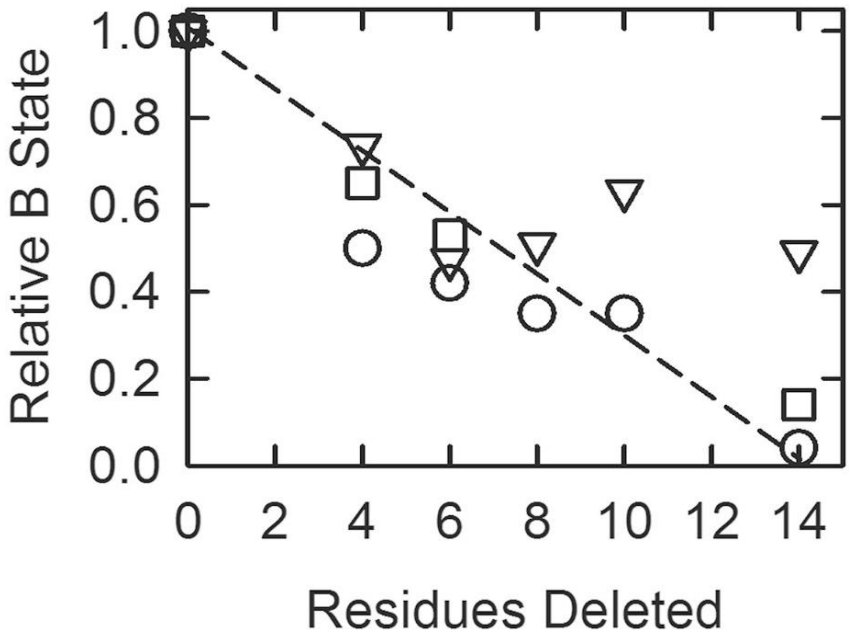

Figure 36: The fraction of actin filaments in the B-state relative to wild-type values at low Ca^{2+} for different troponin T deletion mutants. Values were calculated from acrylodan tropomyosin fluorescence amplitudes (circles), the duration of the lag in binding of excess S1 to actin (squares), and from Eq. 1 (triangles). The latter were calculated using a different rate of binding in Ca^{2+} for each deletion mutant. The dashed line shows the expected behavior if each residue pair contributed equally to the effect measured.

The assumptions used to calculate the blocked state population by the rate of S1 binding to regulated actin are invalid

Equations 3-5 are used to calculate the blocked state from the rate of binding of S1 to an excess of pyrene actin. Equation 4 is dependent on the assumptions that 1) the blocked state is absent at very low calcium concentrations and 2) myosin S1 binds at an approximately equal rate to the closed (C) and open (O) states. Differences in the value of k_{egta} are expected to dictate the relative blocked state population for each troponin mutant while the value of $k_{calcium}$ is expected to be equivalent for each troponin

mutant. The $k_{calcium}$ value is measured from the rate of binding of myosin S1 to excess pyrene actin at saturating calcium.

Contrary to the assumptions of equations 3-5, the rate of binding of myosin S1 to excess wild type pyrene-labeled actin filaments at saturating calcium, $k_{calcium}$, was not at a maximum value at saturating calcium. Rather the rate increased with each successive truncation of troponin T (Figure 20). Either the blocked state is not completely absent at saturating calcium and/or myosin S1 binds more rapidly to regulated actin in the open O state. The former possibility is unlikely as we see no acrylodan fluorescence increase signaling the appearance of the blocked state at saturating calcium (Figure 17).

The relative amount of blocked state calculated from the binding of myosin S1 to excess pyrene actin (triangles) in Figure 36 was calculated using equations 3-5. The deviation of those triangles from other measurements is due to the invalid assumptions made in deriving those equations. Although this method may still be useful for demonstrating relative changes in the blocked state distribution, calculation of the relative blocked state or absolute blocked state using those equations is invalid. This brings into question all of the published data that use this assay to measure the blocked state distribution of different mutants. The Geeves[30] model has been a popular substitute for the more complex Hill[29,85] model. It will be necessary for those who have used the Geeves method to re-evaluate their data.

By globally fitting the rate of myosin S1 binding to excess pyrene actin at very low and saturating calcium, we determined the rates of binding to the blocked, closed and open states to be 3, 6, and 13/sec, respectively. However, each of the traces could not be fit accurately using only two rate constants. Each of the traces at either very low

or saturating calcium concentrations could be fit using those three rate constants. These rate constants could be used to estimate the distribution of the three actin states. However, due to the relatively small differences (approximately 2-fold) between the rates of binding to each state, there is no unique fit to the three amplitudes. For this reason, we cannot accurately calculate the absolute state distribution for each mutant using this method.

Because of this evidence that the myosin S1 binding to excess pyrene actin method is invalid in calculating the absolute blocked state distribution, there is no longer a reliable method of calculating this absolute value. The two other methods used in this project, acrylodan tropomyosin fluorescence and excess myosin S1 binding to pyrene actin, only produce relative distributions in the blocked state. Each of these methods requires a standard value to convert the relative values into absolute values. If we knew the blocked state distribution of wild type troponin regulated actin, we could standardize our acrylodan traces to that value and calculate the state distributions. A future goal for research on contraction regulation will be to find independent methods of measuring the B state.

A possible standard for the blocked state is troponin containing S45E TnI. This is the most inactivating troponin mutant yet observed and it is likely to approach 100% blocked state. This mutant produced an acrylodan tropomyosin fluorescence change corresponding to the closed to blocked transition that was 136% of that with wild type troponin regulated actin[47]. If we assume that mutant stabilized actin nearly 100% in the inactive state, this would allow us to calculate that wild type regulated actin is approximately 73% in the blocked state at very low calcium concentrations and this

value could be used as the standard for converting relative acrylodan fluorescence change values to absolute blocked state populations. To validate this method, we would need to identify a way to verify that the S45E TnI mutant is entirely or nearly entirely in the blocked state. This could possibly be done by using two mutations that each stabilize the blocked state. We showed earlier that the effects of multiple mutations is often additive[69,78].

Stepwise elimination of C-terminus stabilizes the open state in a graded manner

The number of residues removed from the C-terminus also corresponded with progressive stabilization of the open state at saturating calcium concentrations. Removal of all fourteen residues produced about 70% occupancy of the O state at saturating calcium[78]. This is the maximum stabilization that can be obtained through alterations of the C-terminal region of troponin T. That is, all fourteen residues of the C-terminus of troponin T contribute to destabilizing the O state. The last four residues of the C-terminus (residues 285-288) also appeared particularly important for maintaining the open state. Those four residues (29% of the total C-terminus composition) appear responsible for 40% of the open state destabilizing function of the C-terminus (Figure 21).

We had hypothesized that a specific residue or few residues could be attributed to the entire or majority of the C-terminus function of maintaining the blocked and open states. This however, was not the case. Though the terminal four residues (residues 285-288, GRWK) contribute slightly more to this maintenance than the other ten residues (residues 275-284), all fourteen residues make an impact on both the blocked

and open state distributions. Truncation from the highly basic C-terminus corresponded with elimination of positively charged residues. Evidence from our truncation study suggested the positive charge of this region are critical for its function. Additionally, a hypertrophic cardiomyopathy associated mutation within this region, R278C troponin T, exhibits increased calcium sensitivity and force development[86]. These qualities are indicators of stabilization of the open state. Notably, this R278C troponin T mutation eliminates one of the basic charges within the C-terminus.

Basic residues within the C-terminus of troponin T are responsible for stabilizing the blocked state and destabilizing the open state

Based on evidence from the truncation study we developed a troponin T construct where the basic residues within the C-terminus were eliminated via substitution with alanine. For this construct, the seven lysine and arginine residues within the 16 C-terminal residues were substituted with alanine to eliminate all of the positive charge within the region. Additionally, we attached a cysteine residue to the C-terminus, extending the length of the protein by one amino acid. We named this construct HAHA troponin T for high alanine, high activity. The high activity portion of the name was added only after we found the mutant did in fact enhance activity.

Using the acrylodan method, we found the HAHA troponin T construct eliminated the blocked state at low calcium concentrations. Using the pyrene method, we similarly observed a decrease in the blocked state as evidenced by an increase in the rate of binding of myosin S1 to excess pyrene actin regulated by HAHA troponin T relative to that produced with wild type troponin T. Using the myosin ATPase assay, we found the

HAHA troponin T construct stabilized the open state at saturating calcium concentrations.

By each of our measures of the actin state distribution, HAHA troponin T was indistinguishable from our functional measures of Δ14 troponin T regulated actin. Results from these assays with HAHA troponin T suggested that the basic charges within the C-terminus of troponin T are fundamental to its maintenance of the blocked state and the open state. Those basic residues stabilize the blocked state at very low calcium concentrations and destabilize the open state at saturating calcium concentrations.

By eliminating basic residues within the C-terminus, we approximated the effect expected by addition of the negative charge associated with phosphorylation. In doing so, we showed a dramatic change in the state distribution that highlighted the significance of the charge balance of the C-terminus. Though the C-terminus residues 275 and 284 can be phosphorylated via ROCKII or PKC, the physiological relevance of phosphorylation of those residues is unclear as they were not identified to be phosphorylated in mass spectrometric analysis of human tissue or mouse tissue[68]. Pseudophosphorylation by the mutation T285E troponin T has been shown to increase the calcium sensitivity corresponding with destabilization of the blocked state[87]. However, pseudophosphorylation by the mutation T287E did not exhibit any change in measures of tension or ATPase rate[88]. While the physiological relevance of phosphorylation of the C-terminus is questionable, phosphorylation may disrupt the normal mechanism of the C-terminus and shift actin to a more active state in a similar manner to that observed with elimination of the basic residues.

Basic residues within the C-terminus of troponin T increase the K_M of actin

The classical steric blocking model states that troponin places tropomyosin into a position on actin that blocks the myosin binding site. The observation that regulatory proteins are able to increase the ATPase rate to a level higher than unregulated actin is not readily explained by that model. We are interested in the mechanism by which troponin and tropomyosin activate stimulation of the myosin ATPase

Addition of calcium to regulated actin increases the V_{max} of ATPase by 20-fold relative to low calcium conditions but only decreases the K_M by 2-fold and leaves the affinity of S1-ATP for actin relatively unchanged[89]. However, calcium does not give fully activity and only stabilizes actin 30% in the open state[78]. Actin remains 70% in the closed state at saturating calcium. What changes occur going from the closed to the open state that are required for fully activity?

Using N-ethylmaleimide S1 (NEM-S1), to stabilize actin in the fully active state, Williams *et al.* observed that actin in the fully active state produced a greater V_{max} and a lower K_M than regulated actin in the presence of calcium[90]. Those experiments present complications in that NEM-labeled S1 is used at high levels that act as a competitive inhibitor of S1-ATP binding. Thus, rather large corrections must be applied to the data. We took advantage of the troponin mutant A8VΔ14 to stabilize the open state. Using troponin to stabilize the open state does not require corrections.

Our observed V_{max} was 35 (±4) and 35 (±8) /second for unregulated actin and A8VΔ14 regulated actin respectively. There was no appreciable change in the Vmax. The K_M was 258 (±49) and 90 (±36) for unregulated actin and A8VΔ14 regulated actin, respectively. The K_M decreased significantly when actin was regulated by A8VΔ14

troponin indicating that the transition from the closed to the open state population are the result of a decrease in the K_M .This K_M decrease agrees with that reported previously with NEM-S1 stabilized filaments[90].

In muscle cells, the actin concentration is well beyond the K_M (up to 10 mM) and the rates should be near Vmax[91]. However, the Vmax may only be achieved when calcium is saturating. The sarcoplasmic reticulum regulates the calcium concentration in the cytosol of cardiac myocytes. With each heartbeat, the calcium concentration fluctuates between approximately 0.1 and 1 μM[92]. Even though the actin concentration in cardiac myocytes is near that required to reach the Vmax, the rate is also dependent on calcium reaching maximum saturation and possibly the presence of other activators not found in solution studies.

These troponin mutations that apparently effect the K_M should not appreciably affect the myosin ATPase rate when calcium is maximally saturating. The limits of sarcoplasmic reticulum control of calcium concentration are between approximately 0.1 and 1 μM, however, that change is not instantaneous and the calcium concentration for some amount of time is intermediate to those limits. As well, those intermediate calcium concentrations may be more relevant in defects where elevation and/or removal of calcium from the cytosol are impaired.

Both Δ14 and HAHA troponin T are convenient tools for stabilizing the active state of regulated actin. Δ14 troponin T has been exchanged into permeabilized skeletal and cardiac muscle fibers resulting in increased calcium sensitivity and decreased cooperativity of force production[93]. More recently, our colleague Dr. Jose Pinto has exchanged Δ14 troponin T into skinned trabeculae resulting in increased calcium

sensitivity and increased basal force (unpublished). Other colleagues, Drs. John Robinson and Christopher Solis-Ocampo showed actin filaments regulated by ∆14 troponin T produced a 1.8x increase in speed of movement in the in vitro motility assay (unpublished).

The fiber data were collected at conditions that more closely resemble the conditions found in a cell where the actin concentration is significantly higher. It has yet to be shown whether C-terminus mutation can affect the maximal force production in muscle fibers.

The C-terminus of troponin T may interact with tropomyosin in a calcium dependent manner

The previous studies using FRET to map distances within the thin filament take a global approach of mapping a variety of distances between actin, tropomyosin, and troponin subunits for use as constraints in molecular modelling[34,75–77,94,95]. Our study took a more focused approach to specifically measure distances from the C-terminus of troponin T. Our distances will ultimately be merged with those from other groups and used as constraints in molecular modeling simulations. We will not be able to fully analyze our results until those simulations are complete, but we can make conclusions based on the individual distance measurements in the context of what we already know about the interactions of actin, tropomyosin and troponin subunits.

One primary goal of this project was to identify the specific residues of the C-terminus of troponin T that modify the interactions of the C-terminus. We have now identified the basic residues of the C-terminus as being vital to function. The second

primary goal of this project was to identify the interactions of the C-terminus of troponin T and how mutation affects those and other known interactions.

Our leading hypothesis is that residues near 275C in the C-terminus of troponin T have a high affinity for tropomyosin at low calcium and a low affinity at saturating calcium concentrations. Residues near 288K of troponin T have a low affinity for tropomyosin that is less dependent on calcium concentration. Based on this hypothesis, stabilization of the blocked state by the C-terminus occurs through a direct interaction that restrains tropomyosin primarily in that blocked position along actin. We propose the C-terminus of troponin T is in a more folded, less extended state that holds tropomyosin closer to troponin at low calcium concentrations.

With an increase in calcium, we believe the C-terminus undergoes a decrease in folding and becomes more extended. This more extended conformation with an increase in calcium has been suggested previously[77]. Residues near 275C of troponin T dissociate from tropomyosin and release tropomyosin from the blocked state position along actin. Residues near 288K of troponin T remain bound to tropomyosin and limits actin to 30% open state population.

We created a simple scheme to model our interpretation of our data in the context of the known interactions within actin-tropomyosin-troponin (Figure 37). The C-terminus of troponin T is represented in pink and emerges from the IT-Helix (pink with blue outline). The star indicates the approximate location of the very C-terminal residue 288K of troponin T. The colored slices on actin represent the blocked (red), closed (yellow) and open (green) states that tropomyosin (grey) can occupy along actin.

At low calcium concentrations on the left-hand side of Figure 37, the C-terminus of troponin T is in a more folded conformation with extensive interaction with tropomyosin. The inhibitory region (Ip) of troponin I is bound to actin and the hydrophobic pocket on troponin C is not exposed. Tropomyosin is primarily in the blocked state position along actin with some population in the closed state.

At saturating calcium concentrations of the right-hand side of Figure 37, the hydrophobic pocket of troponin C is opened and the regulatory or switch (Sw) region of troponin I is bound to that pocket. The inhibitory region of troponin I is dissociated from actin and interacts with troponin C. Binding of the switch region and inhibitory region of troponin I to troponin C causes a conformational change in the IT-helix that is immediately adjacent to the inhibitory region of troponin I. The conformational change of the IT-Helix induces a conformational change in the C-terminus of troponin T where residues near 275 of troponin T are positioned closer to troponin C. Calcium induced changes in troponin C expose interaction sites with residues near 275 of troponin T to stabilize C-terminus in this conformation.

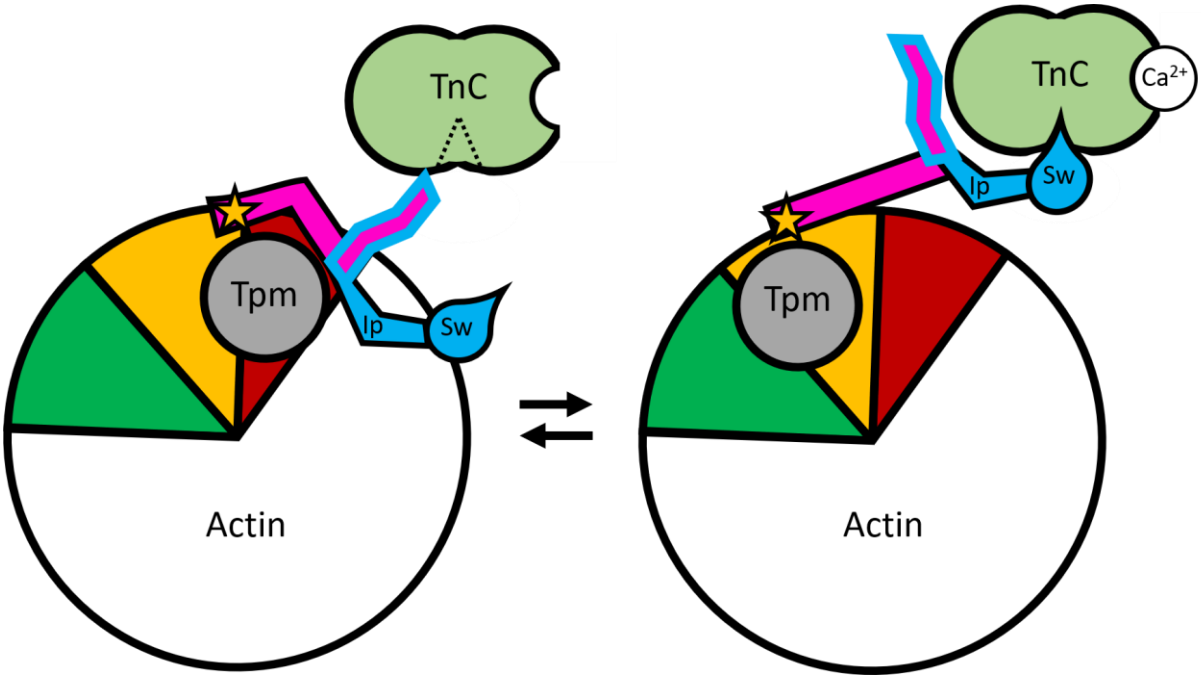

Figure 37: Scheme for our proposed model of the Interactions of the C-terminus of troponin T at low (left) and saturating calcium (right). The large circle represents a single actin monomer viewed looking down a strand of polymeric actin. The colored slices in the circle represent the blocked (red), closed (yellow), and open (green) positions that tropomyosin (grey) can occupy along actin. The C-terminus of troponin T is shown in pink and the star indicates the approximate location of the last terminal residue 288K. The IT-Helix is represented by the pink shape with blue outline. Ip is the inhibitory peptide (or inhibitory region) of troponin I. Sw is the switch region (or regulatory region) of troponin I. Troponin C (TnC) is shown in light green. The dotted section of troponin C without calcium bound represents the hydrophobic patch that opens in response to calcium binding. For simplicity, many protein regions are not shown. One omission is the mobile region of troponin I that interacts with tropomyosin at low calcium but dissociates at saturating calcium.

Changes in the C-terminus conformation resulting from repositioning of the IT-Helix and binding to troponin C stabilize the C-terminus in a more extended conformation. Residues near 288 of troponin T are less dependent on calcium and

remain associated with tropomyosin. The extended conformation allows tropomyosin to move out of the blocked state in response to calcium and partially into the open state. The interaction between residues near 288 of troponin T and tropomyosin limits open state occupancy at saturating calcium.

When the basic residues of the C-terminus of troponin T are eliminated (as in ∆14 or HAHA troponin T), the interaction with tropomyosin is eliminated. At low calcium concentrations, the basic residues of the C-terminus are not available to restrain tropomyosin in the blocked position. Tropomyosin is stabilized almost entirely in the closed position at low calcium concentrations because calcium is still required to relieve some of the other restraints imposed by troponin on the tropomyosin position. When the basic residues of the C-terminus are eliminated at saturating calcium, the open state is stabilized to a greater extent than with wild type troponin because the interaction between residues near 288 of troponin T with tropomyosin are eliminated.

Evidence in support of this model (Figure 37) come from our and from the work of others. For the FRET pair between IAEDANS 275C troponin T and DABMI C190 of tropomyosin, we measured a transfer efficiency of 0.86 and 0.55 at very low and saturating calcium respectively. From this efficiency we calculated a distance of 30 and 39 Å at very low and saturating calcium respectively. The very high transfer efficiency at a very low calcium concentration suggested the possibility that those two locations may interact or are at least close to one another. The large increase in distance for the FRET pair between IAEDANS 275C troponin T and DABMI C190 of tropomyosin suggested that these two regions moved away from each other with an increase in calcium.

IAEDANS 289C troponin T was measured to be further away from C190 tropomyosin at low calcium compared to 275C troponin T. The magnitude of the change in distance between 289C troponin T and C190 tropomyosin however was not as large as that for 275C troponin T. This indicated that the distance between 289C troponin T and C190 tropomyosin was not as significantly affected by calcium.

Because the inhibitory region of troponin I is immediately adjacent to the IT-Helix, binding of the inhibitory region to troponin C may result in a reorientation of the IT-Helix that repositions or changes the conformation of the C-terminus of troponin T. Molecular dynamics simulations provided evidence that a hydrogen bond forms between troponin T residue R278 and troponin C residue D151 in the calcium saturated state[77]. However, this movement of troponin T to troponin C must be verified experimentally. Alternatively, calcium induced changes in troponin C may expose residue D151 for hydrogen bonding to R278 of troponin T. This interaction may in turn induce binding of the regulatory region and inhibitory region of troponin I to troponin C.

We observed a relatively high efficiency of transfer between IAEDANS 275C troponin T and DABMI T143C troponin I at low and saturating calcium. This supports the idea that those region's movement is concerted and that residue 275C of troponin T is repositioned onto troponin C along with repositioning of the inhibitory region of troponin I. A relationship between the inhibitory region of troponin I and the C-terminus of troponin T is also supported by evidence that a troponin T C-terminus mutation (R278C) can recover loss of function to a troponin I inhibitory region mutation (R145G)[69].

A chymotryptic fragment corresponding to cardiac troponin T residues 268-288 was shown to interact with whole troponin I using affinity chromatography, gel filtration, and circular dichroism[96]. This interaction was weaker than with the troponin T fragment (residues 205-259) containing the IT-Helix domain but this indicated that troponin T and troponin I may interact weakly beyond the C-terminus of the IT-Helix. Though this interaction is weak, it may assist in keeping the C-terminus of the inhibitory region close for a concerted calcium response.

Our model requires that the known calcium responses of troponin (hydrophobic pocket of troponin C opening, dissociation of troponin I inhibitory region from actin, binding of troponin I regulatory and inhibitory regions to troponin C) are functional regardless of the presence of basic residues within the C-terminus. This is because troponin must inhibit entry into the open state even when the basic residues of the C-terminus are eliminated. We observed that the distance between troponin I T143C and actin C374 was dependent on the presence of ∆14 troponin T at low and saturating calcium concentrations. The distance for wild type troponin at saturating calcium (58 Å) with ∆14 troponin T at low calcium (50 Å). Although ∆14 troponin T causes some apparent destabilization of the interaction between troponin I and actin, ∆14 troponin T does not eliminate the binding of troponin I inhibitory region to actin.

Time courses of FRET efficiency changes suggests concerted calcium response

The change from the initial efficiency to the final efficiency for the FRET pair between IAEDANS 275C troponin T and DABMI C190 of tropomyosin occurred with a rate of 7.0/second. That value corresponds to the rate of the movement of IAEDANS

275C troponin T and DABMI C190 of tropomyosin relative to one another as actin redistributes from the open state into the closed and blocked states. One of the steps in determining the mechanism of the C-terminus function, is to identify the order of events involved in activation and which appear to be coupled and occur simultaneously. Using the acrylodan probe on tropomyosin, we previously measured that for wild type troponin regulated actin, the closed to blocked state transition occurs at a rate of 6.8/second. The rate of the closed to blocked transition occurs at a nearly equivalent rate to that of the movement of 275C troponin T relative to C190 of tropomyosin. This similarity in rate suggests that the movement of 275C troponin T relative to C190 of tropomyosin is simultaneous with the transition of actin from the open state into a mixture of the closed and blocked states.

The time course of the efficiency change as actin redistributes from the open state into the closed and blocked states was also measured for the FRET pair IAEDANS 289C troponin T with DABMI C190 of tropomyosin. As with the steady state efficiency measurements, this FRET pair is closer when actin is in a more active state although farther apart than the IAEDANS 275C troponin T – DABMI C190 tropomyosin pair. The rate of the transition of these two regions relative to each other is 7.0/second at 10° C indicating this transition also occurs in concert with redistribution from the pen state into the closed and blocked states.

This transition was greatly altered when the basic residues in the C-terminal region of troponin T was replaced with alanine residues. Upon myosin S1 dissociation from actin, the IAEDANS HAHA 289C troponin T-DABMI C190 tropomyosin FRET pair does not exhibit the efficiency change that was observed for the IAEDANS 289C

troponin T-DABMI C190 tropomyosin FRET pair. The efficiency stays relatively constant throughout the redistribution of actin from the O state to the C state. Elimination of this efficiency change over the time course of the reaction is the result of no change in distance between 289C troponin T and C190 tropomyosin due to elimination of the basic residues in the C-terminus of troponin T. This distance change may only occur between the closed and blocked states. As the blocked state is eliminated for HAHA troponin T regulated actin, that distance change was not observed.

Development of a FRET sensor to measure troponin I inhibitory region binding to actin

The FRET pair between IAEDANS T143C Troponin I and DABMI C374 of actin was chosen in part to develop a FRET sensor to monitor the binding of the inhibitory region of troponin I to actin. Residue T143C is in the inhibitory region of troponin I that is known to bind actin at low calcium concentrations and dissociate as the calcium concentration increases. We calculated a distance of 48 and 58 Å at very low and saturating calcium, respectively. This increase in distance as calcium increases corresponds with dissociation of the inhibitory region of troponin I from actin.

This FRET sensor may be useful in measuring how troponin mutation affects the mechanism of the inhibitory region of troponin I binding actin. The distance between these two regions may also be useful in calculating the actin state distribution if the distance is known for actin stabilized in each state. One of the primary goals of this work is identifying the mechanism of disruption to the actin state distribution by mutation in the C-terminus of troponin T. We tested this sensor in the presence of the activating

Δ14 troponin T mutant. Because that mutation eliminates the blocked state, we hypothesized the interaction of the inhibitory region of troponin I with actin would be disrupted.

The FRET pair between IAEDANS T143C Troponin I and DABMI C374 of actin in the presence of Δ14 troponin T resulted in an increase in distance, compared with wild type, from 48 to 50 Å at very low calcium and from 58 to 68 Å at saturating calcium. At low and saturating calcium concentrations, the distance of the FRET sensor is greater when Δ14 troponin T is present, indicating that mutation in the C-terminus of troponin T is coupled to interruption of the binding of the inhibitory region of troponin I to actin. Though the distance is increased resulting from Δ14 troponin T, we do not believe Δ14 troponin T has eliminated this regulatory mechanism.

We measured this FRET sensor IAEDANS T143C Troponin I and DABMI C374 of actin with and without Δ14 troponin T present at several calcium concentrations to determine whether this FRET sensor is responsive over physiologically relevant calcium concentrations. Additionally, we sought to determine whether the presence of Δ14 troponin T affected the calcium sensitivity of the interaction of the inhibitory region of troponin I with actin. Figure 34 shows a plot of this experiment where the efficiency is plotted versus the calcium concentration.

Those data were fit with a Hill equation to determine the pCa50 and Hill coefficient (cooperativity) of the calcium titration. The pCa_{50} was determined to be 4.4 and 4.2 in the absence and presence of Δ14 troponin T respectively. This indicated that this FRET sensor is responsive near the physiological range of calcium concentrations associated with deactivation and activation. The Hill coefficient was reduced from 16.1

to 15.7 with Δ14 troponin T which indicated the transition was slightly less cooperative. Rat cardiac skinned trabeculae produced a hill coefficient of 4.3 and 4.2 for wild type and Δ14 troponin T respectively[97] which agreed with the trend we observed.

The pCa_{50} values indicate that the mutation resulted in a decrease in the calcium sensitivity of the movement of T143C troponin I relative to actin C374. Although the difference in sensitivity is small, it is in opposition to the increase in calcium sensitivity previously with Δ14 troponin T. Rat cardiac skinned trabeculae produced a pCa50 of 5.25 and 5.45 for wild type and Δ14 troponin T, respectively[97]. As previous measures of pCa_{50} were completed in skinned fibers, it is possible that this discrepancy is a result of proteins and geometric constraints that are absent in our solution studies.

This FRET pair between T143C of troponin I and C374 of actin appears useful in measuring the binding of the inhibitory region of troponin I to actin. One disadvantage of this FRET pair is that the efficiency of transfer is low even at low calcium concentrations. Because we know that the inhibitory region of troponin I binds to actin at low calcium concentrations, we would expect a greater transfer efficiency. However, the DABMI probe on actin in this FRET pair is likely in a location distant from the inhibitory region binding site.

An ideal FRET pair would produce a transfer efficiency closer to 0.5 as this value is at the R_0 for a particular FRET pair which can more accurately predict the distance. At very low or very high efficiency values, small changes in efficiency produce large changes in distance. A different acceptor location on actin might produce a greater transfer efficiency with the IAEDANS probe on T143C of troponin. This is more complicated than using the native easily targeted cysteine 374 of actin. A FRET sensor

between the C-terminus of troponin T and actin residue Q41 has been shown to exhibit a high transfer efficiency[34]. That location of actin may be a more ideal acceptor location for measuring the interaction between the inhibitory region of troponin I and actin.

Use of FRET to validate structure-function relationships and potential for use in calculating state distributions

Δ14 troponin T produces a different distribution of states than wild type troponin T. At low calcium concentrations, actin filaments containing wild type troponin T are primarily in the blocked state, but they are in the closed state with Δ14 or HAHA troponin T. At saturating calcium, wild type filaments are in a mixture of 70% closed and 30% open states whereas Δ14 or HAHA troponin T containing filaments are 30% closed and 70% open.

If the motion of the C-terminus of troponin T occurs along a straight trajectory, one can estimate the distance between the inhibitory region troponin I residue T143C relative to actin in each actin state. Wild type troponin regulated actin at low calcium concentrations is primarily in the blocked state and produces a T143C Troponin I - C374 actin distance of 25 Å. Δ14 troponin T regulated actin at low calcium concentrations should be almost entirely in the closed state and produces a T143C Troponin I - C374 actin distance of 50 Å. Wild type troponin at saturating calcium produces a T143C Troponin I - C374 actin distance of 58 Å. We can calculate the distance between T143C troponin I and C374 of actin in the open state using these distance values for the blocked and closed state.

Using the equation 58 Å = 0.7*50 Å + 0.3*M Å we can calculate that the open state distance is 77 Å. Similarly, Δ14 troponin T regulated actin produces a T143C Troponin I - C374 actin distance of 68 Å. Using the equation 68 Å = 0.3*50 Å + 0.7*M Å we can calculate that the open state distance is 76 Å.

We will use molecular dynamics modeling with Dr. Yumin Li (East Carolina University Chemistry Department) to estimate the distances using different probes and generate a more realistic model. It should be possible, as shown in the simple example here, to calculate the distribution of states from FRET analyses. This should solve the problem of calibrating the acrylodan-tropomyosin and pyrene-actin fluorescence changes discussed earlier.

The C-terminus of troponin T does not bind near actin C374 but may bind elsewhere on actin

The FRET pair between IAEDANS 275C troponin T and DABMI C374 of actin produced a distance of 48 and 55 Å at very low and saturating calcium, respectively. The FRET pair between IAEDANS 289C troponin T and DABMI C374 of actin produced a distance of 56 and 58 Å at very low and saturating calcium, respectively. Neither 275C or 289C of troponin T appear to interact near residue 374C of actin at low or saturating calcium concentrations.

The FRET pair between IAEDANS HAHA 289C troponin T and DABMI C374 of actin was investigated to identify how elimination of the basic residues within the C-terminus of troponin T affected the possible interaction between the C-terminus and the

highly negatively charged surface of actin. We calculated a distance of 65 and 63 Å at very low and saturating calcium, respectively.

As the calcium concentration increases from very low to saturating, we know for wild type troponin regulated actin, that the blocked state is eliminated, and actin redistributes primarily into the closed state. During this calcium induced redistribution, residue 275C and 289C of troponin T move further from actin C374. For ∆14 or HAHA troponin T regulated actin, the blocked state is eliminated at low calcium concentrations. The distance between IAEDANS HAHA 289C troponin T and DABMI C374 of actin at low calcium concentrations is greater than the wild type 289C distance at saturating calcium. Although the C-terminus does not appear to interact near actin C374, the distance is affected by elimination of the blocked state.

Because the distance for the FRET pair actin C374 - troponin T 275C is lower than that of the FRET pair actin C374 – troponin T 289C, this suggests that the C-terminus is oriented in a manner where residue 289C is farther from C374 actin and residue 275C extends toward C374 of actin. Molecular modelling simulations will be performed using these distances as constraints to better predict the orientation of the C-terminus relative to actin.

Though our FRET data does not suggest binding of the C-terminus of troponin T near C374 of actin, this does not mean the C-terminus could not bind elsewhere on actin. Of note is that the distance measured between the inhibitory region of troponin I and C374 of actin also did not suggest binding at that site, although we know the inhibitory region binds actin at low calcium concentrations. This hypothesis that the C-terminus of troponin T interacts with actin is based on the observation of spatial and

sequence homology of the C-terminus of troponin T with the inhibitory region of troponin I that is known to bind actin[69].

We additionally presented evidence that a peptide consisting of the C-terminal sixteen residues of troponin T decreased the ATPase rate of unregulated actin in a concentration dependent manner. We showed this was the result of the peptide causing actin to precipitate. This is likely the result of the highly basic C-terminal residues of troponin T binding to the negatively charged surface of actin and making it insoluble. This does not prove that actin is the binding site for the C-terminus of troponin T as many positively charged peptides likely would cause the same outcome. However, this does show that the C-terminus has the potential to bind actin. Whether that interaction is physiologically relevant is still to be identified.

Summary of Conclusions from Each Individual FRET pair

For each FRET pair, we obtained a distance that will be used as constraints in molecular modelling simulations to map the crystal structure of troponin and tropomyosin onto actin. In Table 5, the justifications for each of our FRET pair choices was summarized. Table 10 and Table 11 below summarize the conclusions regarding those justifications based on our data.

Table 10: Conclusions regarding justifications for FRET experiments where DABMI C374 actin is the acceptor

Donor	Acceptor	Result
TnT 275C	C374 of actin	275C of TnT does not appear close enough to interact specifically near C374 of actin though it could interact elsewhere on actin. 275C is closer to C374 of actin than 289C at low calcium concentrations. The distance from this actin location increases with increasing calcium concentration.
TnT 289C	C374 of actin	289C of TnT does not appear close enough to interact specifically near C374 of actin though it could interact elsewhere on actin. 289C is further from C374 of actin than 275C at low calcium concentrations The distance from this actin location increases with increasing calcium concentration.
HAHA TnT 289C	C374 of actin	Elimination of the positively charged residues within the C-terminus of TnT shifts the C-terminus further from this location on actin. The low calcium distance of HAHA TnT resembles that of wild type TnT at saturating calcium
TnI T143C	C374 of actin	The efficiency of transfer is lower at saturating calcium. This agrees with the mechanism of the inhibitory region of TnI dissociating from actin at higher calcium concentrations
TnI T143C Δ14 TnT	C374 of actin	The inhibitory region is further from actin at low calcium concentrations when in the presence of the activating Δ14 TnT mutant. TnT mutation is coupled to inhibitory region binding to actin

Table 11: Conclusions regarding justifications for FRET experiments where DABMI C374 actin is the acceptor

Donor	Acceptor	Result
TnT 275C	C190 of Tpm	These two locations are close and direct interaction may be near these residues. Distance is greater at saturating calcium. 275C is closer than 289C to Tpm C190 at saturating calcium
TnT 289C	C190 of Tpm	These two locations are close and direct interaction may be near these residues. Distance is greater at saturating calcium.
HAHA TnT 289C	C190 of Tpm	Distance is greater in the presence of the activating HAHA TnT mutant. Removal of basic residues disrupts this interaction.
TnI T143C	C190 of Tpm	The distance between inhibitory peptide binding site on actin and Tpm at very low calcium concentrations is approximately 34 Å. The distance between the TnI binding site on TnC and Tpm at saturating calcium concentration is approximately 40 Å
TnI T143C Δ14 TnT	C190 of Tpm	The ∆14 TnT mutant causes the distance between actin inhibitory region and Tpm C190 to increase or the TnI inhibitory region binding to actin is disrupted at low calcium. Also causes the distance between the TnI binding site on TnC and Tpm C190 to increase or the TnI inhibitory region binding to TnC is disrupted at saturating calcium.
TnT 275C	143C of TnI	275C of TnT and inhibitory region of TnI have relatively high transfer efficiency. The two regions may have a shared function. The distance between these two locations is independent of calcium concentration.
TnT 289C	143C of TnI	289C of TnT and inhibitory region of TnI have relatively high transfer efficiency but lower than 275C. The two regions may have a shared function. The distance between these two locations is independent of calcium concentration.

Future Directions

An alternative or addition to this model is that some residues of the C-terminus of troponin T may interact with actin at low or saturating calcium. Though our FRET data do not suggest an interaction, the C-terminus of troponin T could interact elsewhere on actin. The C-terminus might normally position tropomyosin via this actin interaction and set the calcium induced limits of the actin state distribution. Upon elimination of the basic residues of the C-terminus, that interaction would be eliminated. Actin can also be modified with fluorescent probes at C10 and Q41[34]. Those locations might prove to be more useful in identifying an interaction with the C-terminus of troponin T. Additionally, those measurements would be useful as constraints in our molecular modelling simulations.

The distance between the inhibitory region of troponin and actin is increased by the presence of ∆14 troponin T. The inhibitory region of troponin I is believed to bind troponin C at saturating calcium concentrations. It is possible mutation in the C-terminus of troponin T also disrupts binding of the inhibitory region of troponin I to troponin C. Alternatively, mutation to the C-terminus of troponin T might stabilize that interaction. This could be more directly measured with a FRET sensor between inhibitory region of troponin I and troponin C. Measuring that distance might prove to be a more ideal FRET sensor for measuring the mechanism of the inhibitory region of troponin I. Those measurements would also be useful as constraints in our molecular modelling simulations.

The A8V∆14 troponin mutant has been shown to give almost total stabilization of actin in the open state at saturating calcium. We used the ∆14 or HAHA troponin T

mutant in our FRET assays to monitor structural consequence of stabilization of the open state. Though those mutants stabilize the open state, they are not as stabilizing as the A8VΔ14 construct. Incorporation of A8VΔ14 would allow a more direct observation of the structure of the open state.

Sarcomeric modulators such as the peptide consisting of the last sixteen residues of the C-terminus of troponin T may be able to affect the interactions required for the C-terminus of troponin T to maintain the actin state distribution. Since the importance of the high positive charge in this highly conserved C-terminus is now evident, it is likely this region interacts with a negatively charged region. A sarcomeric modulator could disrupt that negatively charged region to destabilize that interaction of the C-terminus of troponin T. If an interaction associated with the blocked state was disrupted, this would destabilize the blocked state and shift the actin state distribution to a more active state. This could be a useful mechanism in restoring contractile activity in heart disease or other diseases where the actin state distribution might be affected.

We currently have limited sarcomeric modulators available for affecting the actin state distribution. Bepridil is a calcium sensitizer that is known to bind the troponin C hydrophobic pocket[98]. Bepridil has been shown to increase ATPase rates and isometric force in muscles fibers[99] presumably by stabilizing the hydrophobic pocket of troponin C. While bepridil increased the activity at low calcium concentrations, it produced a slight inhibitory effect at saturating calcium suggesting stabilization of the closed state[100].

Stabilization of the closed state may be useful in some cases, but the distribution of actin among all three states at both low and saturating calcium must be considered

for restoring contractile activity. A shorter or longer peptide than the Δ16 troponin T peptide we tested may prove more useful for modulating activity. Molecular modelling along with identifying the binding site of the C-terminus of troponin T may allow computation of small molecules that effect the troponin T C-terminus interaction. A small molecule that targets the interactions of the C-terminus of troponin T may prove to be useful in stabilizing the closed state at low calcium concentrations and the open state at saturating calcium concentrations.

Conclusions

We have established that the basic residues within the C-terminus of troponin T are essential in that region's maintenance of the actin state distribution. At low calcium concentrations, those basic residues stabilize tropomyosin in the blocked state along actin. At saturating calcium concentrations, those residues stabilize tropomyosin primarily in the closed position along actin. Elimination of the basic residues within the C-terminus of troponin T results in stabilization of tropomyosin in the closed and open states at low and saturating calcium respectively.

As suggested in part by the 86% transfer efficiency observed between IAEDANS 275C troponin T and DABMI C190 tropomyosin, the most likely target for the C-terminus of troponin T at low calcium concentrations is tropomyosin. The time course of the efficiency change for FRET pairs between the C-terminus and tropomyosin C190 are similar to the time course of the transition from the closed to open state. The movement of the C-terminus of troponin T relative to tropomyosin C190 is simultaneous with repositioning of tropomyosin.

Our model shown in Figure 37 is a working hypothesis based on the evidence obtained in our lab and the known interactions of actin-tropomyosin-troponin. That model is a two-dimensional visualization of a very complicated three-dimensional system. We will incorporate our efficiency and distance measurements into molecular modelling simulations to develop a better visualization of our data. Still, there are many remaining pieces to this puzzle necessary to validate this model.

References

(1) Emilia, B. *Heart Disease and Stroke Statistics-2019 Update: A Report From the American Heart Association*; 2019.

(2) Liu, S.; Rodriguez, C. J.; Mackey, R. H.; Yeh, R. W.; Turan, T. N.; Moy, C. S.; Nichol, G.; Benjamin, E. J.; Mozaffarian, D.; Huffman, M. D.; et al. Executive Summary: Heart Disease and Stroke Statistics—2016 Update. *Circulation* **2016**, *133* (4), 447–454. https://doi.org/10.1161/cir.0000000000000366.

(3) Thierfelder, L.; Watkins, H.; MacRae, C.; Lamas, R.; McKenna, W.; Vosberg, H. P.; Seidman, J. G.; Seidman, C. A-Tropomyosin and Cardiac Troponin T Mutations Cause Familial Hypertrophic Cardiomyopathy: A Disease of the Sarcomere. *Cell* **1994**, *77* (5), 701–712. https://doi.org/10.1016/0092-8674(94)90054-X.

(4) Geisterfer-Lowrance, A.; Kass, S.; Tanigawa, G.; Vosberg, H.-P.; McKenna, W.; Seidman, C. E.; Seidman, J. G. A Molecular Basis for Familial Hypertrophic Cardiomyopathy: A p Cardiac Myosin Heavy Chain Gene Missense Mutation. *Cell Press* **1990**, *62*, 999–1006.

(5) Lu, Q. W.; Wu, X. Y.; Morimoto, S. Inherited Cardiomyopathies Caused by Troponin Mutations. *J. Geriatr. Cardiol.* **2013**, *10* (1), 91–101. https://doi.org/10.3969/j.issn.1671-5411.2013.01.014.

(6) Lynn, M. L.; Lehman, S. J.; Tardiff, J. C. Biophysical Derangements in Genetic Cardiomyopathies. *Heart Fail. Clin.* **2018**, *14* (2), 147–159. https://doi.org/10.1016/j.hfc.2017.12.002.

(7) Hwang, P. M.; Sykes, B. D. Targeting the Sarcomere to Correct Muscle Function. *Nat. Rev. Drug Discov.* **2015**, *14* (5), 313–328. https://doi.org/10.1038/nrd4554.

(8) Shefner, J. M.; Wolff, A. A.; Meng, L. The Relationship between Tirasemtiv Serum Concentration and Functional Outcomes in Patients with ALS. *Amyotroph. Lateral Scler. Front. Degener.* **2013**, *14* (7–8), 582–585. https://doi.org/10.3109/21678421.2013.817587.

(9) Mcnamara, J. W.; Li, A.; dos Remedios, C.; Cooke, R. The Role of Super-Relaxed Myosin in Skeletal and Cardiac Muscle. **2015**, 5–14. https://doi.org/10.1007/s12551-014-0151-5.

(10) Maruyama, K.; Gergely, J. Interaction of Actomyosin with Adenosine at Low Ionic Strength. *J. Biol. Chem.* **1962**, *237* (4).

(11) Gordon, A. M.; Homsher, E.; Regnier, M. Regulation of Contraction in Striated Muscle. *Physiol Rev* **2000**, *80* (2), 853–924.

(12) White, H. D.; Belknap, B.; Webb, M. R. Kinetics of Nucleoside Triphosphate Cleavage and Phosphate Release Steps by Associated Rabbit Skeletal Actomyosin, Measured Using a Novel Fluorescent Probe for Phosphate. *Biochemistry* **1997**, *36* (39), 11828–11836. https://doi.org/10.1021/bi970540h.

(13) Eisenberg, E.; Kielley, W. W. Evidence for a Refractory State of Heavy Meromyosin and Subfragment-1 Unable to Bind to Actin in the Presence of ATP. *Cold Spring Harb. Symp.Quant.Biol.* **1972**, *37* (427), 145–152. https://doi.org/10.1101/sqb.1973.037.01.022.

(14) Geeves, M. A.; Conibear, P. B. The Role of Three-State Docking of Myosin S1 with Actin in Force Generation. *Biophys. J.* **1995**, *68* (4 Suppl), 194S–199S; discussion 199S–201S.

(15) Kawai, M.; Giith, K.; Winnikes, K.; Haist, C.; Riiegg, J. C. European Journal of Physiology. *Eur. J. Physiol.* **1987**, *421*, 394–396.

(16) Dantzig, J. A.; Goldman, Y. E.; Millar, N. C.; Lacktis, J.; Homsher, E. Transition By Photogeneration of Phosphate in Rabbit. *J. Physiol.* **1992**, *451*, 247–278.

(17) Holmes, K. C. Muscle Proteins--Their Actions and Interactions. *Curr Opin Struct Biol* **1996**, *6* (6), 781–789. https://doi.org/S0959-440X(96)80008-X.

(18) Pate, E.; Cooke, R. A Model of Crossbridge Action: The Effects of ATP, ADP and Pi. *J. Muscle Res. Cell Motil.* **1989**, *10* (3), 181–196. https://doi.org/10.1007/BF01739809.
(19) Rayment, I.; Holden, H. M. The Three-Dimensional Structure of a Molecular Motor. *Science (80-.).* **1994**, No. March.
(20) Pate, E.; Cooke, R. Addition of Phosphate to Active Muscle Fibers Probes Actomyosin States within the Powerstroke. *Pflugers Arch. Eur. J. Physiol.* **1989**, *414* (1), 73–81. https://doi.org/10.1007/BF00585629.
(21) White, H. D.; Taylor, E. W. Energetics and Mechanism of Actomyosin Adenosine Triphosphatase. *Biochemistry* **1976**, *15* (26), 5818–5826. https://doi.org/10.1021/bi00671a020.
(22) Hibberd, M. G. Relationships Between Chemical and Mechanical Events During Muscular Contraction. *Ann. Rev. Biophys. Biophys. Chem* **1986**, *15*, 119–161.
(23) Lymn, R. W.; Taylor, E. W. Transient State Phosphate Production in the Hydrolysis of Nucleoside Triphosphates by Myosin. *Biochemistry* **1970**, *9* (15), 2975–2983.
(24) Sleep, J. a; Hutton, R. L. Exchange between Inorganic Phosphate and Adenosine 5'-Triphosphate in the Medium by Actomyosin Subfragment 1. *Biochemistry* **1980**, *19* (7), 1276–1283.
(25) Ma, Y. Z.; Taylor, E. W. Kinetic Mechanism of Myofibril ATPase. *Biophys. J.* **1994**, *66* (5), 1542–1553. https://doi.org/10.1016/S0006-3495(94)80945-2.
(26) Brenner, B. Effect of Ca2 + on Cross-Bridge Turnover Kinetics in Skinned Single Rabbit Psoas Fibers : Implications for Regulation of Muscle Contraction Author (s): Bernhard Brenner Source : Proceedings of the National Academy of Sciences of the United States of Ame. *Proc. Natl. Acad. Sci. U. S. A.* **1988**, *85* (9), 3265–3269.
(27) Lehrer, S. S.; Morris, E. P. Dual Effects of Tropomyosin and Troponin-Tropomyosin on Actomyosin Subfragment 1 ATPase. *J. Biol. Chem.* **1982**, *257* (14), 8073–8080.
(28) Chalovich, J. M.; Chock, P. B.; Eisenberg, E. Mechanism of Action of Troponin Tropomyosin. Inhibition of Actomyosin ATPase Activity without Inhibition of Myosin Binding to Actin. *J. Biol. Chem.* **1981**, *256* (2), 575–578.
(29) Hill, T. L.; Eisenberg, E.; Chalovich, J. M. Theoretical Models for Cooperative Steady-State ATPase Activity of Myosin Subfragment-1 on Regulated Actin. *Biophys J* **1981**, *35* (1), 99–112. https://doi.org/10.1016/S0006-3495(81)84777-7.
(30) McKillop, D. F.; Geeves, M. A. Regulation of the Interaction between Actin and Myosin Subfragment 1: Evidence for Three States of the Thin Filament. *Biophys. J. Vol.* **1993**, *65* (August), 693–701. https://doi.org/10.1016/S0006-3495(93)81110-X.
(31) Resetar, A. M.; Stephens, J. M.; Chalovich, J. M. Troponin-Tropomyosin: An Allosteric Switch or a Steric Blocker? *Biophys. J.* **2002**, *83* (2), 1039–1049. https://doi.org/10.1016/S0006-3495(02)75229-6.
(32) Herzberg, O.; James, M. N. G. Structure of the Calcium Regulatory Muscle Protein Troponin-C at 2.8 Å Resolution. *Nature* **1985**, *313* (6004), 653–659. https://doi.org/10.1038/313653a0.
(33) Miki, M.; Hai, H.; Saeki, K.; Shitaka, Y.; Sano, K. I.; Maéda, Y.; Wakabayashi, T. Fluorescence Resonance Energy Transfer between Points on Actin and the C-Terminal Region of Tropomyosin in Skeletal Muscle Thin Filaments. *J. Biochem.* **2004**, *136* (1), 39–47. https://doi.org/10.1093/jb/mvh090.
(34) Kimura, C.; Maeda, K.; Maéda, Y.; Miki, M. Ca 2 + - and S1-Induced Movement of Troponin T on Reconstituted Transfer Spectroscopy. **2002**, *102*, 93–102.
(35) Pirani, A.; Xu, C.; Hatch, V.; Craig, R.; Tobacman, L. S.; Lehman, W. Single Particle Analysis of Relaxed and Activated Muscle Thin Filaments. *J. Mol. Biol.* **2005**, *346* (3), 761–772. https://doi.org/10.1016/j.jmb.2004.12.013.
(36) Poole, K. J.; Lorenz, M.; Evans, G.; Rosenbaum, G.; Pirani, A.; Craig, R.; Tobacman, L. S.; Lehman, W.; Holmes, K. C. A Comparison of Muscle Thin Filament Models Obtained

from Electron Microscopy Reconstructions and Low-Angle X-Ray Fibre Diagrams from Non-Overlap Muscle. *J Struct Biol* **2006**, *155* (2), 273–284. https://doi.org/10.1016/j.jsb.2006.02.020.
(37) Vibert, P. J.; Haselgrove, J. C.; Lowy, J.; Poulsen, F. R. Structural Changes in Actin-Containing Filaments of Muscle. *J. Mol. Biol.* **1972**, *71* (3), 757–767. https://doi.org/10.1016/S0022-2836(72)80036-6.
(38) Spudich, J. A.; Huxley, H. E.; Finch, J. T. Regulation of Skeletal Muscle Contraction. II. Structural Studies of the Interaction of the Tropomyosin-Troponin Complex with Actin. *J. Mol. Biol.* **1972**, *72* (3), 619–632. https://doi.org/10.1016/0022-2836(72)90180-5.
(39) Miki, M.; Makimura, S.; Sugahara, Y.; Yamada, R.; Bunya, M.; Saitoh, T.; Tobita, H. A Three-Dimensional FRET Analysis to Construct an Atomic Model of the Actin-Tropomyosin-Troponin Core Domain Complex on a Muscle Thin Filament. *J. Mol. Biol.* **2012**, *420* (1–2), 40–55. https://doi.org/10.1016/j.jmb.2012.03.029.
(40) Mathur, M. C.; Kobayashi, T.; Chalovich, J. M. Some Cardiomyopathy-Causing Troponin I Mutations Stabilize a Functional Intermediate Actin State. *Biophys. J.* **2009**, *96* (6), 2237–2244. https://doi.org/10.1016/j.bpj.2008.12.3909.
(41) Johnson, D.; Mathur, M. C.; Kobayashi, T.; Chalovich, J. M. The Cardiomyopathy Mutation, R146G Troponin I, Stabilizes the Intermediate “C” State of Regulated Actin under High- and Low-Free Ca $^{2+}$ Conditions. *Biochemistry* **2016**, *55* (32), 4533–4540. https://doi.org/10.1021/acs.biochem.5b01359.
(42) Takeda, S.; Yamashita, A.; Maeda, K.; Maeda, Y. Structure of the Core Domain of Human Cardiac Troponin in the Ca(2+)-Saturated Form. *Nature* **2003**, *424* (6944), 35–41. https://doi.org/10.1038/nature01780.
(43) Katrukha, I. A. Human Cardiac Troponin Complex. Structure and Functions. *Biochemistry* **2013**, *78* (13), 1447–1465. https://doi.org/10.1134/S0006297913130063.
(44) Johnson, D. Defining the Role of the C-Terminal Region of Troponin T by Analysis of a Series of Truncation Mutants, East Carolina University, 2016.
(45) Li, X.; Tobacman, L. S.; Mun, J. Y.; Craig, R.; Fischer, S.; Lehman, W. Tropomyosin Position on F-Actin Revealed by EM Reconstruction and Computational Chemistry. *Biophys. J.* **2011**, *100* (4), 1005–1013. https://doi.org/10.1016/j.bpj.2010.12.3697.
(46) Vibert, P.; Craig, R.; Lehman, W. Steric-Model for Activation of Muscle Thin Filaments. *J. Mol. Biol.* **1997**, *266* (1), 8–14. https://doi.org/10.1006/jmbi.1996.0800.
(47) Franklin, A.; Baxley, T.; Kobayashi, T.; Chalovich, J. M. The C-Terminus of Troponin T Is Essential for Maintaining the Inactive State of Regulated Actin. *Biophys J* **2012**, *102* (11), 2536–2544. https://doi.org/10.1016/j.bpj.2012.04.037.
(48) Pirani, A.; Vinogradova, M. V.; Curmi, P. M. G.; King, W. A.; Fletterick, R. J.; Craig, R.; Tobacman, L. S.; Xu, C.; Hatch, V.; Lehman, W. An Atomic Model of the Thin Filament in the Relaxed and Ca 2+-Activated States. *J. Mol. Biol.* **2006**, *357* (3), 707–717. https://doi.org/10.1016/j.jmb.2005.12.050.
(49) Yang, S.; Barbu-Tudoran, L.; Orzechowski, M.; Craig, R.; Trinick, J.; White, H. D.; Lehman, W. Three-Dimensional Organization of Troponin on Cardiac Muscle Thin Filaments in the Relaxed State. *Biophys. J.* **2014**, *106* (4), 855–864. https://doi.org/10.1016/j.bpj.2014.01.007.
(50) Zabrouskov, V.; Ge, Y.; Schwartz, J.; Walker, J. W. Unraveling Molecular Complexity of Phosphorylated Human Cardiac Troponin I by Top down Electron Capture Dissociation/Electron Transfer Dissociation Mass Spectrometry. *Mol. Cell. Proteomics* **2008**, *7* (10), 1838–1849. https://doi.org/10.1074/mcp.M700524-MCP200.
(51) Vassylyev, D. G. .; Takeda, S.; Wakatsuki, S.; Maeda, K.; Maeda, Y. Crystal Structure of Troponin C in Complex with Troponin I Fragment at 2 . 3- Angstrom Resolution Author. *Proc. Natl. Acad. Sci. U. S. A.* **1998**, *95* (April).
(52) Kobayashi, T.; Patrick, S. E.; Kobayashi, M. Ala Scanning of the Inhibitory Region of

Cardiac Troponin I. *J. Biol. Chem.* **2009**, *284* (30), 20052–20060. https://doi.org/10.1074/jbc.M109.001396.
(53) Lindhout, D. a; Sykes, B. D. Structure and Dynamics of the C-Domain of Human Cardiac Troponin C in Complex with the Inhibitory Region of Human Cardiac Troponin I. *J. Biol. Chem.* **2003**, *278* (29), 27024–27034. https://doi.org/10.1074/jbc.M302497200.
(54) Talbot, J. A.; Hodges, R. S. Synthetic Studies on the Inhibitory Region of Rabbit Skeletal Troponin I. **1981**, *256* (6), 2798–2802.
(55) Ingraham, R. H.; Swenson, C. A. Binary Interactions of Troponin Subunits. *J. Biol. Chem.* **1984**, *259* (15), 9544–9548.
(56) Brown, L. J.; Sale, K. L.; Hills, R.; Rouviere, C.; Song, L.; Zhang, X.; Fajer, P. G. Structure of the Inhibitory Region of Troponin by Site Directed Spin Labeling Electron Paramagnetic Resonance. *Proc Natl Acad Sci U S A* **2002**, *99* (20), 12765–12770. https://doi.org/10.1073/pnas.202477399.
(57) Li, M. X.; Spyracopoulos, L.; Sykes, B. D. Binding of Cardiac Troponin-I147-163 Induces a Structural Opening in Human Cardiac Troponin-C. *Biochemistry* **1999**, *38* (26), 8289–8298. https://doi.org/10.1021/bi9901679.
(58) ALEX, R.; LIESKA, N.; SPITZ, W. The Amino Acid Sequence of Human Cardiac Troponin-C. *Muscle and Nerve* **1986**, *9* (1), 73–77.
(59) Potter, J. D.; Gergely, J. The Calcium and Magnesium Binding Sites on Troponin and Their Role in the Regulation of Myofibrillar Adenosine Triphosphatase. *J.Biol.Chem.* **1975**, *250* (June), 4628–4633.
(60) Vinogradova, M. V; Stone, D. B.; Malanina, G. G.; Karatzaferi, C.; Cooke, R.; Mendelson, R. A.; Fletterick, R. J. Ca(2+)-Regulated Structural Changes in Troponin. *Proc Natl Acad Sci U S A* **2005**, *102* (14), 5038–5043. https://doi.org/10.1073/pnas.0408882102.
(61) Gomes, A. V.; Guzman, G.; Zhao, J.; Potter, J. D. Cardiac Troponin T Isoforms Affect the Ca2+ Sensitivity and Inhibition of Force Development: Insights into the Role of Troponin T Isoforms in the Heart. *J. Biol. Chem.* **2002**, *277* (38), 35341–35349. https://doi.org/10.1074/jbc.M204118200.
(62) VanBuren, P.; Alix, S. L.; Gorga, J. a; Begin, K. J.; LeWinter, M. M.; Alpert, N. R. Cardiac Troponin T Isoforms Demonstrate Similar Effects on Mechanical Performance in a Regulated Contractile System. *Am. J. Physiol. Heart Circ. Physiol.* **2002**, *282* (5), H1665–H1671. https://doi.org/10.1152/ajpheart.00938.2001.
(63) Tobacman, L. S. Thin Filament-Mediated Regulation of Cardiac Contraction. *Annu Rev Physiol* **1996**, *58*, 447–481. https://doi.org/10.1146/annurev.ph.58.030196.002311.
(64) Mak, A. S.; Smillie, L. B. Structural Interpretation of the Two-Site Binding of Troponin on the Muscle Thin Filament. *J. Mol. Biol.* **1981**, *149* (3), 541–550. https://doi.org/10.1016/0022-2836(81)90486-1.
(65) Stefancsik, R.; Jhat, P. K.; Riya, S. Identification and Mutagenesis of a Highly Conserved Domain in Troponin T Responsible for Troponin I Binding : Potential Role for Coiled Coil Interaction. *PNAS* **1998**, *95* (3), 957–962.
(66) Vahebi, S.; Kobayashi, T.; Warren, C. M.; De Tombe, P. P.; Solaro, R. J. Functional Effects of Rho-Kinase-Dependent Phosphorylation of Specific Sites on Cardiac Troponin. *Circ. Res.* **2005**, *96* (7), 740–747. https://doi.org/10.1161/01.RES.0000162457.56568.7d.
(67) Noland, T. A.; Raynor, R. L.; Kuo, J. F. Identification of Sites Phosphorylated in Bovine Cardiac Troponin I and Troponin T by Protein Kinase C and Comparative Substrate Activity of Synthetic Peptides Containing the Phosphorylation Sites*. **1989**, *1*, 20778–20785.
(68) Zhang, J.; Zhang, H.; Ayaz-Guner, S.; Chen, Y. Der; Dong, X.; Xu, Q.; Ge, Y. Phosphorylation, but Not Alternative Splicing or Proteolytic Degradation, Is Conserved in Human and Mouse Cardiac Troponin T. *Biochemistry* **2011**, *50* (27), 6081–6092. https://doi.org/10.1021/bi2006256.

(69) Brunet, N. M.; Chase, P. B.; Mihajlović, G.; Schoffstall, B. Ca2+-Regulatory Function of the Inhibitory Peptide Region of Cardiac Troponin i Is Aided by the C-Terminus of Cardiac Troponin T: Effects of Familial Hypertrophic Cardiomyopathy Mutations CTnI R145G and CTnT R278C, Alone and in Combination, on Filament Sl. *Arch. Biochem. Biophys.* **2014**, *552–553*, 11–20. https://doi.org/10.1016/j.abb.2013.12.021.
(70) Lehrer, S. S.; Morris, E. P. Comparison of the Effects of Smooth and Skeletal Tropomyosin on Skeletal Actomyosin Subfragment 1 ATPase. *J Biol Chem* **1984**, *259* (4), 2070–2072.
(71) Jin, J. P.; Chong, S. M. Localization of the Two Tropomyosin-Binding Sites of Troponin T. *Arch. Biochem. Biophys.* **2010**, *500* (2), 144–150. https://doi.org/10.1016/j.abb.2010.06.001.
(72) Tanokura, M.; Tawada, Y.; Ono, A.; Ohtsuki, I. Chymotryptic Subfragments of Troponin T from Rabbit Skeletal Muscle. Interaction with Tropomyosin, Troponin I and Troponin C. *J Biochem* **1983**, *93* (2), 331–337.
(73) Morris, E. P.; Lehrer, S. S. Troponin-Tropomyosin Interactions. Fluorescence Studies of the Binding of Troponin, Troponin T, and Chymotryptic Troponin T Fragments to Specifically Labeled Tropomyosin. *Biochemistry* **1984**, *23* (10), 2214–2220. https://doi.org/10.1021/bi00305a018.
(74) Chong, P. C. S.; Hodges, R. S. Photochemical Cross-Linking between Rabbit Skeletal Troponin and a-Tropomyosin. *J. Biol. Chem.* **1982**, *257* (15), 9152–9160.
(75) Wang, H.; Chalovich, J. M.; Marriott, G. Structural Dynamics of Troponin I during Ca2+-Activation of Cardiac Thin Filaments: A Multi-Site Förster Resonance Energy Transfer Study. *PLoS One* **2012**, *7* (12), 1–10. https://doi.org/10.1371/journal.pone.0050420.
(76) Kimura-Sakiyama, C.; Ueno, Y.; Wakabayashi, K.; Miki, M. Fluorescence Resonance Energy Transfer between Residues on Troponin and Tropomyosin in the Reconstituted Thin Filament: Modeling the Troponin-Tropomyosin Complex. *J. Mol. Biol.* **2008**, *376* (1), 80–91. https://doi.org/10.1016/j.jmb.2007.10.078.
(77) Jayasundar, J. J.; Xing, J.; Robinson, J. M.; Cheung, H. C.; Dong, W.-J. Molecular Dynamics Simulations of the Cardiac Troponin Complex Performed with Fret Distances as Restraints. *PLoS One* **2014**, *9* (2). https://doi.org/10.1371/journal.pone.0087135.
(78) Baxley, T.; Johnson, D.; Pinto, J. R.; Chalovich, J. M. Troponin C Mutations Partially Stabilize the Active State of Regulated Actin and Fully Stabilize the Active State When Paired with Δ14 TnT. *Biochemistry* **2017**, acs.biochem.6b01092. https://doi.org/10.1021/acs.biochem.6b01092.
(79) Borrego-Diaz, E.; Chalovich, J. M. Kinetics of Regulated Actin Transitions Measured by Probes on Tropomyosin. *Biophys. J.* **2010**, *98* (11), 2601–2609. https://doi.org/10.1016/j.bpj.2010.02.030.
(80) Sen, A.; Chen, Y. Der; Yan, B.; Chalovich, J. M. Caldesmon Reduces the Apparent Rate of Binding of Myosin S1 to Actin-Tropomyosin. *Biochemistry* **2001**, *40* (19), 5757–5764. https://doi.org/10.1021/bi002724t.
(81) Geeves, M. A.; Chai, M.; Lehrer, S. S. Inhibition of Actin-Myosin Subfragment 1 ATPase Activity by Troponin I and IC: Relationship to the Thin Filament States of Muscle. *Biochemistry* **2000**, *39* (31), 9345–9350. https://doi.org/10.1021/bi0002232.
(82) Gafurov, B.; Chen, Y. Der; Chalovich, J. M. Ca2+ and Ionic Strength Dependencies of S1-ADP Binding to Actin-Tropomyosin-Troponin: Regulatory Implications. *Biophys J* **2004**, *87* (3), 1825–1835. https://doi.org/10.1529/biophysj.104.043364.
(83) Franklin, A.; Baxley, T.; Chalovich, J. M. Properties of the Intermediate State of Actin-Tropomyosin-Troponin. *Biophys. J.* **2012**, *102* (3), 153a. https://doi.org/10.1016/j.bpj.2011.11.836.
(84) Trybus, K. M.; Taylor, E. W. Kinetic Studies of the Cooperative Binding of Subfragment 1 to Regulated Actin. *Proc Natl Acad Sci U S A* **1980**, *77* (12), 7209–7213.

https://doi.org/10.1073/pnas.77.12.7209.
(85) Hill, T. L.; Eisenberg, E.; Greene, L. E. Theoretical Model for the Cooperative Equilibrium Binding of Myosin Subfragment 1 to the Actin-Troponin-Tropomyosin Complex. *Proc Natl Acad Sci U S A* **1980**, *77* (6), 3186–3190.
(86) Szczesna, D.; Zhang, R.; Zhao, J.; Jones, M.; Guzman, G.; Potter, J. D. Altered Regulation of Cardiac Muscle Contraction by Troponin T Mutations That Cause Familial Hypertrophic Cardiomyopathy. *J. Biol. Chem.* **2000**, *275* (1), 624–630.
(87) Schlecht, W.; Zhou, Z.; Li, K. L.; Rieck, D.; Ouyang, Y.; Dong, W.-J. FRET Study of the Structural and Kinetic Effects of PKC Phosphomimetic Cardiac Troponin T Mutants on Thin Filament Regulation. *Arch. Biochem. Biophys.* **2014**, *550–551*, 1–11. https://doi.org/10.1016/j.abb.2014.03.013.
(88) Sumandea, M. P.; Pyle, W. G.; Kobayashi, T.; De Tombe, P. P.; Solaro, R. J. Identification of a Functionally Critical Protein Kinase C Phosphorylation Residue of Cardiac Troponin T. *J. Biol. Chem.* **2003**, *278* (37), 35135–35144. https://doi.org/10.1074/jbc.M306325200.
(89) Chalovich, J. M.; Eisenberg, E. Inhibition of Actomyosin ATPase Activity by Troponin-Tropomyosin without Blocking the Binding of Myosin to Actin. *J. Biol. Chem.* **1982**, *257* (5), 2432–2437. https://doi.org/10.1016/j.biotechadv.2011.08.021.Secreted.
(90) Williams, D. L.; Greene, L. E.; Eisenberg, E. Cooperative Turning on of Myosin Subfragment 1 Adenosinetriphosphatase Activity by the Troponin-Tropomyosin-Actin Complex. *Biochemistry* **1988**, *27* (18), 6987–6993. https://doi.org/10.1021/bi00418a048.
(91) Brenner, B. Molecular Mechanisms and Biochemical Kinetics. In *Muscle Mechanics and Biochemical Kinetics*; Macmillan Press, 1990.
(92) Marks, A. R. Calcium and the Heart : A Question of Life and Death. **2002**, *111* (5), 597–600. https://doi.org/10.1172/JCI200318067.The.
(93) Nakaura, H.; Morimoto, S.; Yanaga, F.; Nakata, M.; Nishi, H.; Imaizumi, T.; Ohtsuki, I.; Morimoto, S.; Yanaga, F.; Nakata, M.; et al. Functional Changes in Troponin T by a Splice Donor Site Mutation That Causes Hypertrophic Cardiomyopathy. **1999**, 225–232.
(94) Miki, M.; Makimura, S.; Saitoh, T.; Bunya, M.; Sugahara, Y.; Ueno, Y.; Kimura-Sakiyama, C.; Tobita, H. A Three-Dimensional FRET Analysis to Construct an Atomic Model of the Actin–Tropomyosin Complex on a Reconstituted Thin Filament. *J. Mol. Biol.* **2011**, *414* (5), 765–782. https://doi.org/10.1016/j.jmb.2011.10.033.
(95) Wang, H.; Mao, S.; Chalovich, J. M.; Marriott, G. Tropomyosin Dynamics in Cardiac Thin Filaments: A Multisite Forster Resonance Energy Transfer and Anisotropy Study. *Biophys J* **2008**, *94* (11), 4358–4369. https://doi.org/10.1529/biophysj.107.121129.
(96) Pearlstone, J. R.; Smillie, L. B. The Interaction of Rabbit Skeletal Muscle Troponin-T Fragments with Troponin-I. *Can J Biochem Cell Biol* **1985**, *63*, 212–218.
(97) Gafurov, B.; Fredricksen, S.; Cai, A.; Brenner, B.; Chase, P. B.; Chalovich, J. M. The ∆14 Mutation of Human Cardiac Troponin T Enhances ATPase Activity and Alters the Cooperative Binding of S1-ADP to Regulated Actin. *Biochemistry* **2004**, *43*, 15276–15285.
(98) Chen, C.; Hurez, V.; Brockenbrough, J. S.; Kubagawa, H.; Cooper, M. D.; Li, Y.; Love, M. L.; Putkey, J. A.; Cohen, C. Bepridil Opens the Regulatory N-Terminal Lobe of Cardiac Troponin C. **2000**, *97* (10).
(99) Solaro, J.; Bousquet, P.; Johnson, D. Stimulation of Cardiac Myofilament Force , ATPase Troponin C Ca Binding by Bepridil1. **1986**, 502–507.
(100) Varughese, J. F.; Baxley, T.; Chalovich, J. M.; Li, Y. A Computational and Experimental Approach to Investigate Bepridil Binding with Cardiac Troponin. *J. Phys. Chem. B* **2011**, *115* (10), 2392–2400. https://doi.org/10.1021/jp1094504.

Appendix A: IACUC Approval letter

East Carolina University

Animal Care and Use Commitee
212 Ed Warren Life Sciences Building
East Carolina University
Greenville, NC 27834

252-744-2436 office
252-744-2355 fax

January 13, 2015

Joseph Chalovich, Ph.D.
Department of Biochemistry
Brody 5E-124
ECU Brody School of Medicine

Dear Dr. Chalovich:

Your Animal Use Protocol entitled, "Proteins of Motility in Rabbits" (AUP #C037g) was reviewed by this institution's Animal Care and Use Committee on 1/13/15. The following action was taken by the Committee:

"Approved as submitted"

Please contact Dale Aycock at 744-2997 prior to hazard use

A copy is enclosed for your laboratory files. Please be reminded that all animal procedures must be conducted as described in the approved Animal Use Protocol. Modifications of these procedures cannot be performed without prior approval of the ACUC. The Animal Welfare Act and Public Health Service Guidelines require the ACUC to suspend activities not in accordance with approved procedures and report such activities to the responsible University Official (Vice Chancellor for Health Sciences or Vice Chancellor for Academic Affairs) and appropriate federal Agencies. **Please ensure that all personnel associated with this protocol have access to this approved copy of the AUP and are familiar with its contents.**

Sincerely yours,

Susan McRae, Ph.D.
Chair, Animal Care and Use Committee

SM/jd

Enclosure

Appendix B: Protein Preparation and Protocols

Skeletal Actin Preparation

Adapted from Ebashi, S.; Kodama, A. *J Biochem* **1965**, *58* (1), 107–108.

Day 1

1. Make 2 liters G-actin buffer
    a. 0.5 mM ATP, 2 mM Tris-pH 7.8, 0.1 mM $CaCl_2$, B-mercaptoethanol
2. Add 270 ml of actin solution /9 g powder. Gently stir every 10 minutes for 30 minutes. Stir gently so as not to extract actinin or tropomyosin.
3. Centrifuge 60 minutes near top speed of Sorvall SS-34 rotor (18,000 rpm)
4. Tare empty beaker. Filter supernatant into beaker through glass wool or Whatman # 541 paper. Approximate volume by mass.
5. Add solid potassium chloride to 3.3 M
    a. assume that potassium chloride increases the volume by 10 %
6. Stir at room temp until the temperature reaches 15° C.
7. Place on ice without stirring until temp reaches 5° C.
8. Centrifuge in Sorvall SS-34 rotor at 18,000 rpm for 40 minutes.
9. Dialyze supernanant against 32 volumes of 2 mM Tris, 1mM $MgCl_2$ pH 7.6. The final concentration of KCl is now 0.1 M. Actin is now in “F” form.

Day 2

10. Add 4 M KCl to the actin to give a final concentration of 0.8 M.
    a. Volume of KCl to add is 0.219 x volume of actin.

11. Stir for 1 hour at 4°C.
12. Centrifuge for 1.5 hour at 45,000 rpm in a Ti 50.2 rotor.
13. Remove pellets into homogenizer with less than 25 ml of G-buffer and homogenize
14. Tare a beaker (150 ml) and add actin to estimate volume by its mass.
15. Add sequentially with stirring: 1.5 ml 100 mM $MgCl_2$, 0.75 ml 4 M KCl, G-buffer to bring total volume to 77.25 ml
16. Place on ice over night or proceed to Day 3\

Day 3

17. Add 18 ml of 4 M KCl and 4.75 ml G-buffer
18. Stir for 1.5 hours at 4°C.
19. Centrifuge 1.5 hours at 45,000 rpm in Ti 50.2 rotor.
20. Remove pellets into homogenizer with less than 25 ml of G-buffer and homogenize.
21. Dialyze against G-buffer with at least three changes of buffer. Change buffer every 12 hours.

Day 5

22. Homogenize G-actin.
23. Centrifuge 1.5 hours at 30,000 RPM in a Ti 50.2 rotor.
24. Weigh the actin to estimate the volume.
25. While stirring vigorously add sequentially: 1 M MOPS pH 7 buffer to get 10 mM, 25 mM $MgCl_2$ to get 1 mM

26. Dialyze in F-actin solution at least 24 hours
    a. 4 mM MOPS, pH 7, 2 mM $MgCl_2$, 0.5 mM ATP
27. Add sodium azide to the actin to a final of 0.01%.
28. Store actin at 4°C

Removal of residual ATP before use

29. Centrifuge at 45,000 RPM for two hours in a Ti 50.2 rotor
30. Pour off supernatant and set aside (check O.D. to ensure low actin concentration)
31. Remove pellet into homogenizer with less than 10 ml F-actin solution and homogenize
32. Measure Absorbance spectrum from 260 nm to 340 nm
33. ATP-free actin should exhibit the following
    a. $A_{280}/A_{290}=1.8$
    b. $A_{280}/A_{260}=1.5$
34. Concentration in mg/ml = $(A_{280}-A_{320})/1.15$

Storage

Store in G-actin form at 5mg/l by adding surcrose to 10mg/ml or by freezing in liquid Nitrogen. Store at -70°C.

Myosin Preparation

Adapted from: Leonard A. Stein, Richard P. Schwarz Jr., P. Boon Chock, and Evan Eisenberg. *Biochemistry* **1979** *18* (18), 3895-3909 DOI: 10.1021/bi00585a009

Day 1

1. Kill 5-6 lb rabbit by bleeding.
2. Dissect back and leg muscles quickly and place on ice
3. Grind and weigh. (Should have about 300 grams)
4. Extract 12 minutes with 3 volumes of ice cold extracting solution. Stir in cold.
    a. 0.5 M KCl, 0.1 M K_2HPO_4, 10 mM PMSF, pH 6.5
5. Centrifuge at 7,000 RPM, 4 degrees Celsius for 15 minutes in GSA rotor.
6. Filter supernatant through four layers of cheesecloth and collect. Estimate volume.
    a. Pellet may be saved for acetone powder prep
7. Carefully adjust to pH 6.6
8. Dilute with 10 volumes ice cold water over the course of 2-3 minutes
9. Check that pH is still below 6.8 and correct as needed
10. Centrifuge at top speed in IEC rotor. Discard supernatant.
11. Weight pellets to estimate volume
12. Add 2 M KCl to 0.5 M to make solution
    a. Liters 2M KCl = 0.303 x volume pellet
13. Pool pellets into one bottle. Rinse residual protein from bottles with 0.5 M KCl. Keep total volume under 550 mL
14. Adjust pH to 6.75 using 0.1 M NaHCO3

15. Measure volume

Day 2

16. Dilute to 0.28 M KCl with ice cold water with stirring
    a. Volume Cold Water = volume solution x 0.786
17. Centrifuge at top speed in Sorvall GSA rotor
18. Discard precipitate
19. Measure supernatant volume
20. Dilute to 0.4 M KCl with ice cold water and stirring
    a. Volume Cold Water = volume solution x 6
21. Allow to stand one hour in the cold
22. Centrifuge at top speed in IEC rotor for 20 minutes
23. Discard supernatant
24. Combine and weigh pellets to estimate volume
25. Bring to 0.5 M KCl with ice cold 2 M KCl and stir to dissolve
    a. volume 2 M KCl = volume pellets x 0.3
26. Dialyze versus 1 liter of 0.5 M NaCl, 0.1 mM DTT

Storage

27. Add ice cold glycerol to 50% glycerol and store at -20 degrees Celsius

Myosin S1 Preparation

Adapted from: Leonard A. Stein, Richard P. Schwarz Jr., P. Boon Chock, and Evan Eisenberg. *Biochemistry* **1979** *18* (18), 3895-3909 DOI: 10.1021/bi00585a009

Day 1

1. Dialyze myosin 50% glycerol stock extensively against 30 mM NaCl, 2 mM MOPS pH 7, 1 mM DTT.

Day 2

2. Centrifuge in Sorvall SS-34 rotor at 18,000 RPM for 1 hour
3. Discard supernatant
4. Estimate pellet volume and dissolve myosin by adding solid KCl to 1 M
5. Suspend the pellets in 0.5 M NaCl, 10 mM MOPS pH 7, 1 mM DTT and dialyze against same buffer

Day 3

6. Measure the concentration and dilute to 15 mg/ml if needed
7. Dialyze overnight against 0.12 M NaCl, 10 mM NaPi pH 7.2, 1 mM EDTA, 1 mM DTT, 0.1 mM NaN3

Day 4

8. Measure myosin volume
9. Prepare 100 mM PMSF by dissolving 34 mg in 1 mL isopropyl alcohol. Dissolve by warming and sonicating.
10. Prepare chymotrypsin by dissolving 5 mg in 1 mL water. Store on ice.
11. Warm myosin to 22-25 degrees Celsius

12. Add chymotrypsin solution using a 1/100 dilution with rapid stirring. Final concentration is 0.05 mg/ml
13. Maintain myosin temperature between 22 and 25 degrees Celsius and stir ten minutes
14. Add 100 mM PMSF using a 1/200 dilution with rapid stirring. Final concentration 0.5 mM.
15. Allow to set in ice 10 minutes
16. Dialyze over night against 40 mM NaCl, 5 mM NaPi, 1 mM DTT, pH 6.5 at 4 degrees Celsius

Day 5

17. Centrifuge at 40,000 RPM for one hour in a Ti 50.2 rotor
18. Collect supernatant
19. Precipitate the S1 by adding 100% ammonium sulfate to 60% saturation
20. Centrifuge at 18,000 RPM in sorvall SS-34 rotor for 30 minutes
21. Pour of supernatant
    a. Pellets can covered with 60% ammonium sulfate at this step and kept on ice for two months
22. Dissolve pellet in 2 mM MOPS pH 7, 50 mM KCl, 1 mM DTT and dialyze versus same buffer

Day 6

23. Dialyze versus buffer of choice before use

Preparation of Ether powder from bovine cardiac muscle for the production of troponin and tropomyosin

Adapted from: Potter (1982; volume 85 of methods in Enzymology)

At 4 degrees C

1) Mince trimmed beef cardiac muscle
2) Add 5 volumes of wash solution and homogenize.
    a. 1% triton, 50 mM KCl, 5 mM Tris pH 8
3) Homogenize 1 minute at high speed (5-7)
4) Centrifuge at 10960 g for 15 min. Discard supernatant.
5) Pellets are suspended in equal volume of wash solution in centrifuge bottle and rehomogenized
6) Centrifuge at 10960xg for 15 min
7) Repeat steps 5-7, 8-10 times (cardiac residue turns almost white)

At room temp

8) Pellets transferred to a 4 Liter plastic beaker
9) Three volumes cold 95% ethanol added
10) Break up pellets with gloved hand
11) Tissue is collected over Buchner funnel on 4 liter filter flask. 26cm diameter, Whatman No. 1 filter paper. Discard filtrate
12) Repeat steps 1-5, 3 more times
13) Repeat steps 1-6 using diethyl ether in place of ethanol
14) Leave to dry overnight on filter paper
15) Weigh and store at 4 degrees C

Preparation of Bovine Cardiac Troponin from Ether Powder

Adapted from: Potter (1982; volume 85 of methods in Enzymology)

1. Bovine cardiac ether powder is extracted in a 20 vol/gram powder of 1M KCl, 20 mM MOPS, pH7.0, 1 mM DTT, 0.01% NaN_3, 25 mg/L Benzamidine, 10 mg/L Leupeptin, 5 mg/L Pepstatin A , 10 mg/L TLCK, 3 mg/l TPCK, 15 mM BME
2. Stir overnight at 4°C.
3. Centrifuge 1 hour at 45,000 rpm in a Ti50.2 rotor.
4. Carefully remove supernatant and adjust to pH 8.0 with 1N KOH.
5. Measure volume
6. Add 167g of ammonium sulfate per liter of supernatant with constant stirring at 4 degrees Celsius
7. Allow to stir one hour
8. Centrifuge in Sorvall SS-34 rotor for 30 min at 15,000rpm.
9. Remove supernatant and measure volume
10. Add 73g/Liter of ammonium sulfate to bring the ammonium sulfate from 30% to 42.5%.
11. After stirring 1 hour, centrifuge 30 min at 15,000 rpm in SS-34 rotor.
12. Save supernatant for Tropomyosin
    a. Collect 65% ammonium sulfate fraction after adding 168 g ammonium sulfate per liter. Proceed to BvC Tropomyosin prep.
13. Dialyze BvC Troponin against 20 mM MOPS pH 7, 50 mM NaCl, 1 mM DTT
14. Equilibrate a Mono Q DEAE column with the same buffer

15. Centrifuge 30 minutes at 40,000 rpm in a Ti 50.2 rotor to remove any precipitate.
16. Load supernatant onto DEAE column and wash with two column of starting buffer.
17. Run a ten column volume gradient to 1 M NaCl
    a. The cardiac troponin should elute in the middle of the gradient
18. Check $OD_{280-340}$ of fractions and run SDS-PAGE gel along with MW ladder to identify clean fractions

Preparation of Bovine Cardiac Tropomyosin from Ether Powder

Adapted from: Potter (1982; volume 85 of methods in Enzymology)

1. The 65% ammonium sulfate pellet from the BvC troponin protocol was brought up in minmal buffer and dialyzed extensively against the same buffer
    a. 1 M KCl, 2 mM MOPS, pH 7.2, 5 mM B-ME
2. Equilibrate a hydroxylapatite column with 1 M KCl, 1 mM PO_4, pH 7.2, 2 mM DTT
3. The sample was spun at 30 minutes at 40,000 rpm in a Ti 50.2 rotor to clarify
4. The sample was loaded onto the hydroxylapatite column
5. The column was washed with two column volumes of equilibration buffer
6. Elute protein with a five column volume gradient of phosphate to 250 mM
    a. Protein should elute near end of gradient
7. Check $OD_{280-340}$ and combine fractions with protein
8. Carefully bring tropomyosin to pH 4.6 and allow to rest overnight on ice
9. Centrifuge at 30,000 rpm for 40 minutes pour off supernatant
10. Dissolve pellet in 4 mM MOPS, 40 mM KCl pH 7 or buffer of choice
11. Run SDS-Page gel along with MW standard to verify purification

Recombinant Troponin C Preparation from 4 L TnI/TnC Culture

Adapted from:

Gafurov, B.; Chen, Y. D.; Chalovich, J. M. *Biophys J* **2004**, *87* (3), 1825–1835.

1) Prepare 2L 6 M Urea, 1 mM EDTA, 20 mM Tris/HCl, pH 8 (Soln. A)
2) Prepare 1L Soln. A + 0.5 M NaCl
3) Suspend pellet w/ about 40 mL Solution A + protease inhibitors
    a. Sigma 8465 cocktail. 43 mg dissolved in ~0.4 mL DMSO, ~1.6 mL water.
    b. Leupeptin to ~10 µM (~2.5 mg dissolved in ~1.0 mL water)
    c. Pepstatin to ~1 µM (~1.0 mg dissolved in ~1.0 mL DMSO)
4) Sonicate 20 seconds x four times on ice
5) Centrifuge at 19K for 1 hour at 4 C. TnI/TnC is in supernatant.
6) Equilibrate DE52 (DEAE) column with cold solution A
7) Add DTT and protease inhibitors
    a. DTT to 1 mM
    b. PMSF to 1mM. (17.4mg in 10 mL isopropanol for 10 mM stock. Store at -20 C)
    c. Leupeptin and Pepstatin (as in step 3)
8) Apply to DEAE column.
    a. TnI shouldn't stick to column. Purify by troponin C affinity column.
    b. TnC should stick
    c. Elute troponin C with gradient to 0.5 M NaCl
9) Gel to confirm troponin C. Combine fractions containing troponin C.

10) Dialyze versus Phenyl sepharose start buffer. 2-3 changes.
    a. 1 M NaCl, 1 mM $CaCl_2$, 50 mM Tris pH 8
11) Equilibrate Phenyl sepharose column w/ start buffer
12) Apply sample to column.
13) Wash column w/ 250 mL start buffer.
14) Wash column w/ 250 mL 1 M NaCl, 0.2 mM $CaCl_2$, 50 mM Tris pH 8
15) Elute troponin C w/ 250 mL 5 mM EDTA, 20 mM Tris/HCl pH 8
    a. Wash further w/ buffer if no peak appears
16) Run SDS-Page gel
17) Dialyze versus experiment buffer or buffer containing at least 200 mM NaCl/KCl and 2 mM DTT
18) Add DTT to 2 mM before freezing in liquid N_2 or dry ice/ethanol. Store at -80 C.

Troponin I Purification using troponin C Affinity Column

Adapted from: Pharmacia Fine Chemicals Affinity Chromatography principles and methods. Sweden, Ljungforetagen AB, Orebro, August 1983

1. Dialyze clean Troponin C against coupling buffer
    a. 0.2 M $NaHCO_3$, 0.5 M NaCl, pH 8.3
2. Suspend freeze dried CnBr activated sepharose in ice cold 1 mM HCl
    a. 1 gram powder gives 3.5 mL gel volume. Use 5 mg protein per mL of gel
3. Wash 15 minutes on sintered glass filter (porosity G3) using 200 mL 1 mM HCl per gram of dry powder in small aliquots. Final aliquot is sucked off until cracks appear in gel.
4. Transfer gel immediately to troponin C solution using a gel to troponin C solution ratio of 1:2
5. Allow to mix 2 hours end over end at room temperature
6. Make 2 M ethanolamine pH solution that is equal in volume to the gel-TnC mixture
7. Add 2 M ethanolamine solution to gel-TnC mixture to give ethanolamine concentration of 1 M
8. Allow to mix end over end for 2 hours at room temperature
9. Allow mixture to settle
10. Suck off superanatant
11. Wash alternately with coupling buffer and wash buffer three times each
    a. Wash buffer: 0.1 M acetate, 0.5 M NaCl, pH 4

12. Suspend in wash buffer and pour into clean, dry column
13. Wash column with ten column volumes of wash buffer
14. Dialyze impure Troponin I from DEAE column from TnC/TnI culture prep against 6 M Urea, 0.1 mM $CaCl_2$, 20 mM Tris/HCl, pH 8.0, 1 mM DTT
15. Equilibrate troponin C affinity column with same buffer
16. Load troponin I onto column and wash with two to four column volumes start buffer
17. Collecting fractions equivalent to about half the loaded volume
18. Elute with 6 M urea, 0.5 M NaCl, 1 mM EDTA, 20 mM Tris/HCl, pH 8.0, 1 mM DTT
19. Run SDS-page gel to verify purification

Recombinant troponin T Preparation from 4L Culture

Adapted from:

Gafurov, B.; Chen, Y. D.; Chalovich, J. M. *Biophys J* **2004**, *87* (3), 1825–1835.

1) Prepare 4L 6 M Urea, 1 mM EDTA, 20 mM Tris/HCl, pH 8 (Soln. A)
2) Prepare 1L Soln. A + 0.5 M NaCl
3) Suspend pellet w/ about 40 mL Solution A + protease inhibitors
    a. About 1.0 mg pepstatin dissolved in 0.1 mL DMSO
    b. About 2.5 mg leupeptin dissolved in ~1.0 mL water
    c. About 0.25 mg TPCK dissolved in 0.1 mL water
    d. About 0.25 mg TLCK dissolved in 0.1 mL water
    e. 43 mg sigma cocktail P8340 dissolved in 0.4 mL DMSO
4) Sonicate 20 seconds x 6-8 times on ice
5) Centrifuge at 19K for 1 hour at 4 degrees Celsius in Sorvall SS-34 rotor.
6) Measure supernatant volume
7) Add 176 g/L ammonium sulfate to 30% saturation. Let stir one hour at 4 degrees Celsius
8) Centrifuge at 19,000 rpm for 30 minutes at 4 degrees Celsius in Sorvall SS-34 rotor
9) Measure supernatant volume
10) Add 94 g/L ammonium sulfate to 45% saturation. Let stir one hour at 4 degrees Celsius

11) Centrifuge at 19,000 rpm for 30 minutes at 4 degrees Celsius in Sorvall SS-34 rotor
12) Measure supernatant volume
13) Add 110 g/L ammonium sulfate to 45% saturation. Let stir one hour at 4 degrees Celsius
14) Centrifuge at 19,000 rpm for 30 minutes at 4 degrees Celsius in Sorvall SS-34 rotor
15) Save precipitate and suspend in about 30 mL solution A + protease inhibitors
16) Dialyze versus 2 L of solution A
17) Centrifuge at 19,000 rpm for 15 minutes to clarify
18) Equilibrate Mono Q DEAE column with solution A
19) Apply sample and wash with one column volume solution A
20) Run 10 column volume gradient of solution A from 0.1 to 0.6 M NaCl
21) Run 1 column volume gradient from 0.6 M NaCl to 1 M NaCl
22) Continue washing with about 5 column volumes 1 M NaCl
23) Check $OD_{280\text{-}340}$
24) Run SDS-PAGE gel to verify purification

Troponin Reconstitution

Adapted from: Kobayashi, T. & Solaro, R. J. (2006) Increased Ca2+ Affinity of Cardiac Thin Filaments Reconstituted with Cardiomyopathy-related Mutant Cardiac Troponin I, *Journal of Biological Chemistry.* **281**, 13471-13477.

1. Dialyze each troponin subunit against 1 M NaCl, 5 mM $MgCl_2$, 5 mM DTT, 20 mM MOPS pH 7
2. Measure concentrations of each troponin subunit using Lowry assay
3. Mix troponin T, troponin I and troponin C at a 1:1:1.05 molar ratio and dialyze against two changes of the same buffer with the addition of 6 M urea
4. Dialyze against two changes of the same buffer without urea.
5. Dialyze against same buffer as step 4 but with 0.3 M NaCl.
6. Dialyze against same buffer as step 4 but with 0.1 M NaCl.
7. Dialyze against 0.1 M NaCl, 5mM $MgCl_2$, and 20 mM Tris/HCl, pH 8.0
8. Centrifuge at 30,000 rpm for 40 minutes in a Ti 50.2 rotor
9. Equilibrate a Mono Q DEAE column with 0.1 M NaCl, 5mM $MgCl_2$, and 20 mM Tris/HCl, pH 8.0.
10. Load troponin onto column and wash with two column volumes start buffer
11. Elute with a linear gradient of 0.1–0.6 M NaCl in the same solution

Modification of tropomyosin with the fluorescent probe acrylodan

Adapted from: Ishii and Lehrer, Biochemistry 29 1160-1166, 1990

1. Dialyze tropomyosin against reducing buffer:
    a. 100 mM KCl, 10 mM Pi buffer pH 6.5, 5 mM EDTA, 1 mM DTT.
2. Add sufficient Pi buffer pH 6.0 to bring the final buffer concentration to 50 mM.
3. Add DTT to 10 mM and incubate for at least 30 min. at 37^{o}C.
4. Dialyze the tropomyosin extensively against 3 mM MOPS, pH 7.5, 0.1 mM EDTA.
5. Add guanidine HCl to the tropomyosin to make it 4 M
6. Add a 5-fold excess of 6-Acryloyl-2-Dimethylaminonaphthalene and allow to react overnight at room temperature in the dark and with a nitrogen atmosphere. Remaining steps are done in dark.
7. Stop the reaction by adding an excess of DTT.
8. Centrifuge 30,000 rpm in a Ti 50 rotor for 20 min. Save the supernatant.
9. Dialyze against at least 20-volumes 4M guanidine HCl, 3 mM MOPS, 0.1 mM EDTA. The dialysis should be changed 4 times at 8-12 hour intervals
10. Dialyze extensively against 40 mM NaCl, 5 mM Mops, pH 7 or buffer of choice

Modification of actin with the fluorescent probe pyrene

Adapted from: Brenner & Korn (1983) JBC 258, 5013-5020

1. Weigh out between 1.4 and 2 mg of pyrenyl iodoacetamide and add dimethylformamide to bring to fourteen mg/ml.
2. Prepare Dilution Buffer:
    a. 100 mM Tris-HCl, pH 8.0, 1M KCl, 20 mM $MgCl_2$, 1 mM $CaCl_2$, 0.1% NaN_3.
3. Prepare Actin Buffer: 1 liter of actin buffer containing 4 mM imidazole, 2 mM $MgCl_2$, 1 mM DTT.
4. To 20 mg of F-actin in actin buffer (4mM imidazole, 2 mM $MgCl_2$) add 1 ml of Dilution Buffer and water to 10 ml.
    a. The water should be added to the dilution buffer prior to addition to actin.
5. Stir in the dark until the actin is homogeneous.
6. Add 0.1 ml of pyrenyl-iodoacetamide and incubate 12 hours at 20^{o}C in the dark.
7. Add a small flake of DTT to stop the reaction.
8. Centrifuge the actin in a 50 Ti rotor for 20 min at 30,000 rpm.
9. Save the supernatant containing the pyrenyl actin.
    a. The pellet is unreacted pyrenyliodoacetamide.
10. Centrifuge the supernatant in the 50Ti rotor at 45,000 rpm for 1h.
11. Discard the supernatant.
12. Add 5 ml of actin buffer to the pellet and allow to stand on ice in the dark for 1hr
13. Homogenize the pellet and dialyze overnight in 500 ml of actin buffer with out DTT.
14. Determine the concentration of actin as described in the Actin prep.

15. Determine the extent of labeling at 344 nm using an extinction coefficient of 2.2E4 $M^{-1}cm^{-1}$.

Protein Detection and Concentration Measure Using Spectrophotometer

1. Set spectrophotometer to measure absorbance at 280 nm and to subtract out absorbance at 340 nm
2. Add protein buffer to each 1 cm path length cell and correct baseline
3. Add protein to cell and collect $A_{280-340}$

Concentration (mg/mL) = ABS/Extinction Coefficient

Concentration (uM) = mg/mL x E6 / MW

Protein	Molecular Weight, MW (grams/mol)	Extinction Coefficient
Myosin S-1	120,000	0.75
Actin*	42,000	1.15*
Myosin	480,000	0.56
BSA	64,000	0.66
HC Troponin T	35,923	0.504
HC Troponin I	24,000	0.397
HC Troponin C	18,400	0.214
Troponin	71,000	0.37

*See actin prep

Lowry Assay

Adapted from: O. H. Lowry, N. J. Rosebrough, A. L. Farr, and R. J. Randall, J. Biol. Chem. 193, 265 (1951).

1. Bring 1-20 μg protein to 0.2 mL with water in a 1.5 mL Eppendorf tube
    a. Make 3 solutions of different concentrations for each protein to be measured as well as 3 solutions of a standard protein (such as BSA) of known concentration. Also make one blank solution with no protein.
2. Add 0.2 mL reagent A to each solution
    a. 1 part CTC, 1 part 0.8 M NaOH, 2 parts 5% SDS
        i. CTC: 0.1% w/v $CuSO_4$*5 H_2O, 0.2% w/v sodium/potassium tartrate, 10% w/v Na_2CO_3
3. Vortex and let stand 10 minutes
4. Add 0.1 mL reagent B
    a. 1 part 2 N Folin reagent, 5 parts water
5. Vortex and let stand 30 minutes
6. Turn on spectrophotometer and set wavelength to 680nm
7. Zero baseline using blank
8. Measure absorbance at 680 nm for each solution
9. Plot each protein absorbance versus the volume of protein added
10. Calculate the slope of each
11. Determine protein concentration using:

$$[\text{Protein}] = \frac{\text{slope unknown}}{\text{slope BSA}} * [\text{BSA}]$$

Pouring polyacrylamide gel

1) Assemble gel cartridge
2) For two 12% gels add the following to a 15 mL conical tube
    a. 3.2 mL sterile H_2O
    b. 4 mL Acrylamide/Bis-acrylamide (30%/0.8% w/v)
    c. 2.6 mL 1.5 M Tris pH 8.8
    d. 0.1 mL 10% SDS
    e. 0.1 mL 10% ammonium persulfate (added immediately before pouring)
    f. 0.010 mL Temed (added immediately before pouring)
3) Quickly close and invert conical. Use disposable pipet to transfer solution to the cartridge. Leave about 2 cm of space from the top.
4) Add solid butanol above solution
5) Allow to sit at least thirty minutes but no longer than 2 hours at room temperature
6) For two stacking gels add the following to a 15 mL conical tube
    a. 3 mL sterile H_2O
    b. 0.67 mL Acrylamide/Bis-acrylamide (30%/0.8% w/v)
    c. 1.25 mL 0.5 M Tris pH 6.8
    d. 0.05 mL 10% SDS
    e. 0.05 mL 10% ammonium persulfate (added immediately before pouring)
    f. 0.005 mL Temed (added immediately before pouring)
7) Quickly close and invert conical. Use disposable pipet to transfer solution to the cartridge. Fill nearly to top.

8) Place loading spacer into cartridge immediately

9) Allow to sit at least thirty minutes

10) Remove spacer

Preparing Samples and Running SDS-PAGE gel

1. Add 30 µL of each protein to 1.5 mL Eppendorf tubes
    a. If protein is close to or greater than 10 mg/mL, use less than 30 µL and bring up to 30 µL with buffer or water
2. Add 7 µL of 5X loading buffer to each
    a. 10% SDS, 10 mM DTT, 20% w/v glycerol, 0.2 M Tris-HCl pH 6.8
3. Boil each tube 5 minutes
4. Transfer poured and polymerized polyacrylamide gel to running apparatus
5. Fill apparatus with Laemmli buffer
    a. 0.2 M glycine, 0.01 M Tris Base, 0.035 mM SDS
6. Load between 5 and 20 uL protein solutions
7. Connect apparatus to voltage source
8. Run at 75 volts until sample is past the stacking gel. Can then turn voltage up to 150 volts if desired.
9. Turn off voltage source once front nears bottom of gel
10. Remove gel cartridge and carefully transfer gel to small container
11. If using coomassie stain, cover the gel with the coomassie solution.
    a. 10% acetic acid, 30% methanol, 0.01% coomassie
12. Optional: Cover loosely with lid and microwave 30 seconds
13. Allow to mix overnight on rocker (or ten minutes if microwaved)
14. Pour off coomassie stain solution
15. Wash gel extensively with destain. 30% methanol, 0.01% coomassie

Obtaining and Analyzing FRET Data

1) After turning on all equipment (ie. Fluorometer, water bath), open FluorEssence software

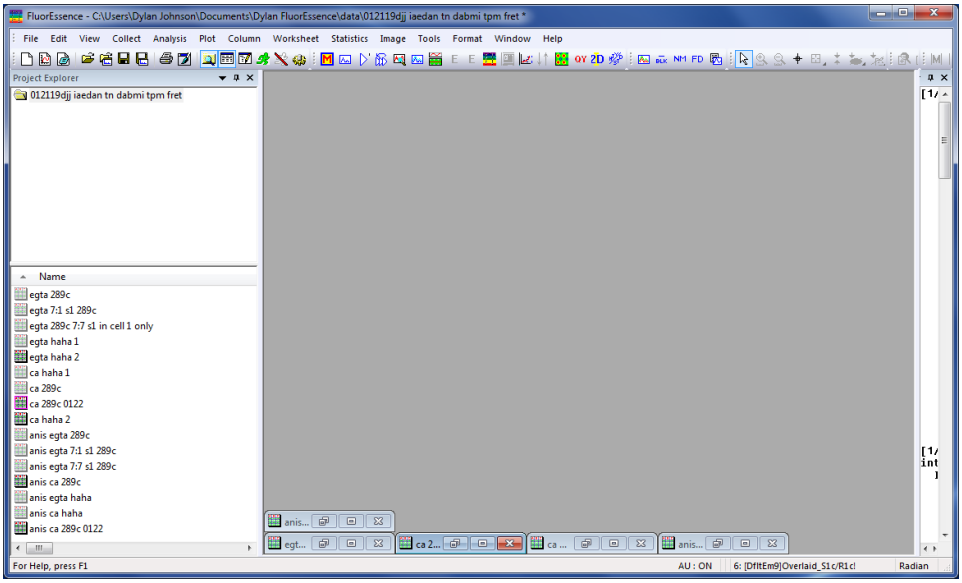

2) Click the red “M” in toolbar. After initialization, click emission.
3) If you already have a blank file, proceed to step 8. A blank file must be created to subtract from your experiments under the same condition. The blank solution should be identical to your experiment solution but in the absence of fluorescent probes. To create a blank file, enter the parameters as in the image below but DO NOT click the checkbox for “Blank Subtraction” (Note these are the parameters used for the IAEDANS-DABMI FRET pair. Different probes may require different values). Use the tabs on the left side of the window to switch between Detector and Monos

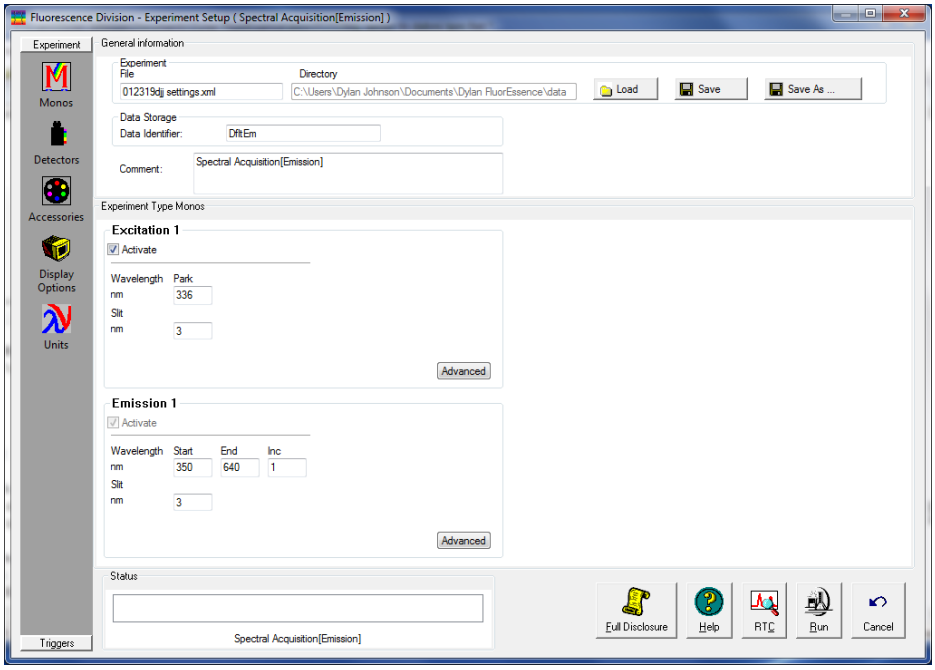

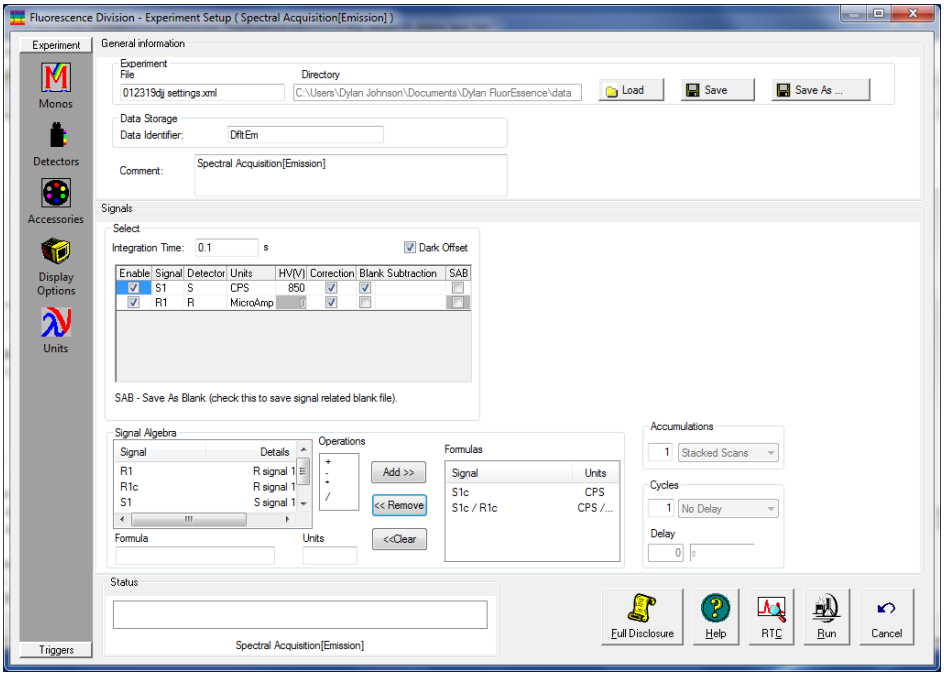

4) Load Blank solution into Cell. Click Run and wait for data collection to finish
5) Now we want to generate a blank file from that data. In the main window click File-HJY Export

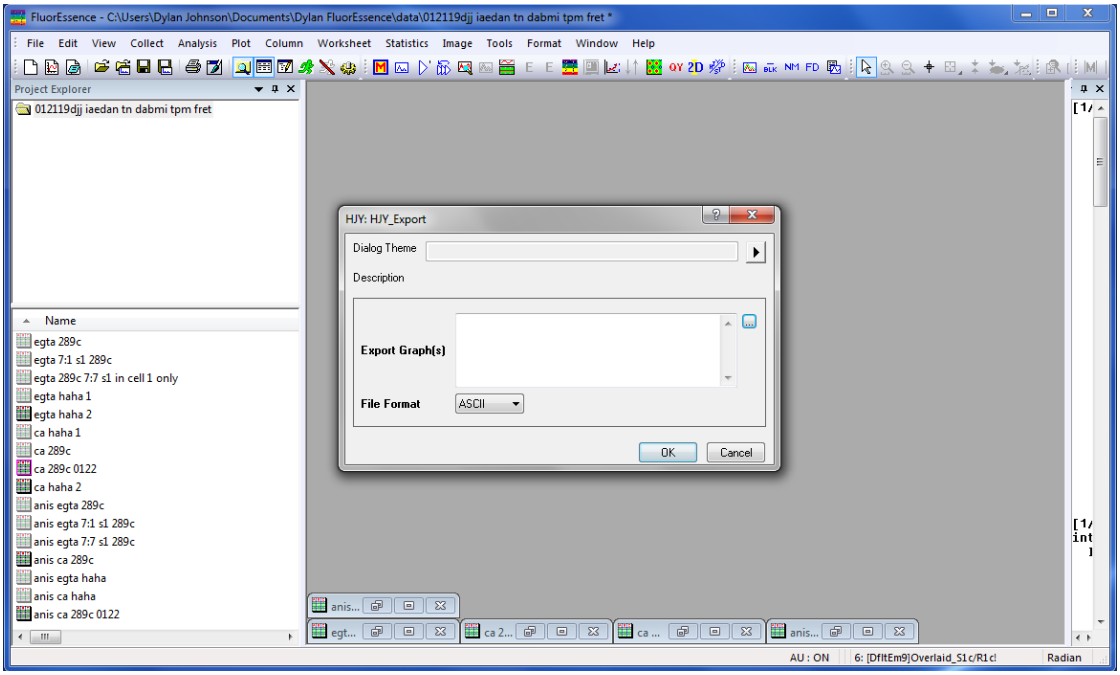

6) Click the "…" button to the right of export graph

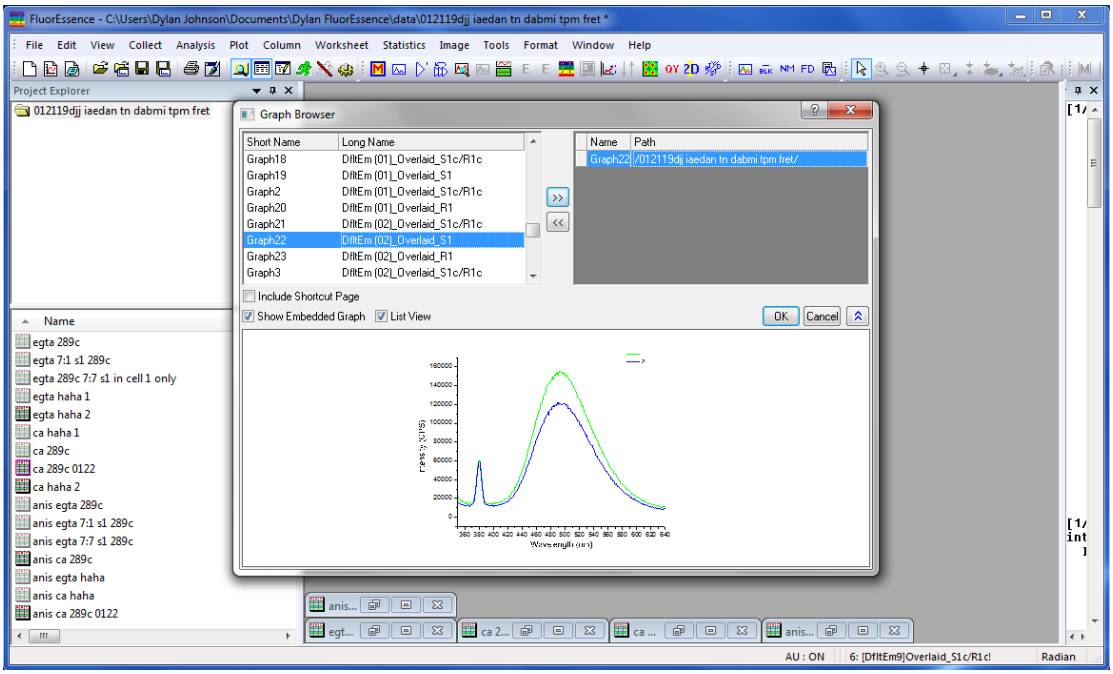

7) Find the plot you wish to save as your baseline. The baseline should be the S1c plot NOT the S1c/R1c plot. Move it into the right column by clicking the ">>" button. Note that the blank file will be created from the plot in position one if there are multiple plots in the file. Click OK. Save the file where you can locate it shortly.
8) Load your experiment solution into the cleaned cell.

9) Click the button to the right of the red “M”. This opens your most recently used parameter settings. Fill in the same parameter settings as in step 3 but this time, check the “Blank Subtraction” box. This will prompt you to locate your blank subtraction file.
10) After loading your blank subtraction file and verifying all parameters are correct, click Run
11) Wait for data acquisition completion.
12) Once complete, use the tabs at the bottom of the following window to cycle between the different data and plots obtained.

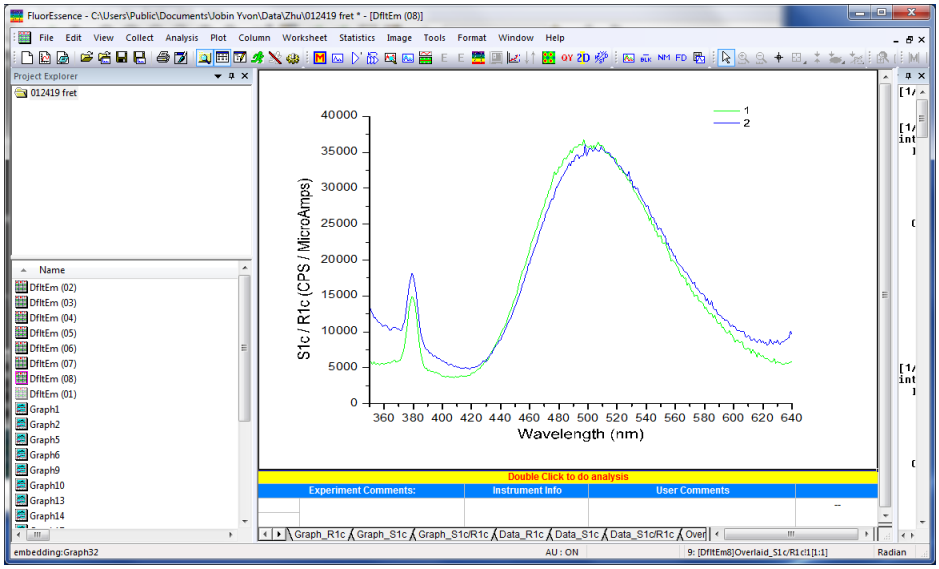

13) Click the Data_S1c/R1c tab. This is the data we will analyze

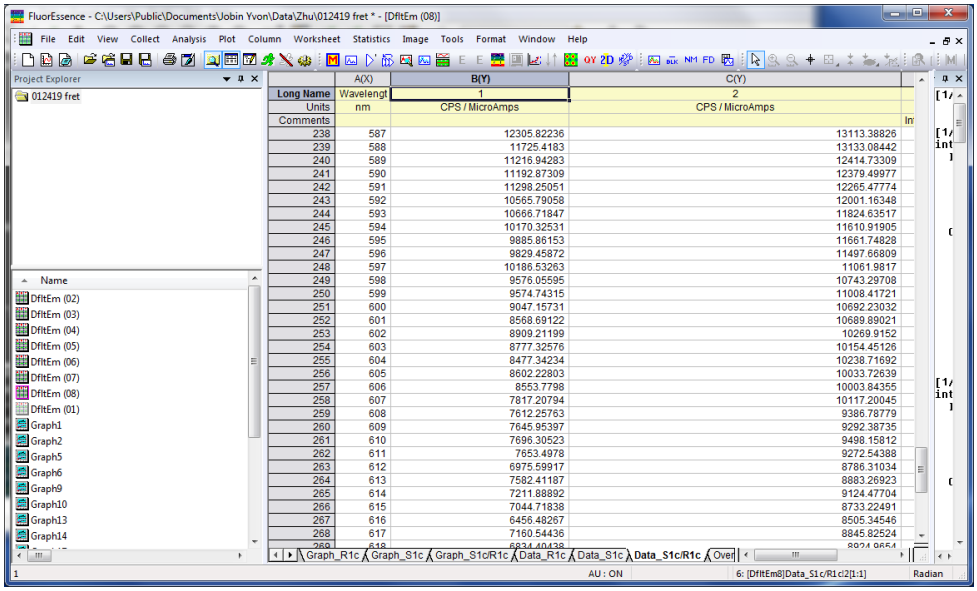

14) We want to create a text file for each set of wavelengths and CPS/microamps values. Copy the data by highlighting and pasting into a new text file. A separate text file should be created for each experiment (ie. With and without acceptor present). Save that file in a location that can be easily located.

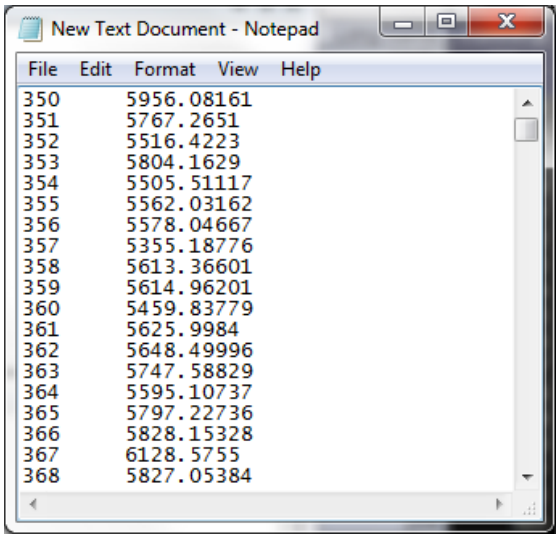

15) Open FITYK software. Click data>quick load file. Locate the text file for one of your experiments just generated. Your data points should appear upon opening. Click the “Baseline Subtraction Mode” button circled in red below.

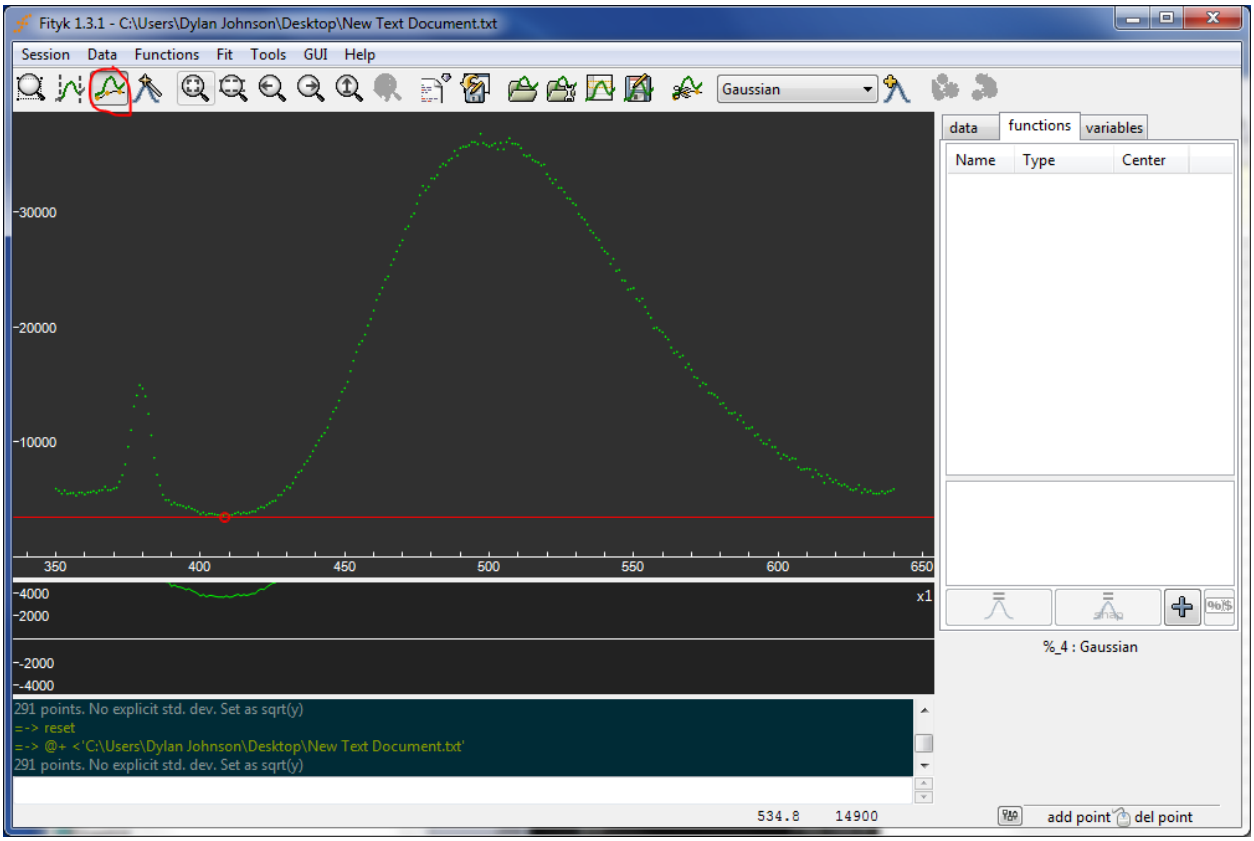

16) Click on the minimum point of the plot. In most cases with this FRET pair, this will be at approximately 410 nm. Click GUI>Baseline handling>Subtract Baseline
17) Click the “Add new peak” button circled in red below FOUR times (three times if there is no appreciable peak around 380 nm). On the right side of the window, note the “functions” tab. Each peak has a Gaussian fit with different parameters that can be modified at the bottom right of the window. One peak should be automatically assigned at approximately 380 nm. Modify the parameters as follows:

380 nm Peak: Lock all automatically assigned values by clicking the lock icon

500 peak:

Height: 10,000

Center: 500, Lock

Hwhm; 40

550 peak:

Height: 10,000

Center: 550, Lock

Hwhm; 40

700 peak:

Height: 10,000, Lock

Center: 700, Lock

Hwhm; 40, Lock

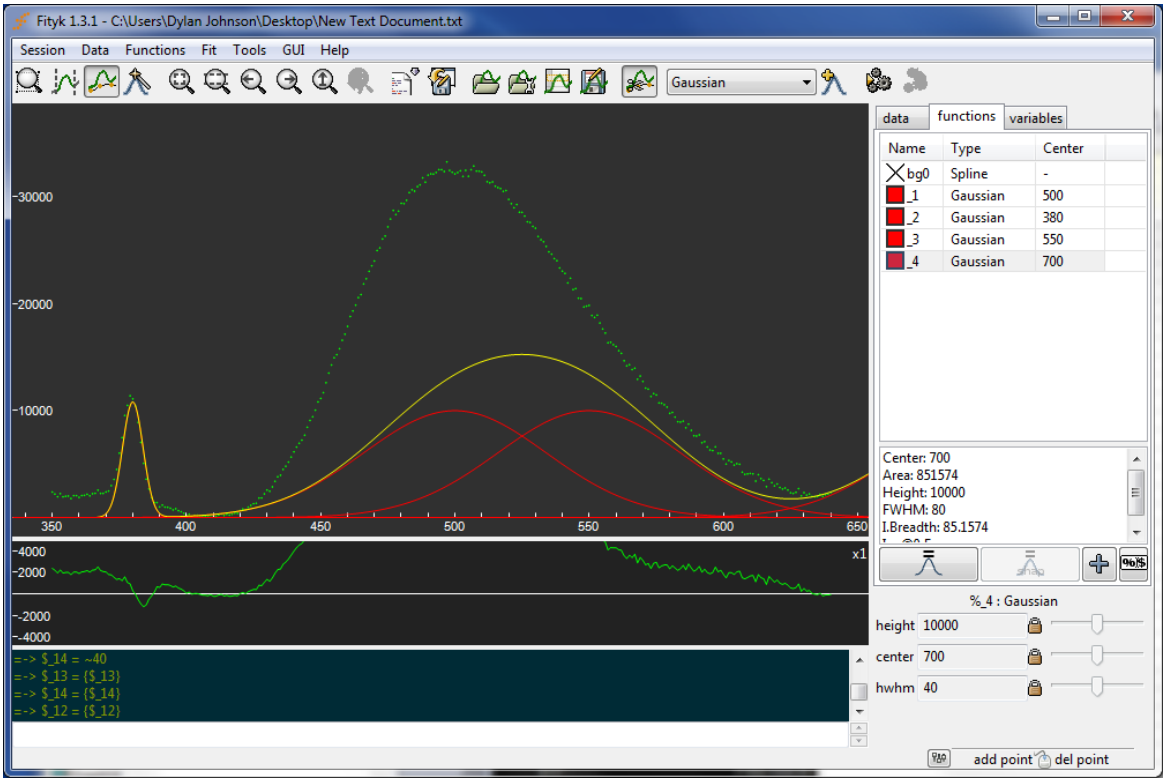

18) Click fit>Run>Ok
19) Unlock the height parameter on the 700 nm peak. Manually adjust to achieve best fit to data. Re-lock the height value.
20) Unlock all parameters on the 500 nm and 550 nm peak
21) Click fit> Run>OK
22) Ensure a good fit of the data. The yellow line is the Fit.

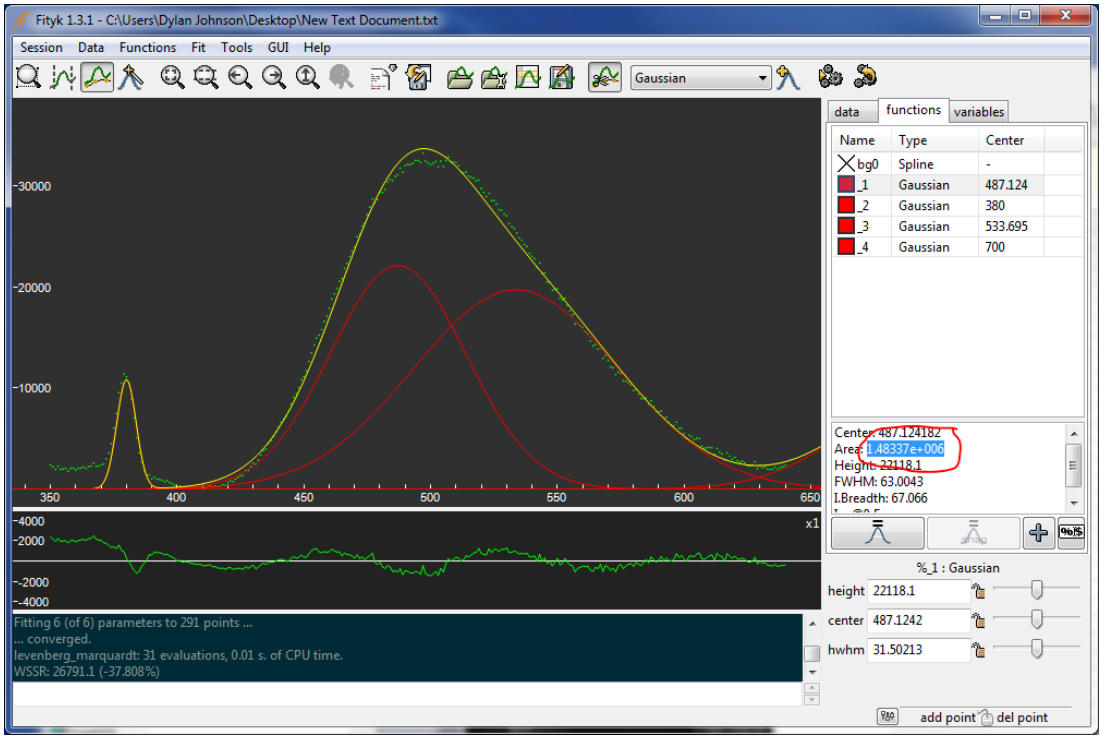

23) For the two peaks corresponding to the main ~492 nm peak of interest, on the right-hand side of the window, add the Area value for each (circled in red above). This is the integrated fluorescence intensity value

24) Once the integrated values have been obtained for the absence and presence of acceptor probe. Calculate the FRET efficiency:

Efficiency= (1-(DA/D))*(1/labelling percentage)

25) Open Fluortools AE software. Click the circled red button as shown in the image below to load the Absorption spectra of the acceptor probe (DABMI tropomyosin in this case) and the emission spectra of the donor (IAEDANS troponin in this case). Note the emission spectra is that obtained in the experiment with all other proteins present in the absence of acceptor probe.

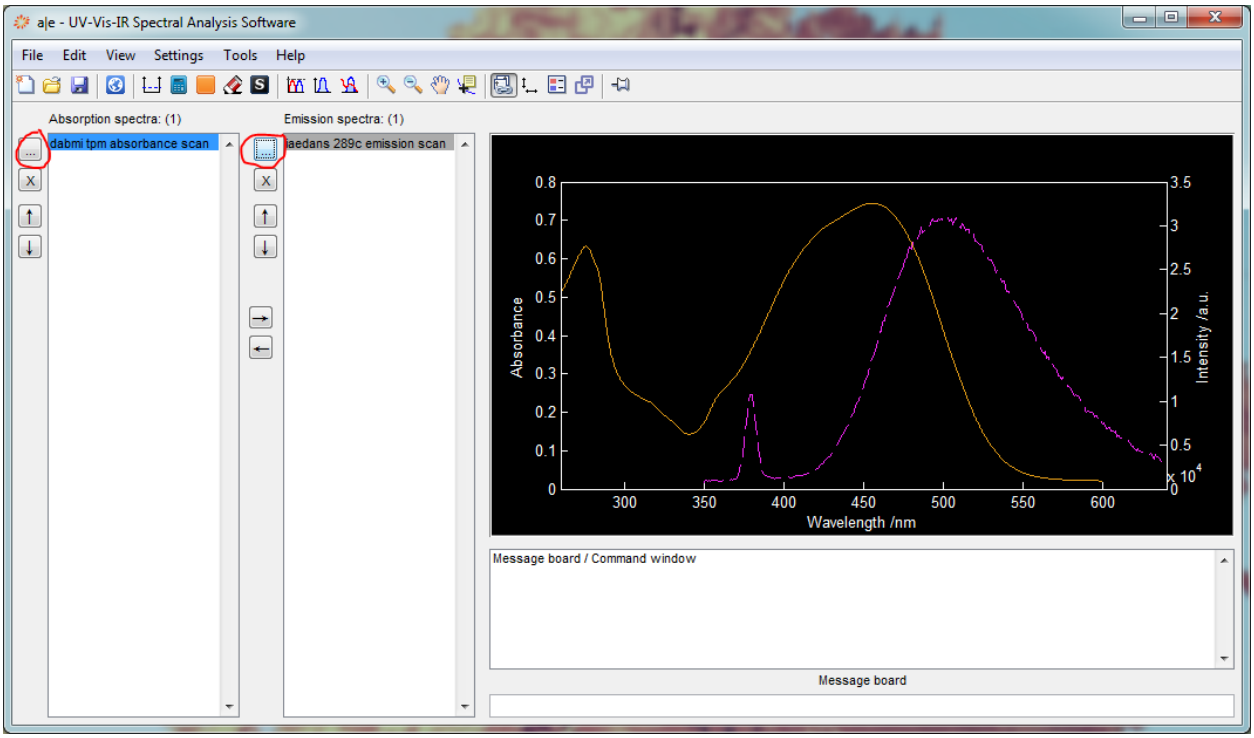

26) The Absorption spectra should be normalized to the extinction coefficient of the probe (For DABMI 24,800 $M^{-1}cm^{-1}$ at 460 nm). For DABMI, this is done by clicking the calculator and multiplying by a factor that makes the absorbance at 460 nm equal 24,800.
27) The emission spectra should be normalized at the emission peak. For IAEDANS, this is 492 nm. Click Tools>Normalize Spectra>Normalize Spectra (at wavelength). Click the Em spectra in the following window then OK. Type 492 nm (IAEDANS), then click OK.
28) Now we can calculate the overlap integral. Click the Button circled in red below. An overlap integral value will be shown in the textbox at the bottom of the window. Record that value.

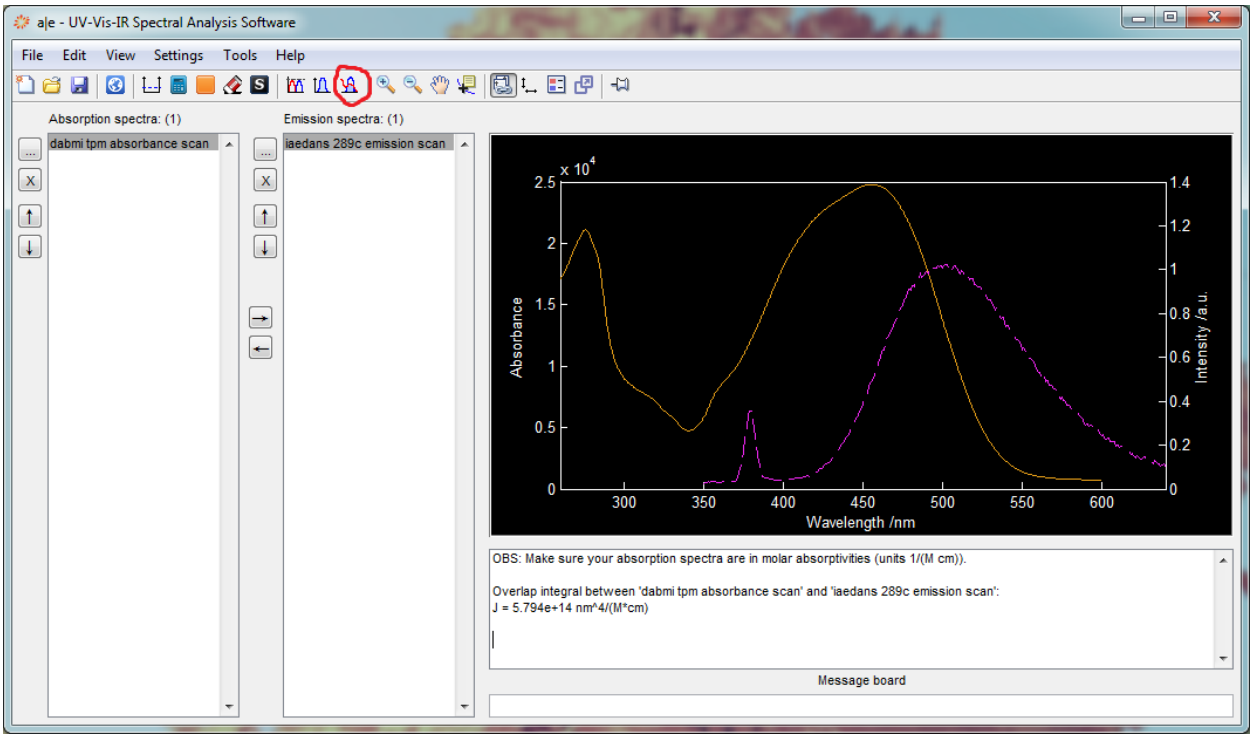

29) Open Wolfram Mathematica and enter the following program. Change the values of the quantum yield (qd), orientation factor (k2), refractive index (nn), overlap integral, and efficiency of transfer (et) as needed. Click shift enter to run the program.

```
ClearAll
qd=0.514;
k2=0.476;
nn=1.33;
j=5.843*10^14;
et=0.8
ro6= 0.0000879*(k2*nn^-4*qd*j)
ro=CubeRoot[Sqrt[%]]
Solve[ro^6/(r^6+ro^6)-et==0,r]
```

30) This program outputs a value of the R_0 (labelled ro) and the Distance in Angstroms. The distance calculation produces multiple values. Only one is not imaginary. Record that value as the distance.

Appendix C: Supplementary Data

Fluorescent Probe Structures

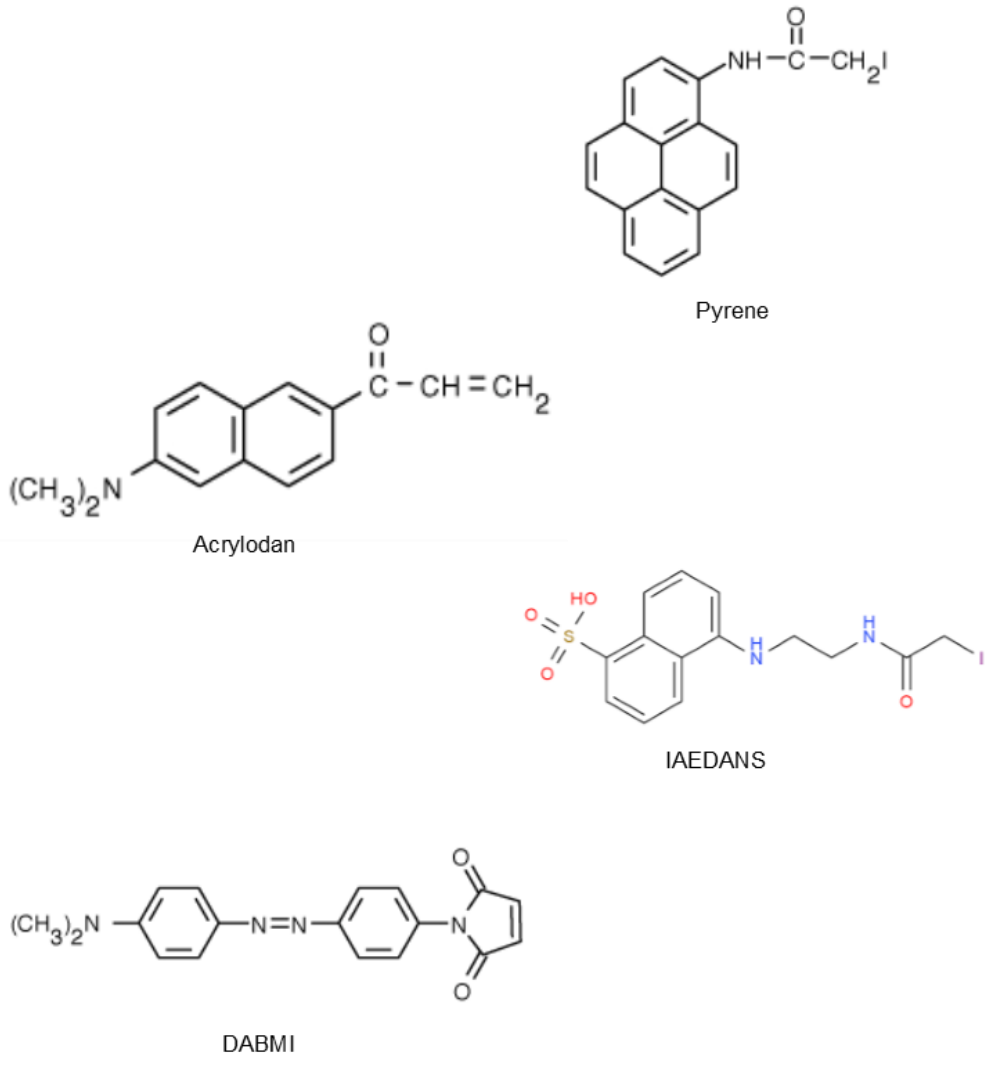

Figure 38: Structures of Fluorescent Probes. Acrylodan, Pyrene, IAEDANS, and DABMI

ATPchase of WT, 275C and ∆14 troponin T

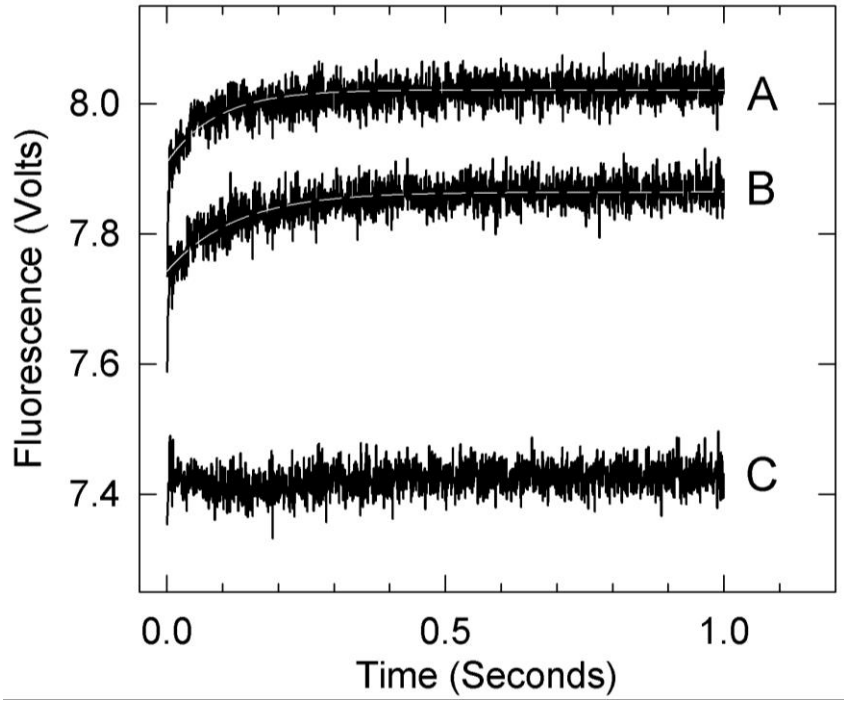

Figure 39: Formation of the inactive B state seen by acrylodan-tropomyosin fluorescence.Time courses of acrylodan fluorescence changes for actin regulated by wild type (1), 275C (2) and ∆14 troponin T (3) following the rapid detachment of myosin S1 in the absence of Ca^{2+} at 10 °C. Traces shown are averages of at least five different measurements. 2 µM actin, 0.43 µM tropomyosin, 0.43 µM troponin and 2 µM S1 in 20 mM MOPS, 152 mM KCl, 4 mM $MgCl_2$, 1 mM dithiothreitol and 2 mM EGTA was rapidly mixed with 2 mM ATP, 20 mM MOPS, 152 mM KCl, 8 mM $MgCl_2$, 1 mM dithiothreitol and 2 mM EGTA. Acrylodan was excited via a monochromator at 391 nm and observed through a 435/451/460 filter.

Representative ATPase data

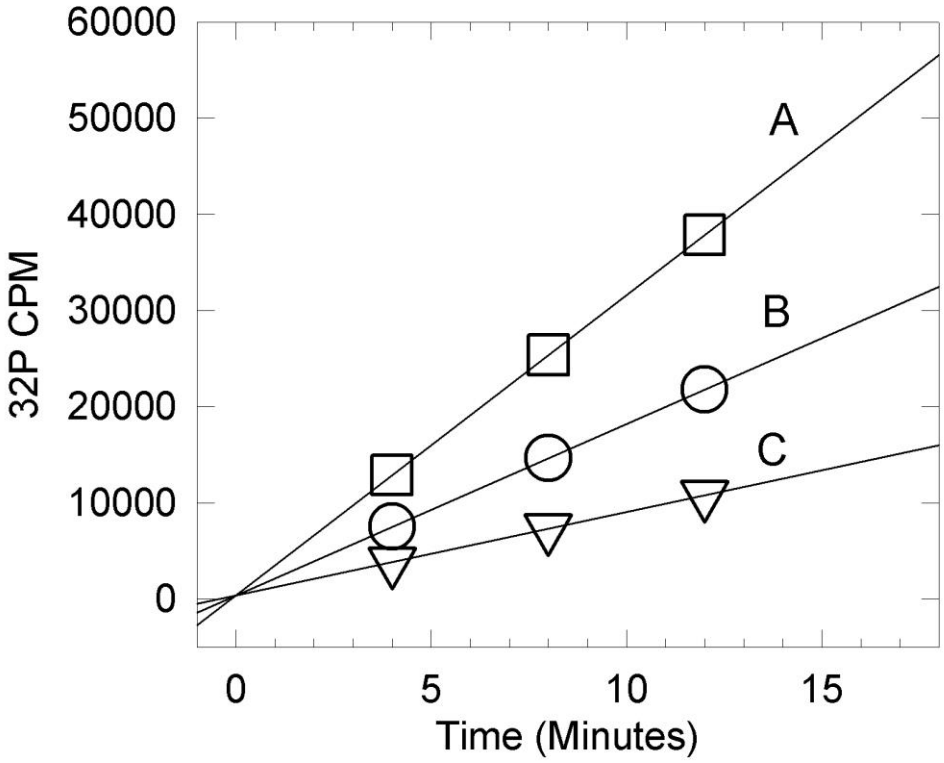

Figure 40: Representative ATPase data at saturating calcium. Regulated actin (squares, A), Unregulated Actin (Circles, B), Actin-tropomyosin (Triangles, C). Measurements were made at 25^{o} C and pH 7.0 in solutions containing 1 mM ATP, 3 mM $MgCl_2$, 34 mM KCl, 10 mM MOPS, 1 mM dithiothreitol and 0.1 mM $CaCl_2$. The concentrations of S1, actin, tropomyosin, and troponin were 0.1, 10, 2.2, and 2.2 µM, respectively

Arrhenius Plot of efficiency of transfer between IAEDANS 289C troponin T and C190 of tropomyosin

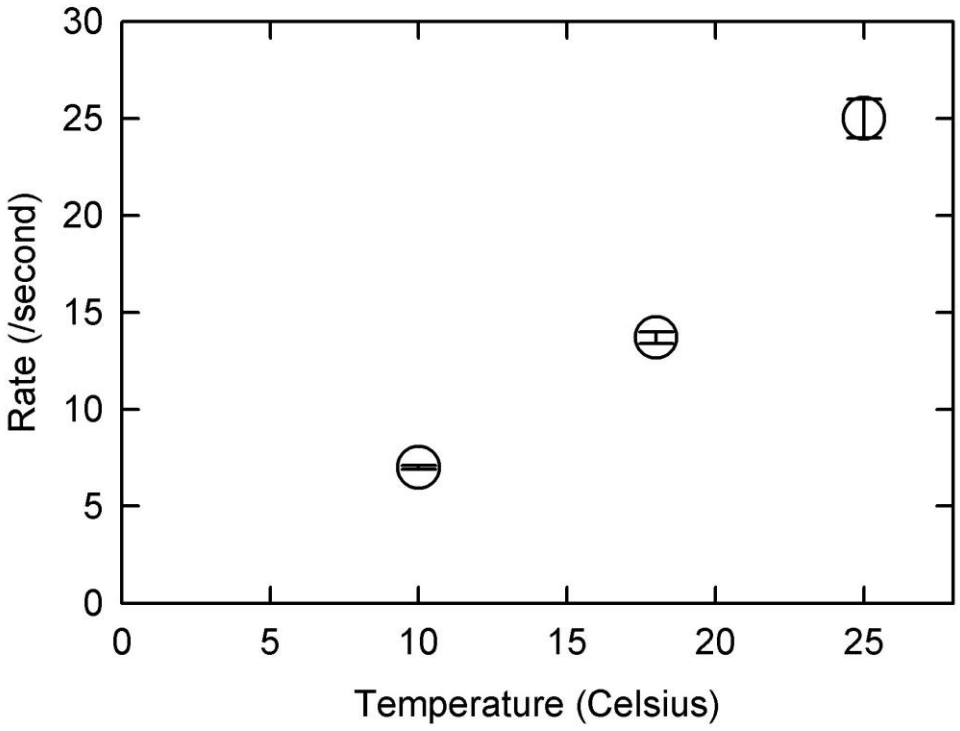

Figure 41 Arrhenius plot of rate of efficiency change between IAEDANS 289C TnT and DABMI fluorescence acceptor probe on C190 of tropomyosin following the rapid detachment of myosin S1 from actin at very low Ca^{2+} concentrations at different temperatures. 2 µM actin, 0.51 µM tropomyosin, 0.43 µM troponin and 2 µM S1 in 20 mM MOPS, 152 mM KCl, 4 mM $MgCl_2$, 1 mM dithiothreitol and 2 mM EGTA was rapidly mixed with 2 mM ATP, 20 mM MOPS, 152 mM KCl, 8 mM $MgCl_2$, 1 mM dithiothreitol and 2 mM EGTA at 25° C. IAEDANS was excited using a 340nm LED and the fluorescence monitored through a 435/451/460 filter. Apparent rates: G, 7.0(±0.1); H, 13.7(±0.3); I, 25(±1).

In-gel digestion and mass spectrometric analysis of wild type, 289C, and HAHA 289C troponin T constructs

1) An SDS-PAGE Gel was run at different concentrations for each troponin T construct. Lane 1 is a MW standard. Lanes 3-5 are wildtype troponin T. Lanes 7-9 are 289C troponin T.

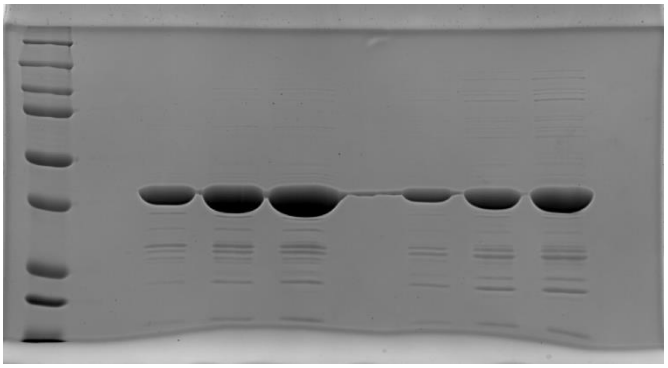

2) A standard protocol was performed for the chymotrypsin in-gel digestion. See: Shevchenko, A., Tomas, H., Havli, J., Olsen, J. V, and Mann, M. (2007) In-gel digestion for mass spectrometric characterization of proteins and proteomes. *Nat. Protoc. 1*, 2856.
3) Liquid chromatography mass spectrometric analysis was performed by Dr. Kimberly Kew. The results for HAHA troponin T are shown below. The sequence of the HAHA 289C troponin T C-terminal residues 251-289 are shown along the top. The colored bars indicate different chymotryptic digest fragments with molecular weights that could be attributed to the molecular weight of sections of the defined sequence. The numbers on the colored bars indicate the time at which the fragment eluted from liquid chromatography. Three fragments were identified that corresponded with the C-terminus of HAHA troponin T where the basic residues were replaced with alanine. This verified that we had successfully substituted those residues.

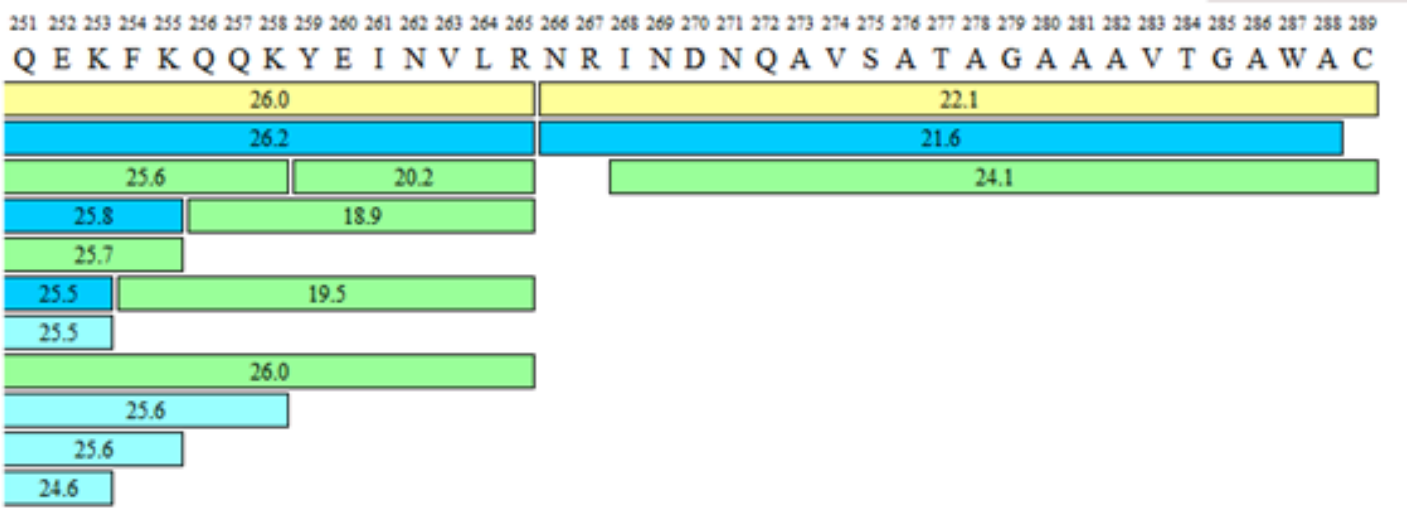

Preparation of Calcium-EGTA buffer

1) 10 grams of calcium chloride and EGTA were weighed into glass beakers
2) The beakers were placed into an over at 170° F overnight to drive off water.
3) Calcium and EGTA were accurately weighed to make a solution that is 100 mM of each.
4) Each was added to a beaker and the volume brought near the total final volume.
5) The solution was brought to pH 7 with NaOH.
6) The solution was added to a volumetric flask and brought to volume.
7) The table below (Table 12) shows the concentration of Calcium-EGTA buffer, calcium, and EGTA that were used to achieve the desired pCa.
    a. These values were calculated using Maxchelator:

        https://somapp.ucdmc.ucdavis.edu/pharmacology/bers/maxchelator/downloads.htm

    b.

Table 12: Ca^{2+}-EGTA buffer, Ca^{2+} and EGTA used to reach desired pCa

Ca^{2+}-EGTA (mM)	Calcium (mM)	EGTA (mM)	Free Calcium (mM)	pCa
4	0	3	6.29E-07	6.20
4	0	0.5	3.70E-06	5.43
4	0	0.1	1.62E-05	4.79
2	0	0	3.05E-05	4.52
8	0	0	6.15E-05	4.21
4	0.2	0	2.09E-04	3.68
4	0.5	0	5.04E-04	3.30
4	4	0	4.00E-03	2.40

SDS-PAGE gel of actin-Δ16 peptide spin down assay

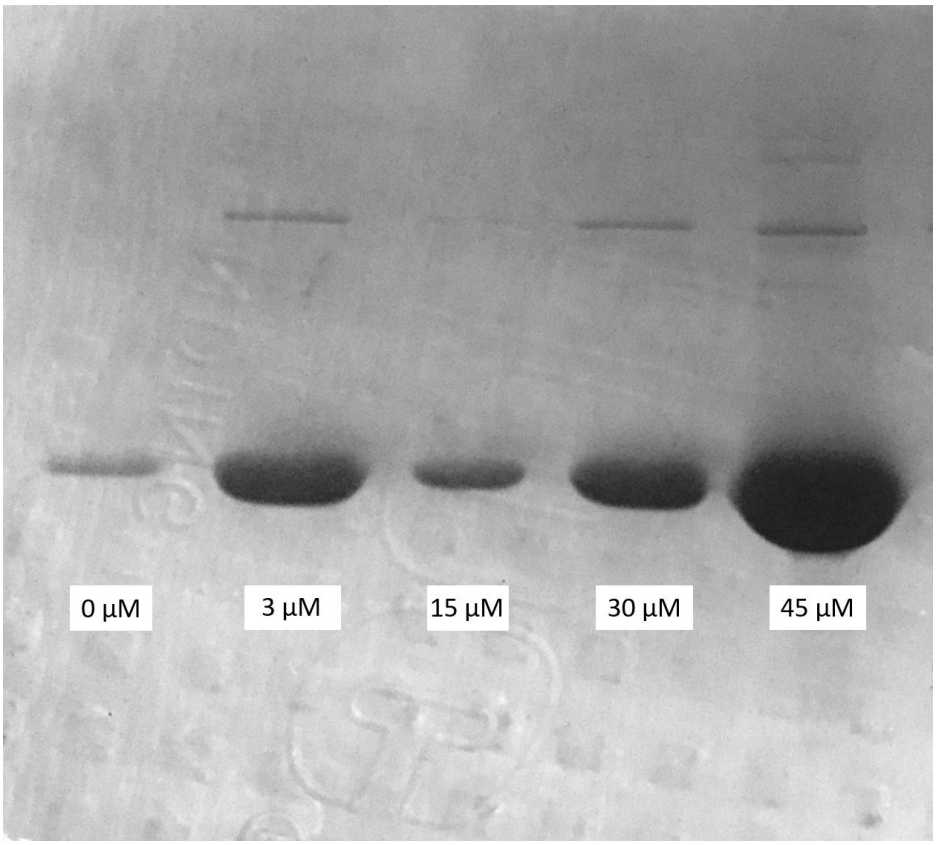

Figure 42: SDS-PAGE gel of actin-Δ16 peptide spin down assay. The major band corresponds to actin. Concentrations refer to the Δ16 peptide concentration.

FRET Titration of DABMI tropomyosin

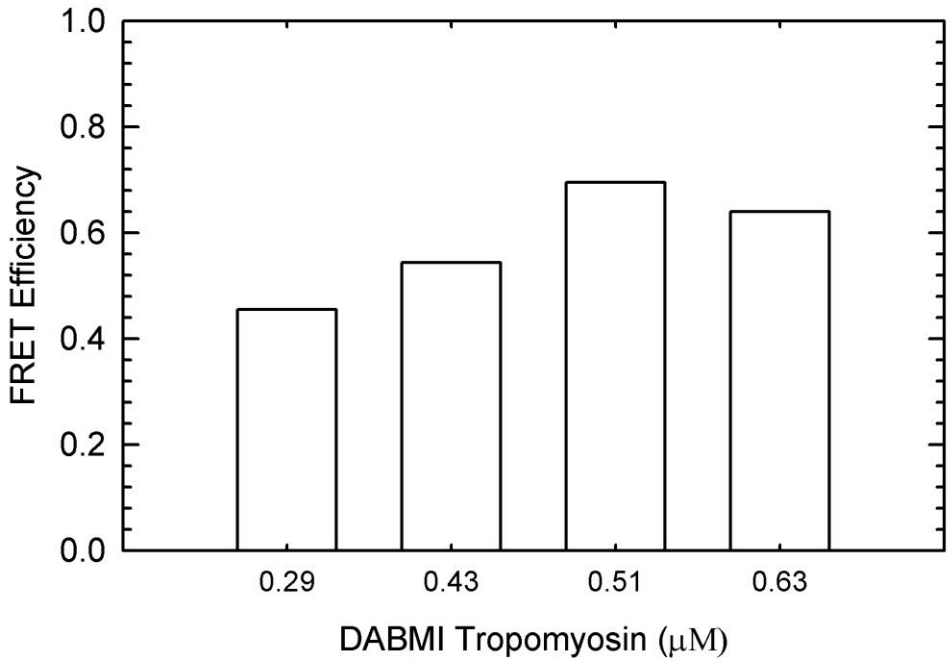

Figure 43: Efficiency of FRET between IAEDANS 289C troponin T and DABMI C190 tropomyosin at different DABMI tropomyosin concentrations. 2 μM actin, 0.29 μM troponin in 20 mM MOPS, 152 mM KCl, 4 mM $MgCl_2$, 1 mM dithiothreitol and 2 mM EGTA. IAEDANS was excited at 336 nm. FRET efficiency determined as described in Chapter 2: Experimental Methods.